

Influence of Interfacial Parameters on the Adhesion of Soft Polymers

zur Erlangung des akademischen Grades eines
DOKTORS DER INGENIEURWISSENSCHAFTEN (Dr.-Ing.)

der Fakultät für Chemieingenieurwesen und Verfahrenstechnik des
Karlsruher Institut für Technologie (KIT)

genehmigte
DISSERTATION

von
Dipl.-Ing. Yana Rüdenuer
aus Sevlievo, Bulgarien

Referent: Prof. Dr. Norbert Willenbacher
Korreferent: Prof. Dr. Peter Müller-Buschbaum

Tag der mündlichen Prüfung: 17.01.2013

Contents

I. Introduction.....	1
II. Tack properties of Pressure Sensitive Adhesives (PSAs)	4
1. Theoretical background.	4
1.1. Adhesion and adhesives.	4
1.2. Methods for evaluation of the adhesion performance of polymers.	6
1.2.1. Mechanisms of bonding.	8
1.2.2. Mechanism of debonding.	10
1.2.3. Parameters of tack test.....	18
1.3. Physical characteristics of polymers and parameters influence the adhesion.	19
1.3.1. Molecular composition of PSAs.....	20
1.3.2. Influence of the bulk parameters: physical characteristic of polymers...	21
1.3.3. Influence of the interfacial parameters: effect on the wetting process...	25
1.4. Mechanical characteristics of polymers: Rheology.	30
1.4.1. Relaxation time. Effect of bonding time on the tack properties.	31
1.4.2. Principles of Rheology. Oscillatory test.....	31
1.4.3. Time-Temperature Superposition (TTS).....	34
1.4.4. Elongational viscosity.....	35
1.4.5. Surface chemical principles. Contact angle and surface energy.	36
2. Materials and methods.....	39
2.1. Materials.....	39
2.2. Methods.....	41
2.2.1. Measurement of shear modulus	41
2.2.2. Measurement of elongational viscosity	43
2.2.3. PSA films preparation and characterization.....	44
2.2.4. Substrate preparation and characterization	45
2.2.5. Crosslinking	48
2.2.6. Contact angle measurements and surface energy determination of polymer films and substrates.	49
2.2.7. Mechanical analysis. Tack measurements.....	52
2.2.8. Video observations.	53

3. Experimental part	57
3.1. Rheological characterization.	57
3.1.1. Characterization of the model system.	57
3.1.2. Characterization of weakly crosslinked acrylate copolymers.....	60
3.1.3. Elongational viscosity.....	62
3.2. Initial conditions	63
3.2.1. Influence of the contact pressure	63
3.2.2. Influence of debonding velocity V_{deb}	64
3.3. Influence of the substrate modifications on the adhesion of PSAs.....	66
3.3.1. Roughness of the substrate.	66
3.3.2. Surface energy of the substrate	78
3.4. Influence of the polymer film modifications on the adhesion of PSAs.....	86
3.4.1. Chemical composition of the polymer	86
3.4.2. Crosslinking	97
3.4.3. Cavity growth modes	112
3.4.4. Surface enrichment	115
III. Summary and Outlook.....	121
IV. Appendix	125
A Data for T_g of acrylate co-polymers measured with DSC	125
B Correction of the tack curves of acrylate co-polymers (example: BA/MA/MMA) according to the compliance of the tack devices.....	127
C Abbreviations and symbols	128
References	132

to my family

PREFACE

This thesis was prepared during 2008 until 2011 in the Institute for Mechanical Process Engineering and Mechanics at the Department of Applied Mechanics at Karlsruhe Institute of Technology. The work was done as a part of a research project financed by Deutsche Forschungsgemeinschaft (DFG).

A number of people who have influenced this work deserve a special acknowledgement for their help in the preparation of this thesis. First of all, I want to thank my supervisor, Professor Norbert Willenbacher, for his patience, advice and support during my work, and Professor Peter Müller-Buschbaum for the inspiring discussions and valuable advice.

I would like to thank Dr. Svetlana Guriyanova for the wonderful time we worked together and for the professional support during my first steps in the area of Pressure Sensitive Adhesives. I am very grateful to Alexander Diethert, Ulrike Licht, and my friends Dr. Katardzyna Niedzwiedz and Dr. Oliver Arnolds for the interesting discussions with me during the work process, to Professor Stephan Naser (TU Darmstadt) for the software program and its systematical updating, to technician Dietmar Paul, Alexandra Reif and Andreas Merk for their technical support. I want to thank also Dr. Olga V. Lebedeva and Dr. Erin Koos for the kindly support with the English language. Many thanks go to all my colleagues, my room colleagues Wiebke Maaßen and Clara Weiss and especially to my friend Beate Oremek, who was always ready to help with all organisations around my project.

I greatly appreciate the financial support provided by the DFG and the scholarship, I received from KIT, respectively Karlsruhe House of Young Scientists (KHYS). I want to thank Mrs. Jana Schmitt (KHYS) for the support.

My greatest thanks go to my parents and my brother for their love and believe in me on every step of my life and to my parents in law and brother in law for their support and love. My husband, Andreas, deserves special thanks for being next to me in good and bad times and for giving me from his optimism over and over again, making every day special. And finally, Anna-Maria, my daughter, thank you, my sweetie, to be such a wonderful baby leaving me time to complete my work. I love you, my family!

Abstract

The influence of the interface phenomena on the debonding mechanisms of pressure sensitive adhesives was systematically studied in this work. The statistical acrylate copolymers used as model systems were investigated using a probe tack test in combination with video-optical observation of the cavitation process. Since the cavitation is an interface phenomenon, analyzing the cavitation process and the factors that influenced it, expand the existing knowledge about the separation of adhesive and adherent. The existence of two types of cavities was confirmed for all polymers investigated here. The rheological properties of all model copolymers were studied using oscillation tests. The increase in the molecular weight of one polymer leads to increase in the storage and loss moduli at low frequency, while at high frequency, they show no difference. It was also observed that incorporating of a polar comonomer results in an increase of shear modulus. Interfacial factors such as surface roughness and surface energy of the substrates used, as well as the chemical composition and crosslinking of the polymers, markedly influence the debonding process of PSAs. The measured surface energies of copolymers were found to be unaffected by the incorporation of comonomers with different surface energy, although, the near-surface composition was changed in a non-trivial manner. Independently of the type of failure in case of rough substrate surfaces, the cavity expansion velocity significantly decreases with an increasing shear modulus of PSA, while on smooth substrate surfaces, this characteristic quantity is insensitive to the bulk properties of the polymer film. For the first time, two different modes of cavity growth have been postulated in this work: lateral growth along the interface on a smooth substrate and omnidirectional growth into the polymer film on a rough substrate

Zusammenfassung

In dieser Arbeit wurde der Einfluss der Grenzflächeneffekte auf den Enthftungsprozess von Haftklebstoffen, auch Pressure Sensitive Adhesive (PSA) genannt, systematisch studiert. Die statistischen Acrylat-Copolymere, die hier als Modell-System zu Grunde gelegt wurden, wurden in einer Kombination aus Tack-Test und Bildanalyse des Kavitationsprozesses untersucht. Da die Kavitation ein Grenzflächenphänomen darstellt, erhöhen die Analyse des Kavitationsprozesses sowie dessen Einflussfaktoren das existierende Wissen über die Enthftung von Polymer und Substrat. Die Existenz zweier Typen von Kavitäten wurde für alle in dieser Arbeit untersuchten Polymere bestätigt. Die rheologischen Eigenschaften der untersuchten Copolymere wurden mit Hilfe von Schwingungsversuchen studiert. Die Erhöhung des Molekulargewichts eines Polymers führt bei niedrigen Frequenzen zu einer Erhöhung der Speicher- und Verlust-Moduln, während sie bei höheren Frequenzen keine Unterschiede zeigen. Es wurde beobachtet, dass die Zugabe eines polaren Comonomers die rheologischen Moduln des Haftklebstoffes erhöht. Die Grenzflächeneffekte, wie die Oberflächenrauigkeit und die Oberflächenenergie der benutzten Substrate, als auch die chemische Zusammensetzung und Vernetzung der Polymere beeinflussen den Enthftungsprozess der PSAs. Die gemessenen Oberflächenenergien der Copolymere zeigen keinen nachweisbaren Einfluss durch die Einbindung der Comonomere mit unterschiedlichen Oberflächenenergien, obwohl die oberflächennahe Zusammensetzung in nichttrivialer Weise geändert wurde. Die Kavitätenwachstumsgeschwindigkeit, welche unabhängig von der Versagensart ist, sinkt mit der Erhöhung der Schubmodule der PSAs im Fall von rauer Oberfläche des Substrates. Im Fall von glatten Oberflächen ist die voranstehend genannte charakteristische Größe unabhängig von den viskoelastischen Eigenschaften des Polymers. Zum ersten Mal wurden mit dieser Arbeit zwei Typen des Kavitätenwachstums postuliert: horizontales Wachstum entlang der Grenzfläche auf glatten Substraten und senkrecht Wachstum in den Polymerfilm hinein auf rauen Substraten.

I. Introduction

Pressure Sensitive Adhesives (PSAs) represent a class of materials with the defining property of sticking to a variety of surfaces under low applied force (1-10 Pa) and short contact time (1-5 s) [1]. This property of pressure sensitivity is called tack. In contrast to all other classes of adhesives, the adhesion process of PSAs occurs without any change of the temperature or chemical reactions. Since neither solvent evaporation nor chemical reaction takes place, these materials are safe and easy to use. To have good tack properties, it is required to have low elastic modulus i.e. to be viscous enough for radial flow, to exhibit an ability to wet the adherent, and at the same time to have the cohesive strength to sustain a minimum level of strength upon debonding. The proper materials, which exhibit such a combination of characteristics as low glass transition temperature, high molecular weight and weak crosslinking, are polymers.

All testing methods of the tackiness of the adhesives are based on the reproduction of test of a thumb being brought into contact and subsequently removed from the adhesive surface. The robe tack test with a flat cylindrical substrate is widely used to test a short-time and low-pressure adhesion [2, 3]. The flat substrate surface has the advantage of applying of uniform stress and strain rate to the adhesive film over the entire substrate surface. Microscopic analysis of the video sequence recorded simultaneously during the separation test is necessary to provide a detailed interpretation of a tack curve and to better understanding the debonding mechanisms, in this case cavitation.

Pressures sensitive adhesives are used in the production of protection films in automotive industry, note pads, labels, masking tapes, analgesic and transdermal drug patches (related with skin contact), and a variety of other products [4]. An advantage of PSA is the ability to separate from the adherent surface without leaving any visible residues. Some of the raw materials mainly used for PSA production are rubber solutions, styrene-butadiene-styrene (SBS), styrene-isoprene-styrene (SIS) hot melt

adhesive, and polyacrylate polymers. Polyacrylate polymers are widely used in industry due to their good stability over a large temperature range, resistance to degradation under ultraviolet light and the possibility to possess viscoelastic properties of PSAs without additives in their formulations. They are mostly statistical copolymers and provide considerable possibilities for modification and formulation. In many cases, polyacrylate polymers are applied as aqueous dispersion [5].

There are two important directions of development in the PSAs applications, namely, the modification of the chemical composition of the underlying components in order to adjust the design to the desired adhesive properties and the prediction of the adhesive properties for use in different applications. The latter is connected to the requirement of comprehensive knowledge of the adhesive behavior with respect to viscoelastic properties of the polymer, and the influence of the interfacial phenomena, such as substrate surface roughness and energy.

Although pressure sensitive adhesives are designed to stick to any kind of surface and are supposed to be insensitive to the adherent, interfacial parameters can influence the adhesive behavior of the polymers. The contribution of the interfacial phenomena to the performance of pressure sensitive adhesives is poorly studied due to the fact that it is superimposed by the viscoelastic properties of the adhesive film, which have a predominating effect. The substrate characteristics, as well as the chemistry of the polymer film, are expected to be key factors in the interaction between the polymer and the substrate. The separation of acrylate copolymers from the substrate is accompanied with formation of cavities that appear at the interface of contact and subsequently grow in the bulk of the polymer film [6]. Due to the fact that the contact defects are an interfacial phenomenon, it is reasonable to suggest that such interfacial parameters as surface roughness and the surface energy, either of the substrate or the adhesive film, can influence the adhesion of pressure sensitive adhesives. Incorporating of a polar comonomer in the polymer chain often changes both the bulk and surface properties and, accordingly, the adhesive performance of PSAs [7]. Another important molecular parameter that affects the adhesion is the degree of crosslinking since it markedly influences the viscoelastic properties of polymers [8].

The goal of this work is a systematic study of the effect of interfacial parameters, such as surface substrate roughness, surface energy, as well as the incorporation of functional comonomers in the polymer chains, on the adhesion of PSAs and investigation of the influence of slight crosslinking of PSAs on their adhesion and debonding mechanism, i. e. the transition of cohesive to adhesive failure. The effect of the substrate characteristics on the adhesion of statistical uncrosslinked and slightly crosslinked butyl acrylate-methyl acrylate copolymers was investigated using substrates with different roughness and surface energy. Additional polar comonomers, namely hydroxyethyl acrylate, methyl methacrylate or acrylic acid were incorporated in butyl-methyl acrylate copolymer in order to investigate the influence of chemical composition of PSA on its adhesion. Finally, the influence of crosslinking on the debonding mechanisms was studied using buthyl acrylate-methyl acrylate copolymers.

The probe tack test was used in combination with video observation. The experimental setup allows for observation of the debonding process and correspondingly cavity formation in situ with high spatial and temporal resolution. The images are recorded during the separation process simultaneously with the contact force-displacement curves at every stage of the tack test. The quality of the obtained images enable us to obtain reliable results for the number of cavities, size of cavities formed, as well as to study of the kinetics of cavitation and evaluation of the cavity growth rate.

II. Tack properties of Pressure Sensitive Adhesives (PSAs)

1. Theoretical background.

1.1. Adhesion and adhesives.

The process of connecting two solids together using polymers as adhesives materials shows wide industrial applications. Certain viscoelastic properties allow polymers to fulfill the requirement for their classification as adhesives [9]. For this purpose the adhesive has to possess a good combination of two characteristic properties: adhesion and cohesion. Adhesion, or the adhesive's stickiness, is distinguished by low viscosity, compulsory for broad contact area and enhanced bond density. Cohesion forces represent the sufficient strength of the physical bonds between the polymer molecules in order to resist externally applied stresses. The cohesion of linear and branched polymer macromolecules is defined only by the partial valence bonds; whereas the adhesion is specified primarily by the secondary bonds. An important advantage of the adhesive joint is the uniform distribution of load over a large area avoiding localization of stress.

Design of adhesives is based on the oriented optimization of the adhesive connection and works successfully both for very small surfaces and for large areas of contact. Plenty of adhesive varieties exist for modification of the structure design in order to get the desired properties suitable for specified commercial applications. The adhesives differ not only by their chemical composition, but also by the thermomechanical properties of the bonded joints, processing methods, as well as types of reactions during the bonding. One can categorize them as chemical reacting glues, reactive hot melts, and physical setting glues [10]. The first type includes both cold and warm hardening adhesives. The process of adhesion requires a chemical reaction, which could be chain or step-growth polymerization, vulcanization, or mild crosslinking. Reactive hot melts are generally crosslinked (cured) after coating, increasing the

cohesive strength and followed by transformation from thermoplasts into a hard material. They present a good combination of physical setting and chemical reacting systems. The hardening ensues with a physical reaction, such as solvent evaporation or temperature cooling. Physical setting adhesives can be classified depending on the process of hardening as follows [10]:

- Hot melts, a mixture of amorphous polyamide with linear molecule chains usually, saturated polyester or ethylene vinyl acetate and tackifier resin, combined mostly with stabilizers and fillers. Higher temperature can bring them in motion, increasing the area of contact, whereas at low temperatures they take the primarily solid state.
- Dispersion adhesives are polymers diluted in solvent/water to obtain a lower viscosity and improved wettability. The hardening starts in parallel with the evaporation of the solvent.
- Plastiols are polymer particles, finely distributed in a tackifier disperse phase without any solvent content. By heating, the plastiols transform into a gel.
- Contact adhesives are polymers, which show relative high strength after applying a low pressure for a short contact time. The process of hardening here is crystallization or diffusion.
- Pressure sensitive adhesives (PSA) are soft, viscoelastic solids, based mainly on polymers: acrylics, styrenic block copolymers and natural rubber. Pressure sensitive adhesives are able to build a joint by the application of a low pressure.

Styrenic block copolymers

This type is representing by high performance thermoplastic rubbers, where styrene-isoprene-styrene triblock (SIS) or styrene-isoprene diblocks are generally used in industry. Typically, they consist of two hard polystyrene end blocks and one soft elastomeric midblock of polyisoprene or polybutadiene. Separated blocks are immiscible and physically crosslinked, which provides good creep properties and reformation under high stress [10]. The important advantage of phase separation by the block copolymers is the resulting enhanced cohesion strength. Nevertheless, they exhibit the mechanical properties of rubbers and the characteristics of the thermoplasts.

Natural rubbers

These polymers have uncrosslinked molecular chains, which place them in the group of thermoplasts. After coating, proceeds crosslinking (vulcanization) in order to prevent creep.

Acrylics

They are statistic copolymers, which consist primarily of a monomer with low glass transition temperature (T_g) and of a secondary “glassy” monomer with high T_g . Under melt/flow conditions, the molecule chains exhibit mobility, leading to continuous reorganization of their positions relative to the other molecules.

Disadvantage of styrenic block copolymers and natural rubbers are their relatively inferior stability and degradation under UV or thermooxidative exposure.

Acrylics exhibit viscoelastic properties for pressure sensitive adhesives without including additives in the formulation and are stable over a large temperature scale.

Acrylic pressure sensitive adhesives are the object of this study.

1.2. Methods for evaluation of the adhesion performance of polymers.

The possibility of the PSA to stick to any kind of surface under a low pressure is called “tack” and is measured in J/m^2 . The importance of quantification of the adhesion leads to development of proper testing methods. All testing methods of tackiness have a goal to reproduce, in one way or another, the test of a thumb being brought in contact and subsequently removed from the adhesive surface. The methods widely used in industry to evaluate the adhesive performance are peel test, shear resistance and the probe tack test.

- *Peel test*

The peel test gives information about the force needed to peel-off an adhesive from the substrate. Peel resistance is an average load per width during the separation process of a thin flexible strip bonded to a rigid substrate and peeled under angle of typically 90°

or 180°. Peel resistance represents the total energy required to break the adhesive bond, which is the sum of the fracture energy and the dissipated viscoelastic energy. The latter is connected to the formation and growth of fibril structures. This is the dominant contribution to the peel resistance force, and shows a strong dependence on test conditions [11].

- *Shear resistance*

The ability of PSAs to sustain shearing forces is known as shear resistance or holding power, where the most widely used method to measure the shear resistance is the static shear test. PSAs are exposed to shearing forces for short or long periods of time at an elevated temperature. The prepared adhesive tape is fixed vertically in the shear tester and the static load is applied on the free end of the tape parallel to the contact area. Additionally, by compressing an adhesive film, the shear deformation result in a radial “cold” flow. Shear resistance of PSAs is closely related to their cohesive strength and creep behavior.

- *Probe tack test*

The most common test for measuring the short-time and low-pressure adhesion is the flat-ended probe tack test with a cylindrical probe (Fig. 1.1). Hammond developed the first probe tack test where the tack of adhesion represented the maximum recorded force [12]. Zosel investigated the debonding mechanisms of soft adhesives using a probe tack test. He recorded the force vs. time debonding curve and implemented an optical observation of the rupture process [3, 13, 14]. Essential information can be gained by analyzing not only the level of maximum stress, but also the whole debonding curve. The curve gives the desired information for the calculation of adhesion dissipative energy and so can elucidate the contribution of the fibril formation to the adhesion process [11].

The probe tack test distinguishes between the linear low strain deformation at the initial stage of detachment and the later nonlinear high strain deformation. The test maintains control over the experimental parameters influencing the tack and provides for good reproducibility. The flat-cylindrical substrate ensures uniform film displacement and

simplifies the analyses of the fibril structures. Axisymmetric substrates allow for large values of the confinement ratio, which is crucial for the investigation of PSAs in a highly confined probe tack test.

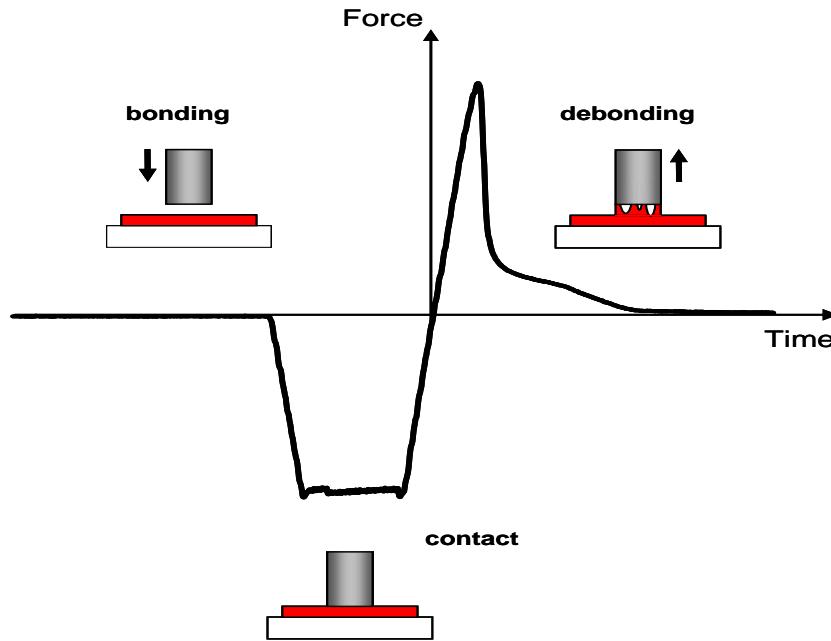


Figure 1.1. Schematic of tack measurements performed on the Texture Analyser. The probe is brought into contact with the polymer (bonding), kept stationary for a certain time (contact) and removed from the film (debonding) [12].

For better understanding of the adhesive process, tack mechanisms can be split into bonding and debonding parts. In this study, entire investigations are focused only on the analysis of debonding. However, it is necessary to notice the importance of the wetting process and bond formation on the adhesion.

1.2.1. Mechanisms of bonding.

PSA have to fulfill the well know Dahlquist criterion to be categorized as a PSA. To bond properly, they have to possess at 1 Hz an elastic modulus lower than 3.3×10^5 Pa [15].

- *Bond formation*

The contact between substrate and polymer is based fundamentally on van der Waals forces, surface chemical bonds, and macromolecular interaction. Bond formation appears at a very limited interface area. For the bond formation, the distance between

the atoms and molecules of the polymer and substrate has to be shorter than 1 nm, which is the length of a chemical bond between the atoms in each material. The interaction energies, atom/atom and atom/molecule, decay with distance d^{-6} for the secondary bond such as dipole-dipole, dipole-induced dipole and fluctuation dipole-induced dipole [16, 17]. As a consequence, very close contact between the polymer and substrate must be established for good adhesion. Uncrosslinked or slightly crosslinked polymers brought into immediate contact with the surface of substrate are able to form an adhesive joint of measurable strength. To establish a nearly complete contact with the surface of the substrate, this polymer must have a low enough viscosity to flow, allowing high quantity of its molecules to achieve contact with the molecules of the substrate.

- *Thermodynamic work of adhesion*

The formation of chemical bonding at the interface between two materials is indicated by the thermodynamic work of adhesion (W_a), which can be calculated with the Dupré equation (1).

$$W_a = \gamma_s + \gamma_l - \gamma_{sl} \quad (1.1)$$

where γ_{sl} is the interfacial energy between liquid (polymer) and solid (substrate), and γ_l and γ_s are the surface energies of the liquid and of the solid, respectively. The meaning of W_a is a change in energy per unit area as one interface is transformed into two separate surfaces. In order to gain energy during the wetting process, the interfacial tension γ_{sl} has to prevail over the sum of the tensions of the solid/air and liquid/air interfaces. The driving force for ability of the adhesive to spread over an adherent surface is governed by the interfacial properties of the both adhesive and adherent. Better wetting can be observed by having: 1) polymers with lower resistances to flow and 2) substrate materials with such interfacial properties that promote strong driving forces, allowing easy spreadability of the adhesive over the contact area. The flow resistance is attributed to the rheological properties of the polymers. Specifically, this viscoelastic character of the polymers induces the demand for applying an external

force to the system, to achieve complete wetting. However, the required pressure for establishing of an adhesion connection using acrylic PSA is very low.

Although the ability to flow is an essential property of the adhesives, not every material that is able to wet the adherent surface can be classified as adhesive. Van der Waals liquids can wet the surface of the adherent almost completely, but the adhesion energy will have the value: $W = 2\gamma_l$, twice the surface energy of the liquid. The van der Waals surface energy can be formulated as the product of the Boltzmann constant and absolute temperature, divided to the square of the molecular size (a_m): $\gamma_l = kT/a_m^2$. The resulting dissipated energy $W \approx 0.1J/m^2$ has a value much smaller than the typical fracture energy of an adhesive joint, which is in range of 100 to 1000 J/m^2 [18]. Actually, exact the efficient dissipation mechanisms of the polymers, which are mainly governed by the plastic deformation of fibrils in extension, give their adhesion properties and are responsible for their high rupture energy. More information about the adhesion properties of polymers and calculation of the rupture energy can be obtained by analyzing the process of debonding.

1.2.2. Mechanism of debonding.

Adhesive measurements are mainly concentrated on studying the process of debonding and the parameters that influence the rupture.

- *Homogenous deformation*

The homogenous deformation of the film in tension is characterized by an increase in the tensile stress caused by the rapid increase of the force with displacement. The initial stage of debonding corresponds to the linear increases in the force on the debonding curve (Figure 1.1), followed by the heterogeneous processes of nucleation and expansion of cavities.

The deformation of a thin elastic film is governed by the confinement ratio, the elastic modulus of the material and the critical energy release rate G_c . G_c depends on the interfacial parameters as interfacial interactions, chain interpenetration, as well as on the dissipation mechanisms near to the interface, and characterizes the energy dissipated during the propagation of crack at the interface PSA/substrate. For an

elastomer adhering to a solid surface, the adhesion energy is determined by the molecular forces which bind two surfaces together, in addition to contributions from the energy expended by dissipative process within the elastomer [19]. The energy release rate G is determined experimentally. The elastic layer is confined between two rigid surfaces (consider axisymmetric geometries). The interface between the adherent and adhesive is the contact area, which can be viewed as crack. Force F applied to one of the rigid substrates is transferred to the elastic layer, due to the adhesive bonding between the adhesive film and the substrate. The stored elastic energy U_E (for elastic material) is equal to the work done to the system during deformation [19] :

$$U_E = \int_0^{\delta_0} P d\delta, \text{ where } \delta_0 \text{ is the final value of the displacement, } \delta, \text{ in the direction of the}$$

applied load. The crack, which separate material in two regions, increases in size and the area of contact decrease from A to $A - \delta$, respectively. Therefore, both, the load which is needed to for achieving a fixed displacement and the strain energy of the samples, decrease. The energy release rate relates to the change in the stored strain

energy with the decrease in contact area: $G \equiv \left. \frac{\partial U_E}{\partial A} \right|_{\delta}$. The lateral confinement ratio, the

contact probe radius divided by the film thickness a/h , is a crucial factor in the compression phase. For large values of a/h then the pressure distribution under the probe is parabolic [11]. Small confinement ratios lead to nonlinear strain, controlled by the initial probe radius a_0 : $(h - h_0)/a_0$. According the theoretical prediction and experiments with viscous mineral oil done by Tirumkudulu and Russel [20], the parabolic distribution of pressure in the film thickness of a very viscous liquid material localizes the cavity nucleation to the middle of the probe, where the pressure has the highest value. Lacroute and co-workers [6] observed, with acrylic copolymers (solid-like material), a random appearance of the cavitation under the probe surface caused by homogeneous negative hydrostatic pressure.

In soft materials with higher values of confinement a/h , the mechanism of detachment proceeds with the appearance of cavitation.

- *Nucleation of cavitation and cavity growth*

In order to decrease the negative hydrostatic pressure in the polymer film, voids appear and grow, forming fibril structures. The cavitation process as a debonding mode has been described in detail previously [2, 21-23]. Voids emerge due to trapped air bubbles during bonding or are caused by impurities on the adherent surface that avoided complete wetting. Usually, they nucleate from pre-existing micro bubbles and grow in the polymer bulk. The localization of the defects and the trapped air bubbles at the contact interface polymer/substrate results in the formation of cavities at the substrate surface. This idea is confirmed experimentally by optical observations of the debonding process, focusing the lens on the polymer surface, which allows the bulk and surface region to be distinguished [6].

Cavity growth during debonding has been studied in more detail [24] using video-imaging, revealing that cavitation starts at a stress level far above the elastic shear modulus of the polymer, and that cavities grow exponentially at a strain rate much higher than the applied external rate.

The schematic side views on the Figure 1.2 illustrate the stages of cavity nucleation, growth, elongation and rupture. The stress-strain debonding curve is synchronized with video images of the contact area, taken from below, at certain times.

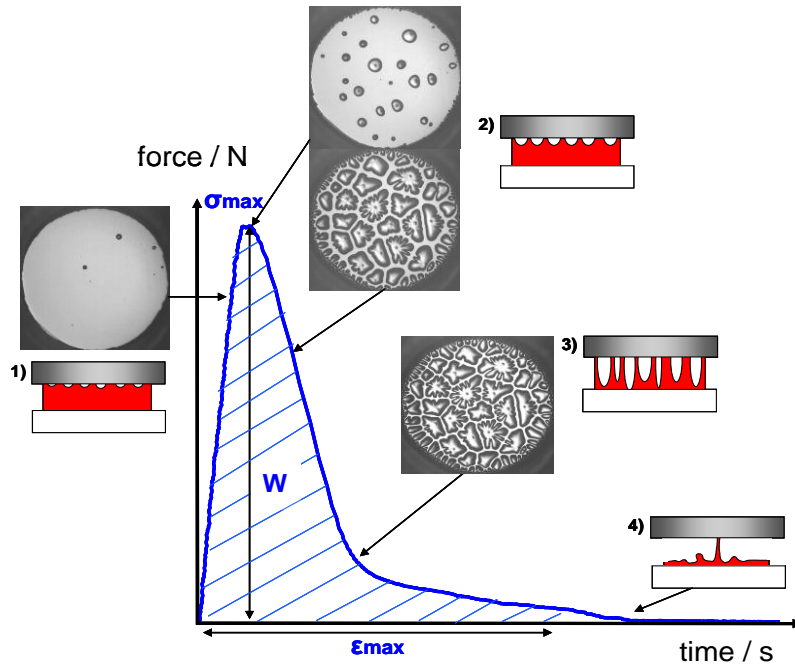


Figure 1.2. Schematic of a typical stress-strain curve synchronized with video images of cavitation of the polymer/substrate surface:

- 1) growth in horizontal direction;
- 2) fibril formation;
- 3) and 4) final rupture.

Tack parameters: work of adhesive (W), nominal stress peak (σ) and deformation at break (ε_{\max}).

1) The first stage of fracture represents cavity nucleation from already existing micro bubbles on the surface of the substrate. The nucleation of cavities is a heterogeneous process, characterized by appearance of cavities in order to minimize the negative hydrostatic pressure in the polymer film. The properties of the substrate surface essentially influence the cavity appearance and their number, while the viscoelastic properties of the polymer have a crucial effect on kinetics of expansion. The first visual observation of cavitation corresponds to the region immediately before the stress reaches its maximum value. If the cavities grow in a low viscosity adhesive, one can expect easy nucleation and expansion of cavities with larger sizes and a reduced number as the cavities grow in the more viscous bulk [21].

Shull and Creton [22] illustrated the mechanisms of cavity growth in the bulk and at the interface with the substrate:

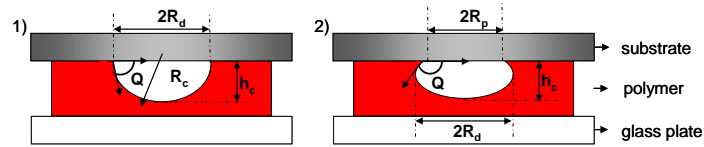


Figure 1.3. Schematic side views of cavities at interface polymer/substrate interface. 1) cavity with circular shape. 2) cavity with ellipsoidal shape and $\theta > 90^\circ$.

If the angle of the cavity and substrate is $\theta > 90^\circ$, then the cavity radius is not uniform and the shape differs from the circular form: the debonding area R_d is larger than the projected radius R_p . For adhesives with dominant viscous component, R_p increase faster than the R_d , which leads to an adhesive type detachment. In the case of $\theta = 180^\circ$, the debonding rate is low, governed by the type of dissipation at the contact line, and results in cohesive failure, leaving residue on the adherent surface.

With adhesive failure, in contrast, the material with a dominant elastic component is able to store higher amounts of energy and detaches without visible residues.

In a recent study, Nase and co-worker [25] created 3D images of the cavitation using a technique based on the Yamaguchi's machine descriptions [26]. They directly observed the air-probe contact angle of poly(dimethylsiloxane) (PDMS) based products and concluded that for viscoelastic solids the contact angle is bigger than 90° , highly crosslinked materials have θ close to 90° and for the weakly crosslinked adhesives no contact between the penetrating air and the probe is observed, which leads to a cohesive failure.

The contact angle between polymer film and substrate is determined by the viscoelastic properties of the polymer film and interfacial characteristic of the substrate, and it governs the failure mechanisms.

2) The second stage is characterized by horizontal growth of pre-existing cavities along the interface between substrate and PSA. An increase in the size of the cavities is accompanied with a radial flow of the polymer surrounding the voids as a result of the minimized pressure near the bubbles during the bulk deformation in tension. When the adhesive has a low viscosity, a Saffman-Taylor instability [27] is observed, characterized by finger-like structures formed by penetration of the outside air into the

polymer bulk. A hydrostatic pressure, higher than the restoring forces from the surface energy, causes this instability.

According to Gent [28] for a neo-Hookean elastic material (incompressible material displaying rubber elasticity), the spherical cavities grow in a highly non-linear way, and the cavities appear and demonstrate unlimited growth when the hydrostatic tension reaches $5/6$ of the value of the elastic modulus E , independent of the defect size. The concentration of the strain in the small volumes of cavities results in an overall reduction of the strain. If the decrease in the strain reaches the critical value near to the value of the elastic modulus E , then the pressure is high and can cause, in some cases, an interfacial rupture.

The radial expansion of cavitation continues until the maximum extension is achieved, which often occurs when the neighbor cavities are reached. The final size of the cavities is controlled by the film thickness, corresponding to the elastic energy, driving the growth process [22].

The second stage of the rupture mechanism is positioned in the area of peak stress on the stress-strain curve and it finished when the cavities achieve such a number and size necessary to reduce the nominal stress. The decrease in the load bearing area is the driving force for cavitation growth, leading to minimizing the pressure in the system. When the cavities achieve their maximum size in the radial direction the vertical extension accompanied by the formation of fibril structures takes place. In some cases, coalescence of the cavities can appear, resulting in rapid and complete detachment of the adhesive from the adherent. The lateral growth of cavities is in competition with the vertical elongation of the walls between them and is governed by the local stress at the cavity edge. The stretching of the fibrils, in contrast, is controlled by the debonding rate during the test [29, 30].

Stage 3) and 4) are part of the second phase of detachment process, namely formation of fibrillation structure and failure or debonding from the probe.

- *Fibrillation and failure*

Fibrils appear from the walls of the maximally expanded cavities being continuously stretched in the tensile direction.

3) The process of separation of two surfaces brought into contact often appears with the formation and elongation of fibrillar structures. Adhesion refers not only to a real density of the interfacial bonds occurring during debonding, but also to the strength of the fibrillar structures formed. The stretching of the fibrils during debonding leads to storage and dissipation of energy. This structure does not appear when the polymer exhibit very low viscosity or is extremely elastic. In the first case, the cohesion forces are too weak and the adhesive flows rather than resisting the strain by building bridges. Due to the high viscosity of the material, in the second case, crack propagation mechanism is observed, which is accompanied by cavity coalescence and fast separation, resulting in low tack energy.

Substrate radius a , film thickness h and radius of crack a_c , as well as the elastic modulus of the adhesive material, debonding velocity and Poisson's ratio control the crack driving force, allowing for the prediction of the fracture mechanism. Crosby and Shull [30] have developed a deformation map using an axisymmetric testing geometry and predicted three distinct deformation modes in order to categorize the early stage of debonding: edge crack propagation, internal crack propagation and cavitation. Creton and co-worker [31] have observed the detachment mechanisms of acrylic adhesive PEHA and block copolymer SIS and described three growth patterns governed by the critical energy of crack propagation and elasticity modulus, offering confirmation to the prediction of fraction by Crosby and Shell:

Edge (bulk) crack propagation

This rupture proceeds by reducing the bond contacts during the separation of a compliant film from a substrate. The main parameters regulating the initial stage of detachment are: the rate of edge crack propagation, the degree of confinement, the elasticity modulus, as well as the relationship between G_{edge} and the velocity (v). Edge crack growth appears for G_{edge} higher than the critical energy release rate G_c . When the elastic component of the material dominates, the critical crack driving force has low values. An internal crack is nucleated of an already existing flat defect at the interface between polymer and substrate. When the defect size exceeds the fraction of critical energy release rate and elastic modulus, nucleated cavities begin to grow, increasing its debonding radius R_d . The expansion of the cavities proceeds mainly at the interface

rather than in the bulk of the adhesive film. The cavities coalesce with their neighbors and rupture appears without a formation of fibril structures. The value of the maximum stress is lower than the value of E , resulting in a reduction in the work of adhesion. The resulting stress-strain curve does not possess the characteristic shoulder denoting fibril expansion and corresponds to stage 3 on Figure 1.3. After reaching the peak, the stress value continuously decreases until it approaches zero.

Interfacial crack propagation

The hydrostatic pressure can lead to the creation of interfacial cracks on a solid substrate. Interfacial crack propagation occurs when G_{cavity} overcomes the critical energy release rate G_c . The nucleated cavities expand spontaneously at a constant rate. The voids grow into the bulk, but G_c is relatively low and the detachment of the cell walls occurs before fibril formation is complete. This mode is characterized by a G_c / E fraction higher than R_d , and results in vertical cavity growth, with an angle $\theta \approx 90^\circ$. The work of adhesion is higher than the value in the edge crack propagation, but is still relative low due to the appearance of cavities at relatively low applied strain. For PSAs, the critical rate depends on the debonding velocity.

The driving force for this pattern is: $G_c = G_l(1 + \varphi(a_T v))$ [32], where G_l is the limiting value energy release rate at low rates and the factor $\varphi(a_T v)$ represents the viscoelasticity.

Cavitation

This mode is controlled by the stress within the layer in contrast to the crack propagation, where the driving force is the energy release rate. Bulk instability occurs when the stress σ overcomes the Young's modulus E : $\sigma > E$. Nonlinear deformation of the material to high strain within the cell walls takes place. Although the high strain, the local energy release rate, acting in individual cavity wall, is relative low. The contact angle in this case is $\theta > 90^\circ$. Competition between elastic extension and adhesive detachment is observed. The horizontal growth of the cavities is inhibited and the walls between the neighbor cavities extend into the fibrils.

As a consequence, depending on its temporal incidence, different growth patterns appear: internal crack propagation if $G_{edge} > G_c$, interfacial crack propagation if $G_{cavity} > G_c$ or cavitation if $\sigma > E$.

The cavitation is preferential for soft material with a low elastic modulus E , with high film confinement a/h and for strong adhesive bonds at the contact interface polymer/substrate (high G_c) [30].

4) Rupture stage. The detachment of an adhesive from a substrate surface proceeds with the propagation of cracks or with fibril formation. With stretching of the orientated polymer chains, the stress increases causing instability followed by a fibril fracture and appearance cohesive debonding. Polymers exhibit high cohesive strain detachment at the end of the fibrils, which is adhered to the substrate. This detachment is known as adhesion debonding process.

1.2.3. Parameters of tack test.

- *Work of adhesion*

The measured tack energy W can be several orders of magnitude larger than the thermodynamic work of adhesive W_a : $W = W_a(1 + \Phi)$, where Φ is determined by the rheological properties of the polymer [33-36]. Tack energy is a product of two terms: thermodynamic work of adhesion and a viscoelastic function of temperature and debonding rate due to the expended energy in the adhesive [37]. A higher amount of adhesive energy is an indicator for the important role of the viscoelasticity in the adhesion process. The quantity of tack is considered to be the dissipated energy (in J) by separation of unit area (in m^2).

$$W = \frac{1}{A} \int F v_{deb} dt \quad [J/m^2] \quad (1.2)$$

where A is contact area (the area to be separated) measured in m^2 ; F is tensile force during debonding (N) and v is rate of separation (mm/s).

This parameter characterized the properties of the polymer for evaluation of their performance as adhesives.

- *Stress-strain curves*

Typical stress-strain curves are displayed in (Figure 1.2). Work of adhesion is the integral of the stress-strain curves (eq. 1.2), the nominal stress is the ratio of the applied force and the contact areas (eq. 1.3) and the elongation is for displacement normalized to the initial film thickness (eq. 1.4):

$$\sigma = \frac{F}{A} \quad [\text{Pa}] \quad (1.3)$$

$$\varepsilon = \frac{h - h_0}{h_0} \quad (1.4)$$

Three more parameters are essential for the characterization of the adhesion performance: maximum nominal stress in the area of the curve's peak, deformation at break and height of the shoulder.

1.3. Physical characteristics of polymers and parameters influence the adhesion.

The adhesion of the PSAs depends on the viscoelastic properties of the adhesive material and the interfacial parameters that characterize the substrate surface. Both govern the wetting process. Variation of the chain size, the density of entanglement (during crosslinking) or the incorporation of monomers with polar functional groups allows for tailoring the polymers' cohesive strength and its possibility to deform thereby resisting high stress. The roughness and the low surface energy of the substrates strongly influence the number of formed cavities, inhibiting the wetting of adhesive materials on substrate surfaces. A crucial point in investigations of the PSA adhesion is gaining control over the bulk and interface parameters in order to increase the value of the maximal stress, which is responsible for failure resistance and to

facilitate cavity nucleation, ensuring fibril stability, and increasing the dissipation of energy. Proper monomer choice in the polymer chains is the basic step to achieve the desired adhesive properties, which one material has to exhibit, in order to be able to join two surfaces together.

1.3.1. Molecular composition of PSAs.

Acrylic PSAs consist of a major monomer 5 - 80%, modifying monomer 10 - 40%, and 2 - 20% of a monomer with the desired functional groups [38]. The monomer selection within the polymer composition is based on different types and amounts of the comonomers with proper glass transition temperatures (T_g). The acrylate adhesives [39] have a chemical composition in the PSAs formulations as follows:

- *Major monomer*

The typically content of PSAs consists of more than 50% major monomer, which exhibits a low T_g and guarantees softness and flexibility, crucial properties for reaching complete contact with the adherent. Acrylic ester of $C_4 - C_8$ alcohol, possess the required low glass transition temperature of around -50°C . 2-ethylhexyl acrylate (EHA) and n-butyl acrylate (BA) are typical acrylic monomers used in industry as major component. However, as homopolymers they do not exhibit high enough cohesive strength to ensure good adhesion properties.

- *Modifying monomer*

The essential cohesion strength necessary for sustaining a shear stress during the rupture is gained by incorporating a modifying monomer with higher T_g . Typically acrylic homopolymers with a T_g over 0°C and sufficient strength are methyl acrylate (MA) and methyl methacrylate (MMA). Major and modifying monomers are often copolymerized in order to obtain the desired viscoelastic properties. Their quantity in the formulation is varied according to the polymer's end purpose.

- *Monomer with desired functional groups*

Incorporating monomers with polar functional groups, such as acrylic acid (AA) or hydroxy ethylacrylate (HEA), into polymer chains leads to the formation of additional H-bonds in the bulk and results in an increase in the cohesion. An orientation of the polar functional groups into bulk, in an opposite direction to the surface, can be observed when an acrylic polymer film is exposed to air. In contrast, when the polymer film comes into contact with a polar surface for a long period of time the monomers with polar groups move in the direction of the interface [39].

1.3.2. Influence of the bulk parameters: physical characteristic of polymers.

The physical characteristics of the polymers, as well as the chemical composition play an important role in the adhesive process. These parameters and their influence on the adhesive process have been exhaustively investigated and are listed below:

- *Glass transition temperature: T_g*

The influence of the glass transition temperature, molecular weight and polydispersity was studied in considerable detail before [14, 40, 41]. T_g is the most important characteristic of adhesion properties of various adhesives. It can be determined from dynamic mechanical analysis and usually it is defined as the temperature at which G'' goes through a maximum. The glass transition temperature of the PSAs has to be below -10°C [42], well below the temperature of bond formation. The requirement for good adhesive properties is a T_g of 50°C to 70°C below the temperature of application [43]. A lower T_g , relative to the test temperature, leads to higher chain mobility and relatively small dissipative losses. Higher T_g , near to the temperature of bonding, the polymer wettability and prevents complete contact. The comprehensive measurements support, for most pressure sensitive adhesives, the relationship between T_g and adhesive properties.

The bulk polymer properties, are controlled mostly by the molecular parameters, such as the weight average M_w , number average M_n , polydispersity, characteristic distribution M_w/M_n , average molecular weight between entanglements M_e and the degree of branching.

- *Molecule weight M_w and number average M_n*

Pressure sensitive adhesives exhibit broad molecular weight distributions and relaxation times, as well as relative narrow ranges of tackiness. Increasing the molecular weight impedes the orientation of the chains in the direction of tension, increasing the cohesion. The main advantage of short chain polymers is their improved wetting properties. Long chains make entanglements resulting in an increase in the cohesive strength, whereas the short chains have high mobility and promote wetting on the substrate [14]. An increase in the M_n results in an increase in the polymer viscosity and the relaxation time [13], which leads to higher dissipated energy.

- *Molecular weight between entanglements: M_e*

The molecular weight between entanglements controls the elastic modulus in the plateau region: $M_e = \rho RT / G_0$, where G_0 is the plateau modulus and can be measured with dynamic mechanical analysis (DMA). Plateau modulus of polymers should not overcome $G_0 = 3.3 \times 10^5$ Pa (Dahlquist criteria), otherwise the material is not able to completely wet the substrate surface and build fibril structures.

In order to form fibrils, the molecular weight between entanglements has to be high. Lack of fibrillation is observed by low M_e materials, which can cause crack propagation [11].

- *Molecular weight between crosslinks: M_c*

PSAs used in industry are crosslinked in order to reduce the maximal elongation required to remove from the substrate without leaving a residue. The degree of crosslinking influences the adhesion properties. Low values for M_c imply high density of the crosslinks and leads to prevention of a fibril formation. An important molecular parameter that influences the adhesion is the degree of crosslinking, and it has a strong influence on the viscoelastic properties of polymers. The adhesive performance of crosslinkable PSAs can be extensively varied, with more densely crosslinked PSAs showing cohesive behavior while slightly crosslinked PSAs are tacky [8, 44]. One of the most preferable methods, recently applied to crosslinking PSA films, is UV technology. Its advantage is that varying the degree of crosslinking by changing the UV dose

enables the manufacture of adhesives with different properties from the single raw material. In [45] it was shown that the work of adhesion reaches its maximum for a degree of crosslinking slightly above the gel point ($G' \approx G''$). With increasing crosslink density, ultimate strain decreases while the stress peak and the height of the plateau remain approximately constant [46]. Fibril formation and ε_{\max} are characterized from the ratio M_c/M_e . A reduction in the value of M_c/M_e results in a decrease in the ε_{\max} . The slight crosslinking is beneficial for the fibril stability, while excessive crosslinking causes premature failure and a reduction in the amount of dissipated energy. The adhesion performance of UV-crosslinkable acrylic PSAs was studied in [47, 48] and it was found that by using high UV doses, the resulting tack and peel resistance are significantly reduced.

- *Polarity of monomers*

Changes in the monomer composition often change both the bulk and surface properties and, accordingly, the adhesion performance of the PSA. Monomers with polar functional groups incorporated into the polymer chains can affect the surface tension and the bulk dynamics of the film. Additional H-bonds appear between the polymer polar groups and increase the cohesion and dissipated energy. Although, there were several studies on the influence of the monomer composition on the viscoelastic and adhesive properties of PSAs [49, 50], it is often difficult to interpret the obtained results. The difficulties arise because changes in monomer composition lead, for example, to variations in the gel fraction and molecular weight distribution and, consequently, changes in the properties of PSA.

Aubrey et al. [7] attempted to separate the bulk and interfacial effects of acrylic acid on the adhesion of PnBA poly-(n-butyl acrylate) by selective carboxylation of the bulk only or the surface only in order to discriminate between bond enhancement by an interfacial effect (presumed to involve interfacial hydrogen bonding) and that by a bulk effect (change in viscoelastic response resulting from carboxylation). It was shown that the presence of 10% weight of acrylic acid in the polymer appears to increase the thermodynamic work of adhesion by a factor of about 1.5. The authors observed a cohesive rupture during a long time of contact peel test, despite that the AA content in the polymer chains increases the interfacial interactions due to the slow migration of

the polar AA comonomer to the interface with the polar substrate. The additional H-bonds work like physical crosslinks. One can distinguish the different influences of the incorporated monomer, due to its nature, the degree of polarity and amount in the formulation. The monomer variation allows for a control of the adhesion properties.

With the addition of AA in polymer, a transition from cohesion to adhesion mechanism of debonding appears due to the increased cohesion forces [51].

Some early studies investigated the influence of comonomer composition/polarity on the adhesion performance of PSAs [49, 50, 51-54].

The adhesion on the steel substrate of the series of non-polar acrylic copolymers, based on 2-ethyl hexyl acrylate (EHA), and polar acrylic copolymers, based on ethyl acrylate (EA), were studied in [52]. In the case of non-polar copolymers, an increase in the EHA content makes copolymers softer and the tack increases. The adhesive values are also closely related to the glass transition temperature of the adhesive. On the other hand, incorporating a small amount of polar comonomer, such as: acrylic acid (AA), methacrylic acid (MAA), hydroxy ethylacrylate (HEA) or acrylonitrile (AN), increases tack. Acid groups have the greatest effect and tack reaches its maximum values at 3-4 mole% either AA or MAA. The authors explain this variation in terms of a competition between improved interfacial bonding due to the polar groups and a reduction in the deformability due to the increase of the shear modulus with increasing content of acid groups.

The effect of varied monomer composition on adhesion of acrylate copolymer with constant T_g and AA content was studied in [49], where it was shown that the tack was constant through all compositions. In this case, tack seems to be determined by T_g or softness of the copolymers, and the constant polar AA concentration.

In [50] the same authors studied the influence of the incorporation of methyl methacrylate (MMA) and styrene (S) comonomer on the adhesion of acrylate PSAs. The incorporation of S decreases, and the incorporation of MMA increases tack values. Another experimental study [53] revealed that incorporating AA in PnBA leads to an increase in the long relaxation times of the polymer and to a significant (60%) increase in adhesion to glassy substrates.

In [51] it has been reported that AA groups have a substantial effect on the large-strain extensional properties of PnBA and cause a change in the characteristic debonding rate at which the transition from cohesive to adhesive failure is observed.

A systematic study on the adhesive and rheological properties, as well as the debonding mechanism of slightly crosslinked acrylic networks based on EHA [54] showed that the addition of polar comonomer (AA) increases both the elastic modulus and the resistance to interfacial crack propagation. The increase in the latter, with increasing AA content, is the dominant effect at low debonding rates/high temperatures, whereas the increase in the elastic modulus becomes predominant at high rates/low temperatures. The addition of a nonpolar comonomer, for example StA (stearyl acrylate), reduces both the small strain modulus of the acrylic network and its resistance to interfacial crack propagation. The decrease in crack propagation with increasing StA content is the principal effect at room temperature and at high rates/low temperatures.

1.3.3. Influence of the interfacial parameters: effect on the wetting process.

Bond formation is influenced by the following parameters:

- magnitude of the applied force and the duration of this contact;
- roughness and tension of polymer film and substrate;
- chemical composition and properties of the adhesive film and substrate.

Reaching a complete contact, is less likely with a higher elastic modulus of the adhesive, high probe roughness or when no external force is applied to the system, as well as with a lack of viscous flow, which can be caused by a high degree of crosslinking [55-57].

The wetting process markedly influences the number of nucleated cavities and the corresponding maximal stress σ_{\max} . Furthermore, the appearance of cavities leads to decreasing nominal stress after the stress maximum is reached.

- *Surface roughness*

Although PSAs are designed to stick to any surfaces and are supposed to be practically insensitive to the surface of adherent, interface properties can alter the adhesion of

PSAs. The average roughness, both of the polymer film and the substrate, influences the process of adhesion, mostly by preventing a complete contact from being reached. Completely smooth polymer surfaces are rarely achieved. Generally, the polymer film covers a much larger lateral dimension than the roughness of the substrate surface. Cavitation occurs near the interface between the probe and the film and it is reasonable to suggest that the roughness of the surface, either of the adhesive film or of the probe, can be an important parameter that affects the adhesion of PSAs.

Roughness of the polymer film

Film surface structures are able to change the values of the dissipated energy and the adhesion forces. Dimitrova et al. [58] have measured the work of adhesion for acrylic PSAs with different contents of nanoparticles. The granular surface structure of polymer film, with higher particle fractions, shows an increase in the tack. Chiche and co-workers have investigated the effect of the roughness using blends such as SIS triblock copolymer and a hydrogenated resin that is miscible with isoprene, on the cavity size and growth rate [59]. They observed qualitative differences between the rough and smooth adhesive surface, where the smooth substrates roughness was measured as $R_a = 10$ nm. On the rough interfaces, where the existence of craters on the surface of the adhesive film is observed, the cavities appear from the initial defects and grow with identical speed, and are a similar size at any given time. In the case of smooth interfaces, the cavity growth rate depends on the time of cavity appearance.

Roughness of the substrate

In an early study, Zosel [60] pointed out that the work of adhesion or fracture energy significantly depends on the probe surface roughness as long as the contact area is incompletely wetted, which is generally the case for low contact forces, short contact times, and high polymer moduli. A limiting value for the work of adhesion was found only at contact times longer than the disentanglement time of the polymer. Persson and Tosatti [61] have discussed theoretically the influence of random rough surfaces of elastic solids on different length scales with full contact. They concluded that a partial detachment transition precedes the full detachment. The effect of the surface roughness on the adhesion of the viscoelastic materials (PSAs) has also been discussed

theoretically [62-64] and it was proposed that the adhesion on the rough surface is limited due to the absence of full surface contact. The model of Creton and Leibler [62] predicts that the true contact area and, hence, the work of adhesion are proportional to the reciprocal of the elastic modulus E of the polymer. In an experimental study [65] on SIS triblock copolymers with steel probes of two different roughnesses $< 1 \mu\text{m}$, it was found that the number of cavities formed during debonding strongly increases with increasing roughness. At low temperatures, the polymer mobility is low and the time of contact not sufficient to fill all the cavities and tack decreases with increasing roughness. At high temperatures, when the wetting is complete, the opposite behavior is observed. Results of a systematic study investigating the role of the surface roughness on the adhesion of model acrylic latex are reported in [66]. It was found that extensive cavitation influences the maximum of the nominal stress, and this stress peak decreases with increasing roughness. Furthermore, the authors claim that the rate of cavity expansion corresponds to the slope of the stress vs. strain curves, which decreases as roughness increases.

A characteristic difference between cavitation and cavity growth on smooth and rough surfaces was pointed out in [59]. On a rough surface, cavitation starts from existing contact defects and all cavities grow simultaneously at a similar rate, while on a smooth substrate, cavities occur sequentially and their growth rate increases with the increasing stress level at which they are formed.

The possibility of reaching complete contact between a polymer film and a rough substrate is limited by asperities. These asperities are responsible for the creation of an inhomogeneous strain field around their peaks with consequential points of residual tensile stress, which act as germs for cavity nucleation, as indicated in Figure 1.4.

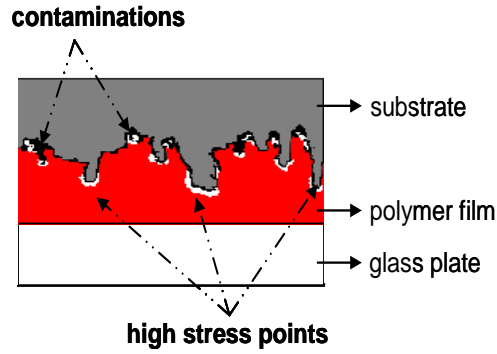


Figure 1.4. Schematic side view of rough substrate. Air bubbles trapped between the substrate and polymer during the contact are nucleated from the contaminations in the holes and the high stress regions of the asperities [67].

The existence of contaminations, such as small particles, usually dust, between the asperities on the substrate surface, facilitates the detachment due to a transformation from polymer/substrate into particle/substrate adhesion. Air pockets, caused by a residual stress, appear around the asperities. The detachment proceeds at the polymer/air interface. New interfaces build as polymer/voids and polymer/weak cohesive dust reduces the adhesive bond strength below the theoretical strength. In [62] was reported that the area of contact A is inversely proportional to the elastic modulus E , proportional to the applied pressure P , and can be represented as: $A \approx P(R/\sigma)^{1/2} / E$, where R is constant radius of asperity curvature. The full wetting of the adherent surface under very low applied pressure is highly reduced with the addition of larger asperities. Zosel [60] observed for polyisobutylene (PIB) and polybutylacrylate (PBA) that after complete wetting on both smooth and rough surfaces, tack energy became insensitive to the applied pressure.

- *Surface energy*

Surface tension, or surface energy, is the stress at the surface of liquids and solids that works to minimize the area in order to achieve a lower energy level. The free surface energy is measured in mJ/cm^2 and is the mechanical work required to increase the surface area by 1 cm^2 . The molecules, at the interface between two systems in contact, have higher potential energy compared to molecules in the bulk. The anisotropy of forces among the molecules at the interface is the dominant microscopic origin of the surface energy.

Polymer surface energy

The average chemical composition at the surface, in some solid polymers, can be distinguished from the bulk. The composition of the polymer film perpendicular to the substrate plane has been investigated by M.B. and co-workers [68] and was found to change with time. The investigated statistical copolymers are with composition sticky component: 90% ethylhexyl acrylate (EHA) and variation 10% of glassy component: styrene (S), maleic acid (MAA) or methylmethy acrylate (MMA). For a given solvent, due to the solubility effects in the fresh sample, either the sticky or the glassy component of the statistical copolymers enriches at the surface irrespective of the majority component. The system minimizes its surface energy during this internal reorganization process, in a way the polymer with the lowest surface energy enriches at the interface [68]. Additionally, the near-surface composition profile of P (80EHA-stat-20MMA) was tuned by exposing the samples to atmospheres with different relative humidity (RH) [69]. The content of the more polar component (MMA) close to the surface increases with increasing RH. However, the measurements show no change in the surface tension with sample aging or with increasing RH.

Substrate surface energy

In some earlier studies [3, 31, 70, 71] the effect of the substrate surface energy on the adhesion of PSAs was investigated. In [70, 71] it was shown that maximum tack is achieved with adherents whose surface tensions are slightly higher than that of the adhesive. Good wetting of the adherent by the adhesive is also very important for high tack, which is satisfied if the adherent has a higher surface tension than the adhesive [3]. In [31] the adhesion of commercial SIS block copolymers on steel and hydrophobically modified steel substrates were studied. The surface properties were described by a critical energy release rate. This interfacial parameter influences the value of the adhesion energy as well as the mechanisms of debonding. In the recent studies [72- 76] the adhesion of various PSAs on low-energy surfaces, such as PE, PP and polytetrafluorethylen (PTFE), was compared to the adhesion on the high-energy surface of steel, traditionally used for the adhesion tests. There have been attempts to study the influence of the composition of PSAs on their adhesive performance on the

low-energy surfaces and to synthesize PSAs with good adhesion. In [70] and [71] the relationship between wetting and adhesion of PSA was investigated using substrates with different surface energy. The adhesion forces were found to depend on the critical value of the surface energy, γ_c , of the substrate, which was determined graphically from the plot of $\cos \theta$ vs. surface tension of aqueous solution of dipropylene glycol. The measured tack increased with increasing the critical surface energy of the substrate until it reached a maximum value of γ_c about 33 - 39 mJ/m² and drop. Agirre et al. in [72] have improved the compatibility between the adhesive and low energy substrates, in particular for non-treated polypropylene (NTPP) and PTFE, by introduction of stearyl acrylate (SA) in the polymer backbone. Furthermore, the presence of SA in the polymer composition reduced the peel strength on more energetic surfaces as treated polypropylene (TPP). The adhesion properties of bilayer films made from acrylic solutions (one layer being more cohesive and the other more dissipative) have been investigated and reported in reference [74]. The authors carried out a probe tack test in order to understand the mechanisms that determine the bulk and the interfacial contributions to the debonding. It was observed that the presence of a composition gradient enhanced the adhesive properties, particularly on a low-energy surface such as PE. On steel, the presence of a more elastic adhesive in contact with the substrate can transform the fracture from cohesive to adhesive.

1.4. Mechanical characteristics of polymers: Rheology.

The abovementioned interfacial effects that influence the adhesion of PSAs by affecting the wetting process cannot be reliably analyzed without taking into account the superposing influence of the rheological properties. The energy release rate at the edge of the expanding cavities is proportional to the elastic modulus: G' (for a given strain). The viscoelastic properties have been exhaustively reviewed in references [54, 74, 77-80] and in various other works.

1.4.1. Relaxation time. Effect of bonding time on the tack properties.

The viscoelastic properties of PSAs are very important during the compression for bond formation as well as during the deformation stage for debonding. Mechanical and rheological properties show time dependence. The Deborah number characterizes the materials and refers to the ratio of the stress relaxation time and the observations time. De can either be varied by changing the temperatures or the time of observation [42].

For PSAs, the Deborah number is defined as: $De = \frac{\tau_r v_{deb}}{h_0}$, where v_{deb} / h_0 is the initial macroscopic strain rate (the ratio of substrate velocity v_{deb} and initial film thickness (h_0)), and τ_r is the relaxation time of the adhesive. High values of De are an indicator for primarily elastic behavior of a PSA, at low values a relaxation of the stress takes place. The smaller the Deborah number, the more fluid the material appears in certain process [81].

Although, the relaxation time in linear viscoelastic region is insensitive to the observation time, storage G' and loss G'' moduli depend on both relaxation and observation time. Shorter relaxation time results in an increase in the values of the viscoelastic modules.

1.4.2. Principles of Rheology. Oscillatory test.

Rheology is the science of deformation and flow of matter. Some materials act as solids and others as liquids. Materials, that possess characteristics of both a solid and a liquid, are called viscoelastic. Viscoelastic fluids are solid-like at high frequencies, and begin to flow at significant low frequencies or long times, respectively. Pressure sensitive adhesives are part of this group. The ability of the PSA to flow and wet the substrate, increasing this way the area of the contact is related to its viscoelastic properties, which can be determined from rheological measurements. Small amplitude oscillatory shear tests are frequently used to characterize the linear viscoelastic properties of fluids. When applying small angle sinusoidal strain γ to a system, it responds with a stress τ , which is also sinusoidal and has the same frequency as long as the deformation is in the linear regime.

$$\gamma = \gamma_0 \sin(\omega t) \quad (1.5)$$

, where γ_0 is the deformation amplitude (maximal deformation), ω - is the angular frequency.

The response of the deformation is measured and for the linear viscoelastic region (LVE) have the same frequency $2\pi f$ as the deformation input excitation, but with phase shift δ .

$$\tau = \tau_0 \sin(\omega t + \delta) \quad (1.6)$$

, where τ_0 is the stress amplitude.

By the sinusoidal oscillation the phase difference between stress and strain is the phase angle δ [rad]. The phase angle in case of pure viscose materials is $\delta = 90^\circ$, while in pure elastic is $\delta = 0^\circ$.

The storage modulus G' characterizes the elasticity and stiffness of viscoelastic material and is proportional to the deformation energy stored during one load cycle:

$$G' = \left(\frac{\tau_0}{\gamma_0}\right) \cdot \cos \delta \quad [\text{Pa}] \quad (1.7)$$

The viscous properties are presented by the loss modulus G'' , which is proportional to the amount of energy irreversibly dissipated during a load cycle.

$$G'' = \left(\frac{\tau_0}{\gamma_0}\right) \cdot \sin \delta \quad [\text{Pa}] \quad (1.8)$$

The relationship between the stored and dissipated energy is represented during the dimensionless number - los factor:

$$\tan \delta = \frac{G''}{G'} \quad (1.9)$$

- *Amplitude-sweep*

During the amplitude sweep, the strain amplitude is varied and frequency is kept constant. The measured storage and loss moduli are plotted versus deformation, as shown in Figure 1.5. The region at low deformation, where the moduli have constant values is the linear viscoelastic regime, characterized with no change in the structure of the material. The frequency dependence of the linear viscoelastic material parameters G' and G'' provides valuable information about the application properties of PSAs. Prior to the variation of frequency one has to determine the linear viscoelastic regime (LVE), i.e. the range of deformation and stress amplitudes for which the material responds linearly to the applied strain or stress.

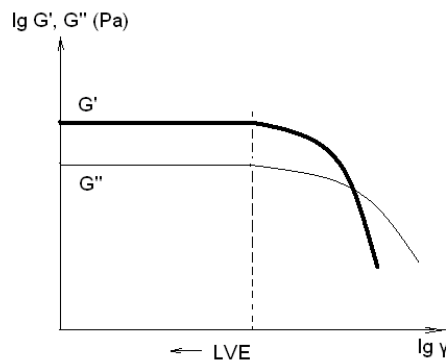


Figure 1.5. Viscoelastic moduli (storage modulus G' and loss modulus G'') as a function of the deformation in log - scale. LVE is a linear viscoelastic region.

- *Frequency-sweep*

During the frequency test the frequency is varied, while the amplitude is kept constant. The low frequency range corresponds to long term behavior of the tested materials, the molecules have enough time to relax which leads to predominating viscous behavior. At high frequency elastic behavior dominates over the viscous due to the short time for molecular reorganization.

The devices used to examine the rheological properties of the fluids are mechanically limited. Very high and very low frequency is not able to be measured by varying the frequency. The accessible frequency range of conventional rotational rheometers is limited (typically 10^{-3} rad/s - 10^2 rad/s) but for many polymeric materials the

accessible frequency range can be expanding using time-temperature superposition (TTS).

1.4.3. Time-Temperature Superposition (TTS).

Time-temperature superposition principle is based on the idea that during the deformation of the polymer the change in the deformation rate correlates to the change in temperature. TTS is used not only in linear rheology, but also in large deformation, what is, for example, the case of probe tack test [82].

In order to characterize completely the mechanical behavior for some viscoelastic materials, a large frequency range is required. However, the standard rheological devices work usually in narrow frequency ranges, 3 to 4 decades. To get the needed information about the behavior in lower and higher frequency, one can measure the sample at different temperatures and then shift the obtained curves along the frequency axis to one reference temperature. The temperature strongly influences the chain mobility and with increasing the temperature the mobility of the polymer chains increases. The influence of the temperature variation on the molecules motion is identical with the effect of time variation. However, measurements by extremely low frequency are hard to maintain. With shifting the data measured at different temperatures (Figure 1.6) horizontally along the time axis results in a so-called master curve representing the linear viscoelastic properties of a material in a wide frequency range.

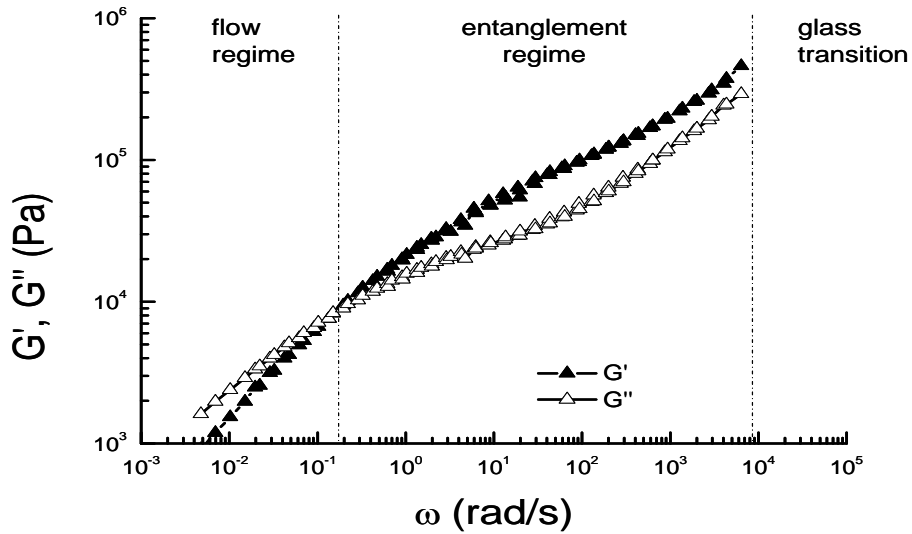


Figure 1.6. Master curve (G' - storage modulus and G'' - loss modulus) for MA/BA with $M_w=600$ kg/mol, measured between 0° and 70°C and shifted to reference temperature $T_{ref}=23^\circ$.

The shift factors a_T given by the universal equation of the William - Landel - Ferry [82].

$$\log a_T = \frac{-C_1(T - T_{ref})}{C_2 + T - T_{ref}} \quad (1.10)$$

, where T = temperature during the experiment, T_{ref} = reference temperature and C_1, C_2 = material constants. Generally T_{ref} is chosen to be about 50°C above T_g . Generally, TTS can be applied as long as no structural change or phase transition occurs within the investigated temperature range.

Curves, recorded for each temperature, are shifted to the reference temperature. At temperature below the reference the segments are shift to the left corresponding to the higher frequency and at higher as the reference temperature/low frequency - to the right.

1.4.4. Elongational viscosity.

Elongational viscosity of polymers has been studied earlier in [83, 84]. Problems often appear by preparations for extensional measurements of high viscosity fluids as reported in [85]. Münsted and Laun, found a possible correlations between the shape

of extensional flow curves and the molecular weight distribution for low density polyethylene (LDPE) [86]. Extensional experiments of low viscosity polymer fluids faces some other difficulties: it is hard to provide a well-defined flow kinematics during the measurements, often different fluid elements experience different deformations, therefore the obtained data depend on the used measurement method [87, 88]. It is also difficult to hold a sample of low viscosity polymer in such way that slow elongation and steady value of stress are achieved.

Rheological measurements can be performed on a SER (universal testing platform), which can be mounted on a commercial torsional rheometer systems. SER consists of two oppositely moved drums. During the rotation of the drums, the sample is stretched over an unsupported gap.

For a constant drive rotation rate, a constant Hencky stain rate $\dot{\epsilon}_H = 1/L(dL/dt)$ (where L is the length of the sample) is applied to the sample specimen. The resistance to elongation results in a tangential force $F(t)$, acting on both moving drums. The cross-section area $A(t)$ of elongated sample, decreases exponentially with time (for constant Hencky strain rate experiments). The tensile stress growth function, $\eta_E^+(t)$, of the stretched specimen, for constant Hencky strain rate, can be expressed as [89]:

$$\eta_E^+(t) = \frac{F(t)}{\dot{\epsilon}_H A(t)} \quad (1.11)$$

1.4.5. Surface chemical principles. Contact angle and surface energy.

The basic parameter for characterization of the spreading behavior of liquid wetting a solid is the contact angle Fig. 1.7.

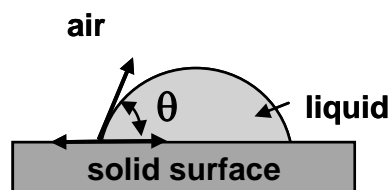


Figure 1.7. Contact angle of a liquid sample

The Young equation, relates the contact angle θ to the surface tension between solid and vapor (air) γ_{SV} , the surface tension between solid and liquid γ_{SL} , and surface tension of the liquid in equilibrium with vapor γ_{LV} :

$$\cos \theta = \frac{\gamma_{SV} - \gamma_{SL}}{\gamma_{LV}} \quad (1.12)$$

The difference between surface energy substrate/vapor and substrate/liquid is the static adhesion force.

Systematic studies of the contact angle [90-92] were starting point for extensive studies on wetting phenomena. According to Zisman, contact measurements affect the chemical composition of the solid surface. Langmuir [93] reported that the range of the acting forces acting on the non-polar solid are of order of a few nanometers.

The surface non-uniformity as chemical heterogeneity and surface roughness, affect contact angle measurements. In the analysis of contact angle hysteresis, Shuttleworth and Bailey [94] concluded that for very rough surfaces and high contact angles contact can be establish on the top of the asperities without the liquid to penetrate, and a minimum energy state may not appear but could exist a metastable state. With increasing the roughness, the contact advancing angle increases, which prevent the establishing of a complete contact.

The wetting process is influenced by the polarity of the acting forces between the molecules and atoms of the system in contact. Polar forces exist between dipoles and hydrogen bridges, while dispersions forces are counted among non-polar component. Interfacial energy can be presented as sum of a polar and a disperse part:

$$\gamma_{SL} = \gamma_{SL}^p + \gamma_{SL}^d \quad (1.13)$$

$$\gamma_{VL} = \gamma_{VL}^p + \gamma_{VL}^d \quad (1.14)$$

If non-polar systems are brought in contact, the value of the interface energy consists only of contribution of non-polar part, while the polar part is zero. However, if polar systems (with high or low polarity) interact, the value of interfacial energy is separated between the polar and non-polar part. In reference [3] it was reported that the adhesion

work is high when the surface energy of the substrate is higher than the surface energy of the adhesive. This assumption does not work for example for polyethylene melts, which possess low surface energy, wet well the high energy steel, but this interaction result in low work of adhesion, due to the lack of dipole molecules.

The interfacial energy can be calculated by using of test liquids for experimental definition of the contact angle. Most common way to determine γ_{sl} for metals seems to be the so-called sessile drop method [95].

2. Materials and methods

2.1. Materials

The PSAs used in this study are model statistical acrylic copolymers with different composition. The model copolymers p(nBA-stat-MA), p(nBA-stat-MA-stat-HEA), p(nBA-stat-MA-stat-MMA) and p(nBA-stat-MA-stat-AA) were synthesized in BASF SE in Ludwigshafen via radical solution polymerization in a semi-batch procedure at 80°C in methyl ethylketone (MEK), for the low and intermediate molecular weight samples, or in n-butyl-acetate, for the high molecular weight sample, with 80% solids-content and a peroxide starter.

For additional investigations of surface enrichment additional systems were used.

The additional model copolymers were synthesized in BASF SE in semi-batch procedure in iso-butanol at 100°C and 70% solids content with a peroxide starter. The molecular weight of the model copolymer were following: $M_w = 182$ kg/mol for EHA/S, $M_w = 187$ kg/mol for EHA/MAA, $M_w = 165$ kg/mol for EHA/MMA and additionally, 80% EHA and 10% MMA with $M_w = 248$ kg/mol.

Molar mass distribution of studied polymers M_w and their polydispersity M_w/M_n were determined with Size Exclusion Chromatography (SEC), a widely used method for polymer characterization. The measurements were performed at BASF SE (see Fig. 2.1.).

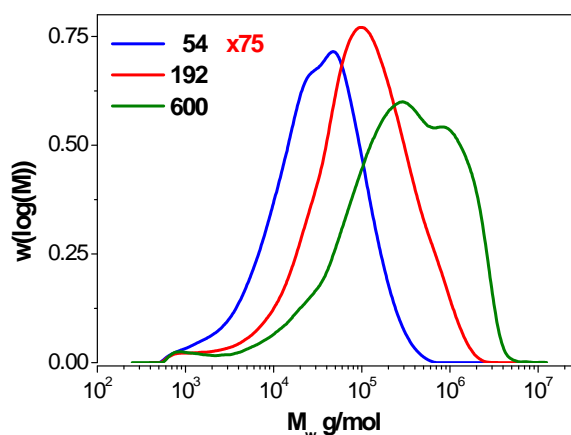


Figure 2.1. Molar mass distribution measured (SEC data) for BA/MA with three different molecular weights. The $w(\log(M))$ is multiply $\times 75$ for the lowest M_w to allow the presentation of all M_w in the same diagram.

The SEC method is based on the fact, that the hydrodynamic volume of the dissolved polymers determines its transition through porous beads. From the data shown in Fig. 2.1 the number average molecular weight $M_n = \sum n_i M_i / \sum n_i$ has been determined, as well as the weight average molecular weight $M_w = \sum n_i M_i^2 / \sum n_i M_i$ and the polydispersity index $PDI = M_w/M_n$. PDI typically exhibit values of 1 and higher, and if PDI approaches 1, the polymer chains approach uniform length. Characteristic features of studied copolymers are given in Table 1. All samples show broad molar mass distributions.

Table 2.1. Model copolymers.

Composition	Ratio*	M_w (kg/mol)	M_w/M_n	Supplied as
BA/MA	79.7/20	54	3.9	71% solution in MEK
BA/MA	79.7/20	192	6.4	80% solution in MEK
BA/MA	79.7/20	600	13.6	49.4% solution in n-butyl-acetate
BA/MA/HEA	79.7/15/5	193	6.7	80.6% solution in MEK
BA/MA/MMA	79.7/10/10	195	7.0	65% solution in MEK
BA/MA/AA	79.7/15/5	191	7.0	80% solution in MEK

BA = butyl acrylate, MA = methyl acrylate, AA = acrylic acid, MMA = methyl methacrylate, HEA = hydroxy ethylacrylate, MEK = methyl ethylketone.

* All copolymers contained 0.3% of photoinitiator

The molecular structures of monomers are shown in Fig. 2.2 and Fig. 2.3.

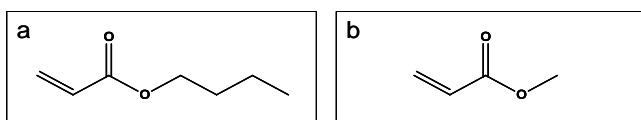


Figure 2.2. Molecular structures: a) BA; b) MA.

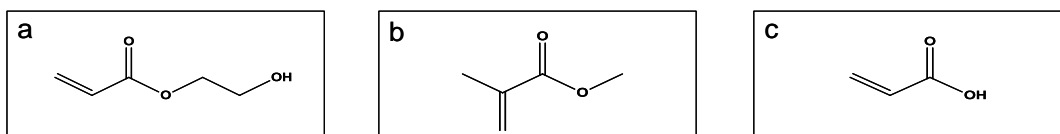


Figure 2.3. Molecular structures: a) HEA; b) MMA; c) AA.

Glass transition temperature T_g can be calculated from the Fox equation:

$$\frac{1}{T_g} = \sum_{i=1}^n \frac{W_i}{T_{g,i}} \quad (2.1)$$

where W_i is the weight fraction of monomer species i . T_g of investigated polymers were measured using differential scanning calorimetry (DSC) and the results are given in Table 2.2.

Table 2.2. Glass transition temperature of BA/MA; BA/MA/HEA; BA/MA/MMA and BA/MA/AA, measured using differential scanning calorimetry (DSC 30 from Mettler).

Composition	T_g
BA/MA	- 43.8
BA/MA/HEA	- 40.7
BA/MA/MMA	- 37.8
BA/MA/AA	- 36.4

- *Materials used in the probe tack test*

Transparent glass plates (200×50×3 mm) were purchased from Hera Glas GmbH, Germany, abrasive papers (Bühler GmbH, Germany), and the acetone was purchased from Carl Roth GmbH + Co. KG, Germany. The probes used for the tack measurements were flat-ended cylinders with a diameter of 5 mm made of stainless steel, type 1.4034 (Eisen Schmitt GmbH & Co. KG, Germany), glass (Hera Glas GmbH, Germany), transparent low density polyethylene LD-PE (Fritz Bossert, Germany) and silicone Si-Wafer (SiTec, Germany).

2.2. Methods

2.2.1. Measurement of shear modulus

Rheological measurements were performed on a rotational rheometer RS-150 (ThermoHaake GmbH, Germany) using cone and plate fixtures with cone diameter of

20 mm and cone angle $\alpha = 1^\circ$. The schematic of cone plate geometry is shown on Fig. 2.4.

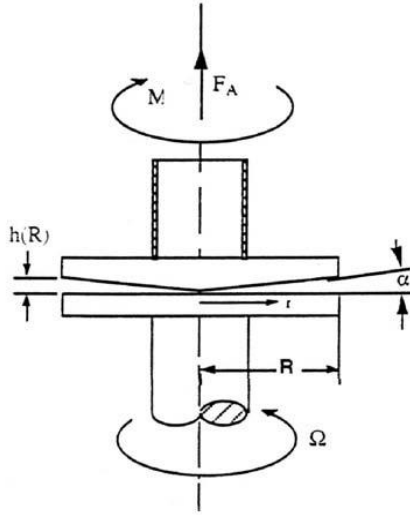


Figure 2.4. Schematic of cone-plate rheometer. R - cone radius; M - moment of force; α - cone angle; Ω - angular velocity; $h(R)$ - gap; r - distance; F_A - force.

The polymer sample is placed between the cone and the plate and is sheared. The shear rate is related to the angular velocity and the cone angle:

$$\dot{\gamma} = \frac{\Omega}{\alpha} \quad (2.2)$$

The shear rate is radius independent, i.e. it is constant through the gap. According to the small cone angle, the area of the cone does not differ much from the one of the plate and can be considered as equal. Therefore, torsional moment is measured on the cone or the plate, and can be represented as follows:

$$M = \int_0^R r \cdot \tau \cdot 2\pi \cdot r \cdot dr \quad (2.3)$$

Torsional moment is required for calculation of the shear stress:

$$\tau = \frac{3 \cdot M}{2 \cdot \pi \cdot R^3} \quad (2.4)$$

Cone-plate rheometers ascertain the true values for the shear rate, and the shear stress for both Newtonian and non-Newtonian fluids.

The measured storage and loss moduli were plotted as a function of the deformation. The region, where G' and G'' exhibit constant values, a low deformation area, is a linear viscoelastic region. The limit deformation value, in the linear viscoelastic region, was used in the frequency sweep. During the frequency sweep, the angular velocity was varied from 0.1 to 100 rad/s. The oscillation amplitude (percentage of strain) was determined during the amplitude sweep, for all polymers used here, in order to perform rheological measurements in the linear viscoelastic region. The range of frequency from 0.1 to 100 Hz corresponds to the wetting and creep properties of PSAs. Measurements, with variation of frequency, can be performed in short interval due to the mechanical restriction of the rheometers.

2.2.2. Measurement of elongational viscosity

Elongational viscosity was measured using SER Universal Testing Platform (M.L. Sentmanat, US Patent No. 6578413) mounted on a commercial rotational rheometer ARES G2, without any additional alteration on its system. Filament stretching rheometers with SER unit are described in detail in [96, 97]. SER consist of two cylinders, which stretch, the polymer sample (Fig. 2.5).

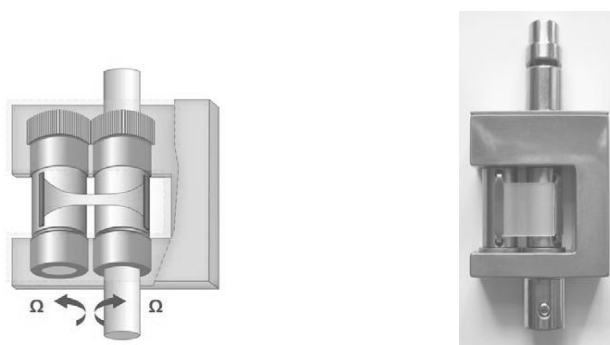


Figure 2.5. Universal testing platform SER (right) and detail of SER with polymer sample (left) [98].

The polymers were filled in a rectangle form, in order to obtain constant shape sample for increasing of the reproducibility. Prepared samples were fixed directly on the cylinders. The measurements of the elongational viscosity were carried out at room temperature ($T = 23^{\circ}\text{C}$), under two extensional strain rates: 0.3 and 1 s^{-1} .

2.2.3. PSA films preparation and characterization

Pressure sensitive adhesives are typically used in industry in form of thin polymer films. Adhesive films were prepared with $50 \pm 5 \mu\text{m}$ thickness, by coating the PSA solutions onto clean glass plates. For the experiments, doctor blades with different gaps and an automatic film applicator coater ZAA 2300 (Zehntner GmbH, Switzerland) were used. Variation of the solution concentration or the gap size of the film applicator enabled the adjustment of the polymer film thickness. The coating speed was found to show no effect on the film thickness, but was kept constant at 20 mm/s, in order to become a uniform film with reproducible thickness. Freshly prepared films were stored at room temperature overnight, for at least 12 h, for slow solvent evaporation avoiding bubble formation, followed by evaporation of the remaining solvent at 120°C, for about 1.5 h, achieving smoother polymer surface.

For estimation of the thickness of PSA film, two independent methods were used. Film thickness was measured by a dial gauge with a flat-ended feeler using silicon paper to avoid an adhesion between the feeler and the film. Alternatively, the film thickness was determined from force-distance curves obtained from tack measurements. The distance was calibrated to zero at the surface of the glass substrate. The difference between the known substrate position and the position at which the first contact with polymer material takes place, i.e. the position at which the first negative force value is detected, gives information about the film thickness. Both methods provided similar results.

The composition of the PSA films was studied using X-ray reflectivity [99]. The measurements were performed on Siemens D5000 Diffractometer (Siemens AG, Germany), according to the method detailed in [68]. The reflectivity curves and the corresponding fits are plotted on Fig. 2.6a in Fresnel-normalized representation. As a result of the data analysis, the refractive index profiles (Fig. 2.6b) perpendicular to the sample surface, can be extracted. Since only two components are involved and the refractive index is proportional to the electron density, one can read this as a composition profile.

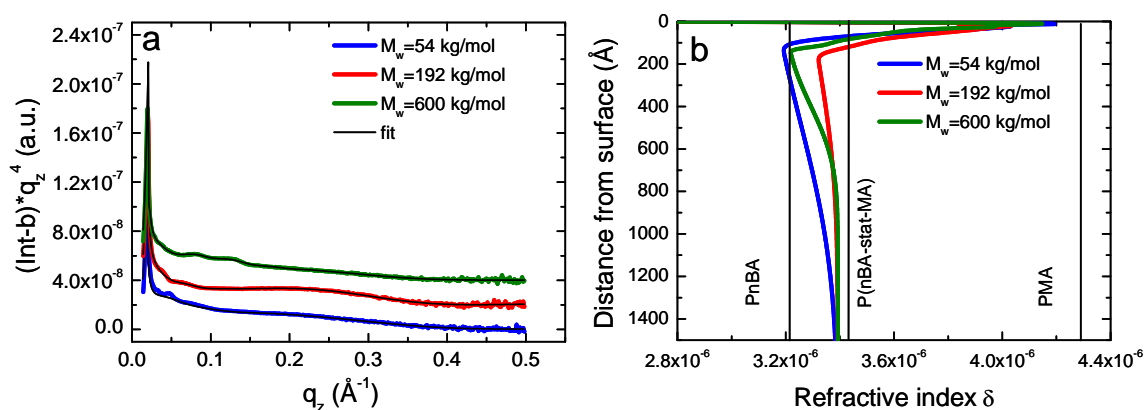


Figure 2.6. X-ray reflectivity data and corresponding fits in Fresnel-normalized representation of BA/MA films of three molecular weights (a) and corresponding refractive index profiles of the surface-near region of the shown fits (b). X-ray measurements were performed by A. Diethert (Technical University Munich) and published in [68].

The horizontal lines mark the values of the involved homopolymers and the statistical copolymers, as shown by the label. The composition of the PSAs films near the surface defers from the composition in the bulk film. The latter is the average composition of the copolymer, which is 80% PnBA and 20% PMA (neglecting the small amount of photoinitiator). At the surface, however, a thin enrichment layer of PMA is detected. This is followed by an enrichment region of PnBA with a thickness of approximately 100 nm, before the homogenous bulk composition is reached.

2.2.4. Substrate preparation and characterization

The substrates used for tack experiments were flat-ended cylinders prepared from a stainless steel, polyethylene (PE), glass and Si-wafer with a diameter of 5 mm (Fig. 27a). Flat-ended substrates were chosen since it allows establishing a uniform stress distribution, which is related to the fibrillation formation.

Flat, stainless steel, cylinders were polished to different degrees, with abrasive papers and with a diamond dispersion (1 μm particle diameter), in order to prepare probes with various average surface roughnesses $R_a = 2.9, 41.2$ and 291.7 nm. The substrates were polished using rotating disc device. The probes were kept near to the edge of the disc, in constant direction, in order to obtain non-isotropic surface with quasi-periodic grooves.

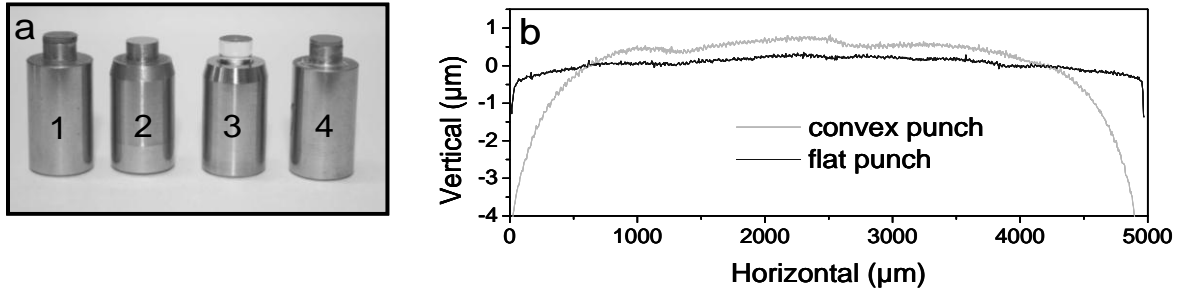


Figure 2.7. (a) Images of the substrates: polyethylene (1); stainless steel (2); glass (3) and Si-wafer (4)
 (b) Profiles of the steel substrates after polishing along the whole diameter (measured with confocal white light microscope NanoFocus μ Surf®)

The substrate surfaces were characterized using a white light confocal microscope NanoFocus μ Surf® (NanoFocus AG, Germany) and Q-Scope™ Scanning Probe Microscope (SPM) (Ambios Technology, Inc., USA).

In order to characterize the curvature of substrate's flat end after the polishing procedure, a profile along the entire probe diameter was made, using NanoFocus μ Surf®. This characterization is required, due to the threat of an edge roundness appearance during the polishing procedure, and therefore, a convex curvature, which prevent a homogeneous contact pressure to be achieved during the tack measurements. Fig. 2.7b shows the examples of a flat and a convex substrate. Only the substrates with a flat profile were used in this study. We avoid the appearance of convexity by creating a proper holder to fixing the substrates during polishing.

The Scanning Probe Microscope SPM images were done in a contact mode, using silicon contact tips (CSC17, Mikromash). The substrates surfaces were scanned, line by line, during the radial moving of the cantilever (about 10 nm tip radius), over the scanning area (Fig. 2.8). The three dimensional motion of the tip is controlled by a piezoelectric element. An optic sensor (laser beam) is oriented in the direction to the cantilever and its reflection is measured with detector. Contact mode is preferably used by roughness measurements of rigid substrate surfaces (Fig. 2.8 right). Direct contact was established between the tip and the rigid surface, during the surface scanning. The spring has to be soft enough to detect the smallest force application and at the same time has to possess high resonance frequency to resist against oscillation instability. However, by scanning of soft materials some damages of the surface structures could

appear, as negative consequences of the direct contact with the tip. The average substrate roughness R_a was determined from the SPM images, and is defined as an average deviation from the mean surface plane:

$$R_a = \frac{1}{N} \sum_{n=1}^{n=N} |Z_n - \bar{Z}| \quad (2.5)$$

Fig. 2.8 shows the profiles taken from the SPM images at the positions shown by lines. Substrate surfaces of all roughness, in this study, have peak to valley distances far smaller than the adhesive film thickness.

The surfaces of the probes were cleaned with acetone prior to each test.

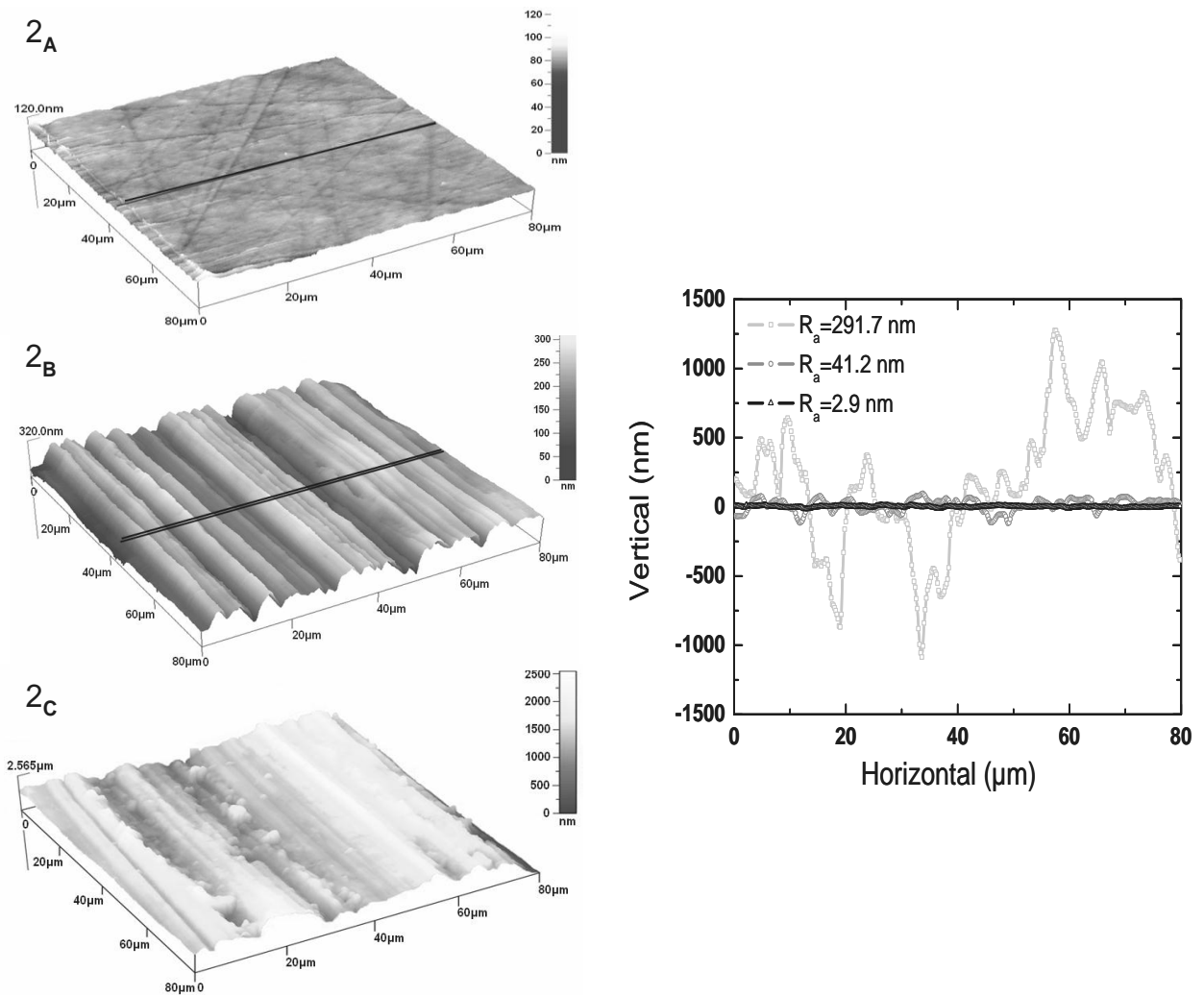


Figure 2.8. SPM images (left) of the substrates (2A) $R_a = 2.9$ nm; (2B) $R_a = 41.2$ nm; (2C) $R_a = 291.7$ nm and profiles (right) taken from the images at the place shown by lines.

Table 2.3 present the values of surface roughness measured with NanoFocus and SPM in different areas. The values of substrates roughness obtained with SPM (80×80 μm²) were used in this work.

Table 2.3. Values of average surface roughness for stainless steel substrates measured in different areas with SPM and NanoFocus.

substrate	R_a		
	10×10 μm ² (SPM)	80×80 μm ² (SPM)	320×320 μm ² (NanoFocus)
2 _A	1.0	2.9	10.5
2 _B	28.1	41.2	60.5
2 _C	147.0	291.7	472

For the preparation of the PE probe ($R_a = 49.5$ nm), a transparent foil of a low density PE was glued onto a Si-wafer to ensure high quality imaging of the cavitation process. Transparent glass cylinders was cut using an ultrasonic saw to prepare the glass probes ($R_a = 2.36$ nm). The glass probe was soaked for an hour in Acetone to clean the surface and was hydrophobized using thrimethylchlorosilane TMCS [100, 101]. To obtain a contact angle of 100° with distilled water, similar to the one on PE, we used 100% TMCS. Si-wafer cylinder was cut using ultrasonic saw, to prepare Si-wafer probe ($R_a = 1.6$ nm). The diameter of all probes was 5 mm and the R_a of the probe surface was measured using a Q-Scope™ Scanning Probe Microscope (SPM) (Ambios Technology, Inc., USA) as described in [102].

2.2.5. Crosslinking

One of the most preferable methods recently introduced for the crosslinking of PSA films is using UV technology. The advantage is that the degree of crosslinking and the adhesion-to-cohesion ration of PSAs, can be varied by controlling the UV dose, and this makes it possible to manufacture, from a single raw material, a wide range of adhesives with different properties [44].

One can vary the UV dose by changing the time during which the sample stays under the radiation. Long time corresponds to high UV dose and vice versa. It is important to

note, that UV light has a limited depth of penetration into the polyacrylate films. As a consequence, an adhesive with a film thickness above this penetration depth will be only weakly crosslinked. Moreover, it is impossible to determine the profile crosslinked density by dynamic mechanical measurements, and the moduli G' and G'' represent an average over the density distribution [8].

The UV crosslinked samples were prepared with the following procedure. BA/MA films, deposited onto the glass slides, were cured using a UV lamp (UV-Handlampe NU-15 KL, Benda, Germany) with an intensity of 1.45 mW/cm^2 measured at the distance of 4.5 cm and a wavelength of 254 nm. The used exposure times were 0, 21, 28, 34 and 69 seconds corresponding to the UV doses 0, 30, 40, 50 and 100 mJ/cm^2 , respectively.

2.2.6. Contact angle measurements and surface energy determination of polymer films and substrates.

Contact angles of test liquids onto all substrates and polymer films used in this study were measured according to the sessile drop method using Contact Angle System OCA (DataPhysics Instruments GmbH).

Distilled water, diiodomethane and paraffin oil were used as test liquids. Fig. 2.9 shows the contact angle in equilibrium of distilled water, on substrates made of different materials: stainless steel, polyethylene, silica and glass.

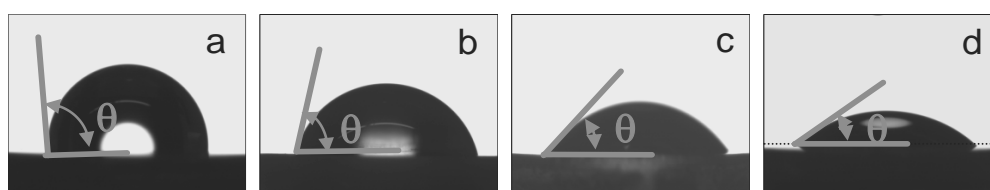


Figure 2.9. Images of contact angles with distilled water on different surfaces: (a) PE; (b) steel; (c) Si-wafer and (d) hydrophilic glass.

The change in contact angles of all substrates and all acrylate polymers, used in this study, were measured with the test liquids in a test interval of 60 seconds. On Fig. 2.10 one can see an example of contact angle change in time between the test liquids and BA/MA/MMA PSAs. The droplets of the test liquids do not obtain equilibrium at the

time of contact with solid surface. The transient contact angles, both on different probes and copolymer films, were recorded automatically as a function of time, at a rate of 10 frames/second.

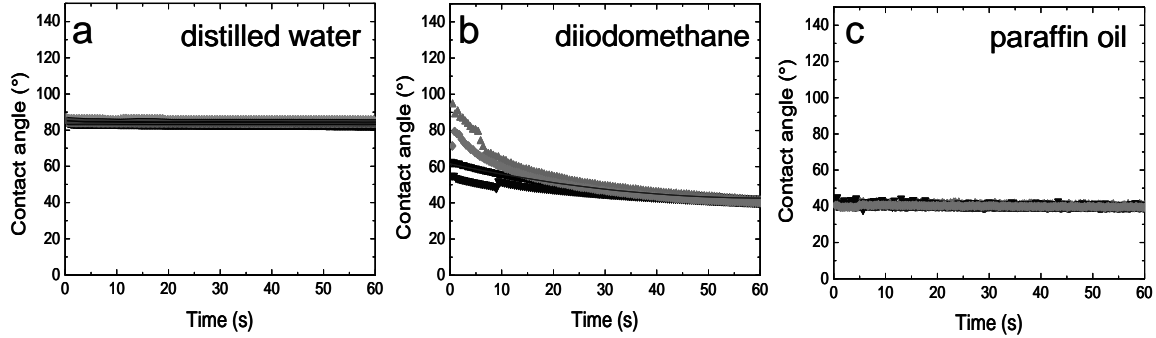


Figure 2.10. Contact angel as a function of time for three test liquids: a) distilled water, b) diiodomethane and c) paraffin oil on a film of BA/MA/MMA.

If no constant value of θ was reached within this time interval an exponential decay function $\theta(t) = \theta_e + (180^\circ - \theta_e) \exp(-K(t - t_0)^n)$ (see [103]), was fitted to the experimental data in order to obtain the equilibrium values θ_e (see e.g. Fig. 2.10b). The t_0 is the time when the drop gets in contact with the substrate and $\theta(t_0) = 180^\circ$, θ_e is the contact angle in equilibrium, K , n are fitted parameters, which reported the kinetics of the drop by spreading on the substrate [103]. An average value was then calculated from 6 independent experiments.

Surface energy values were calculated from the measured contact angles according to the method of Owens and Wendt described in reference [104].

$$\frac{(1 + \cos \theta)\gamma_{VL}}{2\sqrt{\gamma_{VL}^d}} = \sqrt{\gamma_{SL}^d} + \sqrt{\gamma_{SL}^p} \sqrt{\frac{\gamma_{VL}}{\gamma_{VL}^d}} - 1 \quad (2.6)$$

, where θ is contact angle; γ_{VL} - surface energy of liquids; γ_{VL}^d - dispersive component of liquid, $\gamma_{SL}^{d,p}$ - dispersive and polar component of substrates.

The test liquids have the values for surface tension and dispersion component plotted in Tab. 2.4.

Table 2.4. Surface tension and dispersion component of the test liquids [105, 106].

	γ_{VL} (mJ/m ²)	γ_{VL}^d (mJ/m ²)
distilled water	72.8	21.8
diiodomethane	50.8	49.5
paraffin oil	28.9	28.9

The equation (2.6) is plotted on the Figure 2.11 and by fitting with linear function of the data, the surface energy were determined for all polymers and substrates. The square root of dispersive components is the slop of the linear function, and the square root of the polar component is the y-axis intercept.

The surface energy was obtained by summing the determined values:

$$\gamma_{SL} = \gamma_{SL}^d + \gamma_{SL}^p \tag{2.7}$$

Additionally, from equation (2.6) and (2.7), the surface tensions of the substrate surfaces were calculated in the same way as for the polymer film.

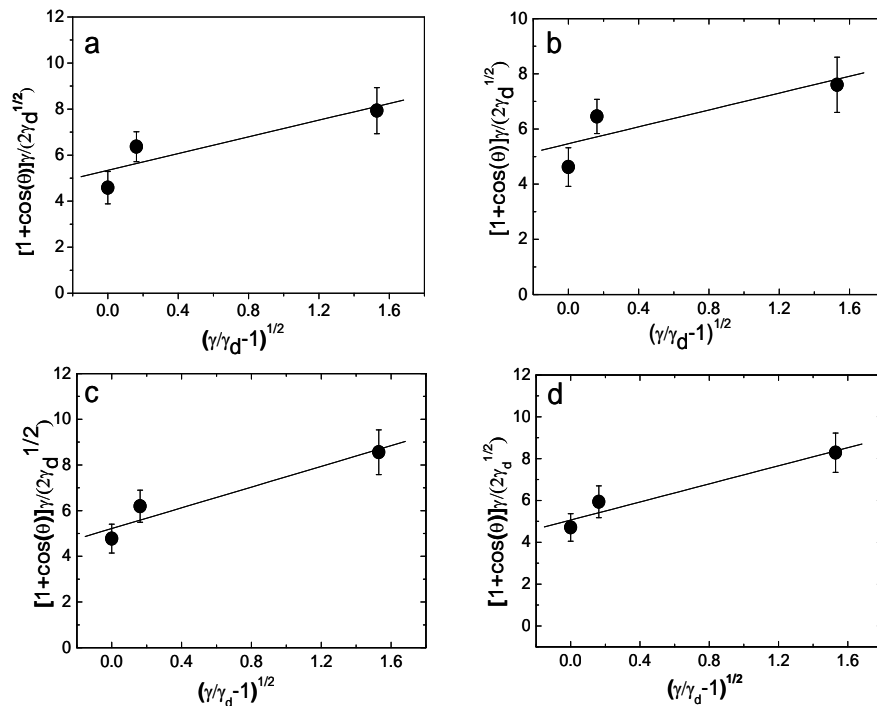


Figure 2.11. Owens-Wendt plots for (a) BA/MA; (b) BA/MA/HEA; (c) BA/MA/MMA and (d) BA/MA/AA for each test liquids : distilled water, diiodomethane and paraffin oil. The lines are the linear fit to the data.

Table 2.5 provides all obtained mean values of contact angle with distilled water, surface energies and the standard deviation.

Table 2.5 Contact angle and surface energy values of substrate and polymer films used in this study.

	type	contact angle θ (°)*	surface energy γ (mJ/m ²)
substrate	PE	97.9 ± 2.5	30.2 ± 1.5
	steel	67.7 ± 4.8	43.3 ± 4.7
	Si-wafer	33.8 ± 3.7	63.8 ± 5.6
	glass 25°	24.6 ± 2.4	68.0 ± 4.8
	glass 100°	99.5 ± 1.8	25.8 ± 4.1
polymer film	BA/MA	89.0 ± 1.0	31.8 ± 6.0
	BA/MA/HEA	91.5 ± 1.0	31.4 ± 5.9
	BA/MA/MMA	84.4 ± 0.9	32.1 ± 6.1
	BA/MA/AA	86.4 ± 0.9	30.3 ± 6.1

* Contact angle with distilled water

2.2.7. Mechanical analysis. Tack measurements.

The experimental set-up used for the tack measurements and video-optical observation (Fig. 2.12) is based on the commercial device Texture Analyzer TA.XTplus (Stable Micro Systems, UK) with a measured compliance of 2.75 $\mu\text{m}/\text{N}$ and modified with a quartz force sensor (Kistler Instrumente GmbH, Germany) with a force range ± 500 N and a threshold of 1 mN. The glass slide with the deposited PSA film is positioned on the home-built vacuum table. The probe tack tests were performed as follows: The probe approached the sample with a rate 0.1 mm/s, contacted the adhesive film with a contact force of 10 N and was held at a constant position for 1 s. The probe was then withdrawn with a constant rate of 0.1 mm/s. The resulting force-distance curves were recorded simultaneously with video images of the contact area. Testing was performed at a temperature of 23 °C. The surface of the probe was cleaned with acetone before each test. To get reliable average values each sample was tested at least 5 times.

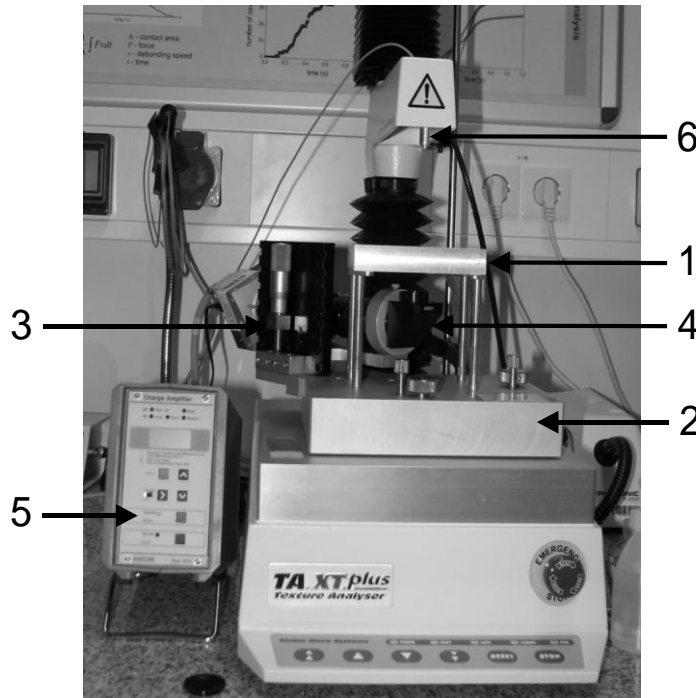


Figure 2.12 Experimental set-up for tack measurements and video-optical observation: 1-vaccum table; 2-platform; 3-video camera; 4-objective (90°); 5-charge amplifier; 6-substrate.

As already described in detailed above, stress peak σ_p and the deformation at break ε_B were determined from the stress vs. strain curves. The measured force F was converted to a nominal stress $\sigma = F/A_0$, where A_0 is a true initial contact area, measured from the optical images, taken at the beginning of the pull-off period. The tack value was obtained from the area under the nominal stress vs. nominal strain curve. The latter was calculated from the time-dependent film thickness h as

$$\varepsilon = (h - h_0) / h_0, \text{ where } h_0 \text{ is the initial film thickness.}$$

2.2.8. Video observations.

The debonding of acrylate copolymers is accompanied by the cavitation. Cavities occur at the interface between the substrate and the polymer and they are affected by the interfacial parameters. The detailed analysis of the cavitation can allow to quantify the influence of the interfacial parameters on the adhesion of PSAs. An optical observation of the debonding allows for observation of the cavitation and determination of the cavity growth rate.

Texture Analyzer TA.XTplus was equipped with a high-speed camera mounted under the vacuum table, where a transparent glass plate with the deposited sample is positioned in order to record a video sequence simultaneously with the stress-strain curves. The video images were obtained with a high-speed camera KL MB-Kit 1M1 (Mikrotron GmbH, Germany) used in combination with a zoom objective 90° KL-Z6 and a cold light source KL3000B. The camera allows to record 124 frames/s at maximum resolution of 1280×1024 pixels. At maximum resolution one pixel is approximately 5 µm.

The force-time curve was synchronized with the video sequence. The first image recorded, corresponds to the moment when it was observed that the probe touches the surface of the polymer film. The point of the force curve where the force value differs from zero represents the contact of the substrate with the sample and corresponds to the image of the first contact. The videos were quantitatively analyzed using Visiometrics Image Processing System (IPS) software, developed by Prof. Dr. Stephan Naser, University Darmstadt. The true contact areas, cavity size, as well as the velocity of cavity growth, were obtained.

Data analysis

Information about the cavitation during the debonding process can be gained by analysis of the recorded images. Video data analysis includes the following steps:

1. Determination of the contact area. In this step, one can enter either the diameter of the probe surface or the size of 1 pixel, which is around 5 µm. Using IPS software one can calculate the true area of contact from the manually marked probe surface on the first image of every video sequence.
2. Contrast between substrate and polymer: Different materials reflect the light in different way. Polymer films absorb and reflect less light compared to the steel substrate. On the Figure 2.13 one can see the polymer film in green color, while the substrate (the wholes inside and outside the cavities) is black.

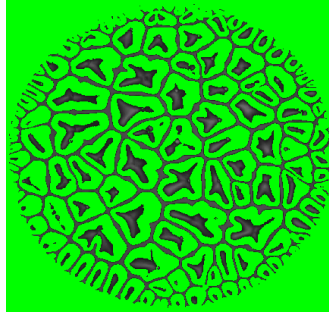


Figure 2.13. Contrast between the cavities and the background. Threshold adjustment in the IPS software.

IPS recognizes light and dark regions on the images. The problems, which could appear during the determination of the threshold, are the following:

- Some groups of pixels, which are parts of the cavity border or inside of cavities, could be marked by the software, separately and later erroneously recognized as a new cavity. A phantom cavity will appear in the data analysis.
- Defects on the surface by using rough substrates may also be marked and further mistakenly recognized as cavities by the software.

These problems can be avoided with a precise definition of the threshold. A marked area is recognized as a cavity, when its size exceeds a size of manual predefined pixels amount. Therefore, the cavities which appear at the border of the substrate, as a result of penetrated air into polymer bulk during debonding, represent physically different phenomena. Such cavities are not considered in the statistical analysis of the cavitation process.

3. Definition and numeration of Regions Of Interest (ROIs). Cavities can be numbered manually or automatically. According to the first method, a line was manually drawn around every cavity, along the maximal size it can reach. All ROIs receive the number. All data about the size of the cavities are saved under these numbers during the analysis. The second method allows the automatic recognition and numbering of all cavities. The main problem here is the additional recognition of the black colored places in the middle of the cavities as extra cavities, as well as the additional counting of the cavities occurring at the border of contact area. Manual correction is required.

To obtain reliable results 3 tack measurements were performed for each sample and on the images of every video sequence 15 to 20 cavities appearing at the different places of the polymer/substrate contact area were marked and analyzed. Fig. 2.14 shows the

change of the cavity size on the images of the same video sequence, analyzed with IPS software.

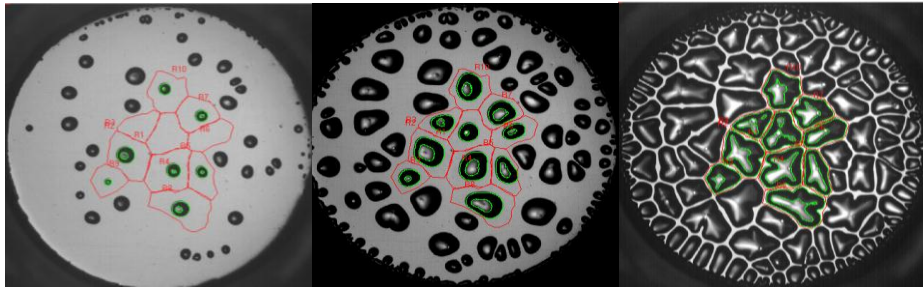


Figure 2.14. IPS recognized the cavities in the ROIs and the change in there size.

IPS software recognizes the cavities in the ROIs on all images and delivers the parameters such as ROI number, size, etc. These parameters are used for creating of a diagram and analyzing the change of cavity size as a function of time, as well as the cavity growth rate.

3. Experimental part

3.1. Rheological characterization.

3.1.1. Characterization of the model system.

Two groups of model acrylate copolymers were used for the investigation of the interfacial phenomena on the adhesive properties of PSAs:

- acrylate copolymers with the same composition, but with different molecular weight
- acrylate copolymers with the same molecular weight, but with different chemical composition

First group, containing copolymers with the same chemical composition (BA/MA copolymers), but with three different molecular weight was used for the estimation of the influence of the roughness of the substrate on the adhesion of PSAs. Second group, containing copolymers with the same molecular weight, but with different chemical composition (BA/MA copolymers with additional incorporated functional comonomers) was used for the estimation of the effect of functionality on the adhesion. Rheological properties of all above mentioned copolymers were investigated (Fig. 3.1a and 3.1b). Information about the behavior of the copolymers at very low and very high frequencies can be gained by varying the temperature at which the measurements are performed. The characteristic master curves were obtained with time-temperature superposition (TTS) by shifting the curves measured at different temperatures to a reference temperature.

Fig. 3.1 shows the master curves of storage G' and loss G'' moduli as a function of the angular frequency for a) BA/MA copolymers with three different molecular weights, and b) BA/MA copolymers with an incorporated different functional comonomers: hydroxy ethylacrylate (HEA), acrylic acid (AA) or methyl methacrylate (MMA). The samples were measured at different temperatures between 2 and 120°C and the data was shifted to a reference temperature, which was chosen to be room temperature $T_{ref} = 23^\circ\text{C}$.

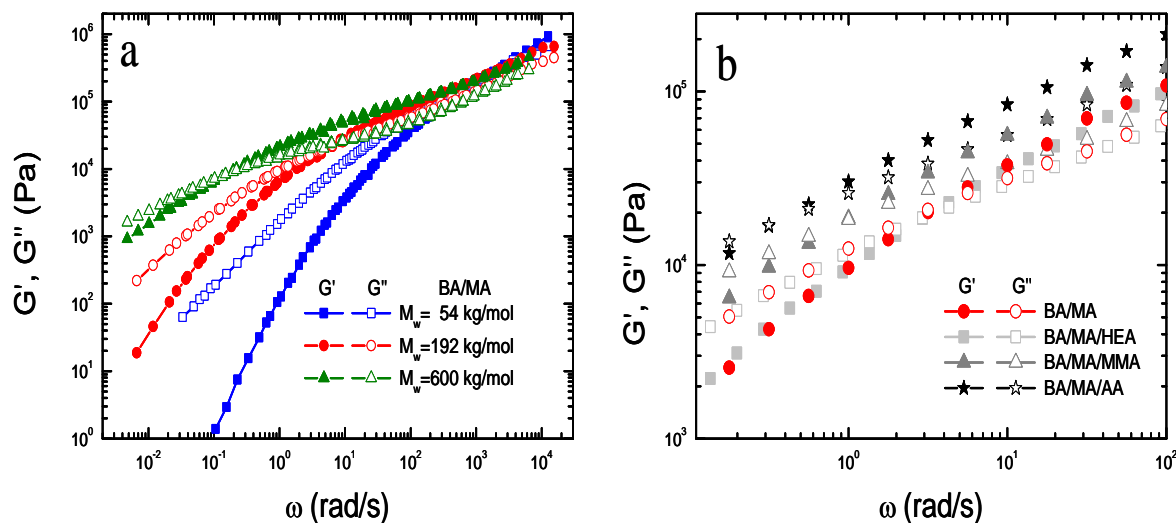


Figure 3.1. Shear modulus (G' – storage modulus; G'' – loss modulus) as a function of frequency (a) TTS for MA/BA PSAs with different molecular weights and (b) PSAs with different composition ($M_w \sim 190$ kg/mol) measured at room temperature.

There is a correlation between the viscoelastic properties of PSAs and their adhesion performance [11]. The process of adhesion for all PSAs contains two parts: low rate bonding, characterized by the ability of the adhesive to flow under light pressure, and high rate debonding, characterized by the deformation of the polymer film under stress until the film separates from the substrate.

In contrast to bonding, during the debonding process the polymer should be cohesive, i.e. internally strong in order to resist the applied stress. Additionally, the bonding process corresponds to low oscillatory frequency behavior, and the debonding process to high oscillatory frequency.

As shown in Fig. 3.1a, viscous behavior ($G'' > G'$) dominates the copolymer response at low frequencies, whereas at high frequencies, the elastic component ($G' > G''$) prevails. Such behavior is typical for PSAs and has been explained in earlier studies, e.g. [107]. In case of a predominantly viscous component, the polymer dissipates energy during deformation, which results in easy adherence to the substrate accompanied with a formation of good contact. A higher value for the elastic component indicates storage of deformation energy in the polymer bulk. Increased energy will be necessary for the separation of surfaces in contact. Nevertheless, acrylate copolymers studied here show values for storage modulus G' below 3.3×10^5 Pa at low frequencies (around 1 Hz), when

the T_g is adjusted, and, consequently, they fulfill the Dahlquist criterion for the performance of polymers as PSAs [15] and therefore they can be used as PSA model systems. As expected, the increase in the molecular weight leads to an increase in the longest relaxation time, characterized by a crossover in the storage and loss moduli, where the crossover point of G' and G'' is shifted to lower frequencies/high temperatures with increasing molecular weight. By increasing the molecular weight of the polymers, the terminal region that indicates an increase in the cohesion of the adhesive materials shifts to lower frequencies. Therefore, the increase in the molecular weight results in an increase in the viscoelastic moduli in the low frequency region. Stress relaxation is regulated from short-range chain motion, and shows no dependence on the molecular weight, which explains the superposed TTS master curves at high frequencies. No occasional crosslinking of the acrylate polymer is indicated, since the frequency dependence of the rheological moduli corresponds to the one of flexible, linear polymers.

Fig. 3.1b shows the shear moduli G' and G'' as a function of frequency for acrylate copolymers with different composition. The variations in the monomer composition often lead to changes in the bulk and surface properties of the polymers and, accordingly, the adhesion performance of PSA [7, 52]. The increase in G' and G'' results from increasing the polarity of the additional functional comonomer (HEA < MMA < AA). Higher rheological moduli indicate that deformation of the adhesive, during the bonding to the substrate, will be more difficult. In the case of additional AA groups, for example, H-bonds appear in the polymer chain that increase the internal strength of the copolymer and these bonds act as a physical crosslinking. Incorporating HEA leads to virtually no change in the rheological properties. In contrast, incorporating a small amount of AA changes the PSA's behavior to predominantly elastic behavior, $G' > G''$. The longest relaxation time is slightly shifted in the low frequency direction, due to the increase in polarity. This effect becomes much more pronounced by increasing the length of the polymer chains (3.1a).

The tack of a polymer is related to the linear viscoelastic moduli in the frequency range between 1 and 100 rad/s. Since the applied debonding velocity during tack measurements has a low value, $V_{deb} = 0.1$ mm/s, and the film thickness is $h_0 = 50$ μ m, the characteristic deformation rate V_{deb}/h_0 is 2 s⁻¹. In this frequency range, the

viscoelastic signature of the studied model system, changes from predominantly viscous (for the lowest M_w , and crossover $G' = G''$ for intermediate M_w) to predominantly elastic behavior (for the highest M_w) (Fig. 3.1a). Moreover, BA/MA PSA with an additional comonomer (HEA or MMA) shows predominantly viscous behavior, while incorporating of AA comonomer changes the behavior of PSA to predominantly elastic.

3.1.2. Characterization of weakly crosslinked acrylate copolymers.

The adhesive properties of acrylate copolymers cured with UV doses between 0 and 100 mJ/cm² were also studied. The crosslinking of polymers changes their viscoelastic properties and also the mechanism of debonding. Generally, the light crosslinking of PSAs increases their cohesion, which results in a higher value for the work of adhesion. Therefore, curing of polymers can lead to a change in the debonding mechanisms - from cohesive to adhesive failure.

Fig. 3.2a represents the shear moduli G' and G'' as a function of frequency for BA/MA copolymers with molecular weight $M_w = 192$ kg/mol and $M_w = 600$ kg/mol, and for BA/MA with $M_w = 192$ kg/mol cured with a UV dose of 100 mJ/cm². Curing the copolymers with a UV light leads to crosslinking of the chains and an increase in the shear moduli. Moreover, the crosslinked BA/MA copolymers exhibit values of the shear moduli similar to the high molecular weight copolymers values, but in contrast to the uncrosslinked systems, no crossover ($G' = G''$) is observed. Therefore, in the observed frequency range, crosslinked copolymers do not show a terminal flow. Crosslinked copolymers have larger longest relaxation times than uncrosslinked - shifted in the direction of low frequency. In the frequency range of the tack measurements, the crosslinked BA/MA with $M_w = 192$ kg/mol has similar values for G' and G'' as the uncrosslinked BA/MA with higher molecular weight. Increasing the length of the polymer chains or crosslinking them leads to an increase in the shear moduli of copolymers, i.e. their cohesion. However, crosslinked copolymers of intermediate M_w and uncrosslinked copolymers with higher M_w have different failure mechanisms, adhesive and cohesive, respectively. The first mechanism is characterized by debonding from the substrate surface without visible polymer residue left behind,

while the second mechanism is accompanied with a rupture in the polymer film with polymer residue left on the substrate after debonding.

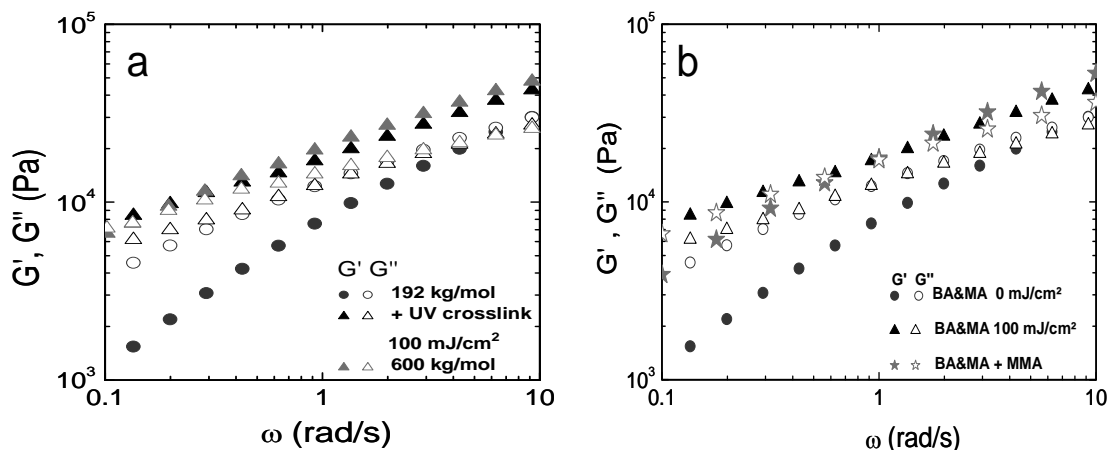


Figure 3.2. Shear moduli (G' - Storage modulus and G'' - loss modulus) as a function of frequency for (a) MA/BA PSAs with $M_w = 192$ kg/mol (uncrosslinked and crosslinked with 100 mJ/cm², 2) and $M_w=600$ kg/mol; (b) MA/BA PSAs (uncrosslinked and crosslinked with 100 mJ/cm²) and MA/BA with additional functional comonomer MMA, all with $M_w \sim 200$ kg/mol. Measurements are performed at room temperature.

Fig. 3.2b shows the shear moduli G' and G'' as a function of frequency for uncrosslinked and crosslinked, with 100 mJ/cm², BA/MA, and BA/MA with incorporated functional comonomer MMA, all with similar $M_w \sim 200$ kg/mol. As already mentioned above, crosslinked or larger polymer chains can increase the shear moduli as does the incorporation of a small amount of polar comonomers. Different additional functional comonomers influence the rheological properties with differing intensities, therefore it is difficult to distinguish between the influence of the polymer bulk and the polymer/substrate interface on the adhesion properties. The investigation of the isolated effect of the interface on the adhesion of the PSAs, could be realized by adjusting the viscoelastic properties during a curing process to similar values of shear moduli. The curing of BA/MA with a UV dose of 100 mJ/cm² increased the values of G' and G'' in the direction of the values of shear moduli for BA/MA/MMA, but in a different way, as expected. In the frequency regime of the tack measurements, crosslinked BA/MA shows predominantly elastic behavior, while non-crosslinked copolymer BA/MA/MMA curves have crossovers where $G' = G''$. The longest

relaxation time of crosslinked BA/MA is much larger than of the non-crosslinked BA/MA with incorporated MMA. This indicates that for the studied acrylate copolymers, an adjustment of the viscoelastic properties of the acrylate copolymers with incorporated functional comonomer cannot be achieved by curing with UV.

3.1.3. Elongational viscosity

Extensional viscosity measurements were performed in order to study the deformation characteristics of BA/MA copolymer and BA/MA copolymer with various incorporated functional comonomers. In Fig. 3.3 the viscosity is plotted against time in a constant velocity experiment for BA/MA and BA/MA/AA. The elongational viscosity and the shear viscosity are compared. The elongation viscosity was measured at two different elongation rates: 0.3 and 1 s⁻¹.

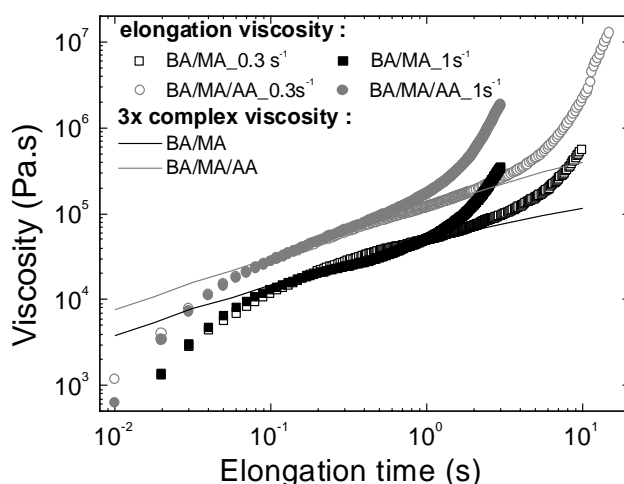


Figure 3.3. Elongation and the mirror image of $3\times$ shear viscosity as function of the elongation time for BA/MA and BA/MA/AA. Elongation velocity measured at 0.3 and 1 s⁻¹. Measurements were performed at room temperature.

Typically, at the beginning of the elongation, the increase in the elongational viscosity curves has a slope of order 1. At short times, in logarithmic scale, the rate of increase goes through a plateau followed by a rapid exponential increase (inflection point), corresponding to strain hardening of the tested adhesive [108].

Similar observations of the elongational behavior for copolymers have been reported in a previous study, where n-butyl acrylate and 2-ethyl-hexyl acrylate, were used as PSAs [109].

3.2. Initial conditions

The performance of PSAs is strongly influenced by such experimental parameters as the compressive stage duration, i.e. contact time and pressure, as well as the temperature or the debonding velocity. Both contact time and contact pressure are responsible for the size of the contact area as well as the degree of the relaxation during debonding [12]. These two parameters, which define the initial condition of the tack measurement and can be varied at the compressive stage, have an influence on the initial stage of the process of debonding. The effect of the initial conditions as t_c and p depend on the bulk properties of the polymer film and the polymer/substrate interface (such as the degree of roughness). Therefore, it is necessary to fix all experimental parameters in order to study the influence of the surface substrate roughness, the surface energy, as well as the polymer chemistry on the adhesive behavior of PSAs.

3.2.1. Influence of the contact pressure

In order to examine the role of the contact pressure, several measurements were carried out at various compression forces in a range from 3 to 20 N. The contact pressure was calculated as the ratio of the load to the area of contact that was determined from the images. The effect of the contact pressure on tack values of BA/MA PSAs for three different substrate roughnesses is shown in Fig. 3.4. The tack values for all PSAs studied here increase with increasing contact pressure irrespective of the roughness of the steel substrates.

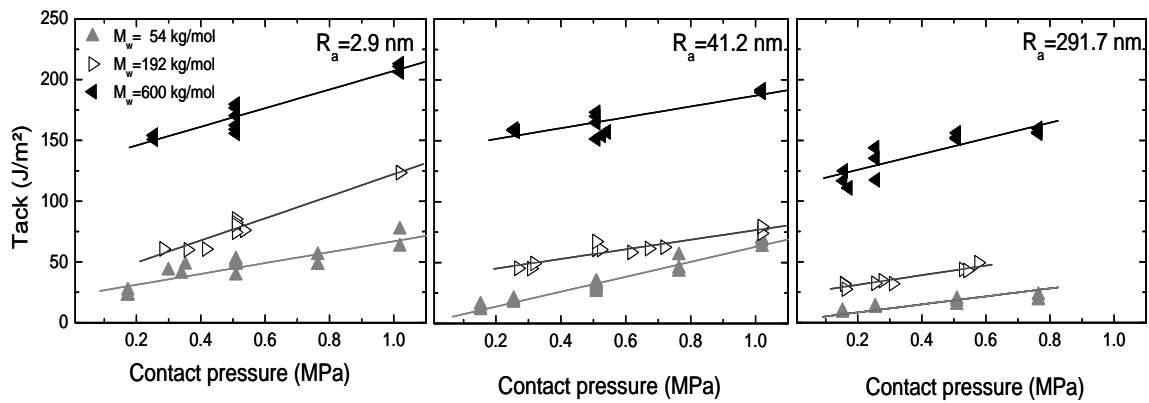


Figure 3.4. Tack vs. contact pressure for BA/MA PSAs of $M_w = 54$ kg/mol, $M_w = 192$ kg/mol, $M_w = 600$ kg/mol and roughness $R_a = 2.9$ nm, $R_a = 41.2$ nm and $R_a = 291.7$ nm. Lines are to show trends.

In contrast to earlier investigations, no limiting value for the tack is reached because unlike in commercial PSAs, the polymers used for the investigation of the effect of substrate roughness were uncrosslinked [14]. Under the experimental conditions chosen here, as expected for uncrosslinked copolymers, the mechanism of failure is always cohesive. The variation of tack with contact pressure is insensitive to molecular weight or surface substrate roughness. The contact pressure was fixed at 0.51 MPa in all subsequent measurements.

3.2.2. Influence of debonding velocity V_{deb} .

The debonding velocity is related to the strain rate of the adhesive polymer. The debonding process is characterized by heterogeneous shear and elongational flow [30]. At the initial stage of separation, the strain is homogeneous. Increasing the velocity of debonding in the cohesive regime, i.e. low De , results in an increase in the adhesion energy. This regime is characterized by bulk yielding separation. A further increase in V_{deb} leads to a decrease in the tack values, and a transformation of the separation into adhesion failure occurs. When the strain rate is high enough to prevent substantial polymer relaxation, the possibility for fibril formation is minimized, which leads to a reduction of the adhesion energy. A change in the failure mechanism - from cohesive to adhesive separation - for the copolymers studied here occurs at $V_{deb} > 8$ mm/s for the low molecular weight and at over 10 mm/s, for the intermediate and high M_w .

However, the crosslinked samples show an adhesive failure even at $V_{deb} = 0.1$ mm/s. The deboning velocity was kept constant at 0.1 mm/s during all measurements.

Variations in temperature can also affect the adhesion of PSAs. Changing the temperature modifies the relaxation time of polymers, which results in a change in the rheological behavior. The storage modulus decreases when increasing the temperature, resulting in increasing the area of contact with the substrate due to improved wettability of the polymer. As a result, the adhesion energy increases. A further increase in the temperature leads to a decrease in the cohesion strength of the polymer, followed by a reduction in the adhesion energy. Maximum tack energy was observed around 50°C above the glass transition temperature of the polymer. All tack measurements here were performed at room temperature.

Varying adhesive film thickness has also an effect on the adhesion process. Tordjeman and co-workers [110] attributed the increase in the nominal stress peak with decreasing film thickness to the different viscoelastic properties of the adhesive with decreasing film thickness and increased confinement. These results were later confirmed by Chiche and Creton [59] who reported that for a “smooth” interface (smooth adhesive film or substrate) the stress overshoot increases markedly with decreasing the film thickness. In order to investigate the influence of parameters such as roughness, surface energy, chemical composition or crosslinking and to be able to analyze the quantitative difference, it is important to keep the film thickness constant (50 μm) for all measurements.

An increase of contact time results in increasing the real contact area by wetting because of the deformation of the viscoelastic adhesive by the compression. Leibler and co-workers observed a pronounced maximum in the adhesion energy approximately 50°C above the T_g at short contact times. Increasing of the time of contact, however, suppressed a maximum of the work of adhesion W [62]. Nevertheless, short contact times suppress the diffusion and surface contamination of the adhesive. Therefore, for all measurements short contact time was chosen, $t_c = 1\text{s}$.

3. 3. Influence of the substrate modifications on the adhesion of PSAs.

3.3.1. Roughness of the substrate.

The influence of the substrate roughness on the adhesion was theoretically discussed first for elastic and later for viscoelastic polymers [111]. The experiments have shown that in contrast to all other classes of adhesives, the use of substrates with high roughness has a negative effect on the adhesion of PSAs. The reason for this effect is the existence of asperities, which reduce the real size of contact with the polymer [62, [63]. The effect of the roughness increases with the elastic modulus of the polymer film.

- *Stress-strain curve*

Deformations, which appear in adhesive film during the tack measurements, are complex. At the first stage of separation, the shear stress predominates, which is accompanied by cavitation. The next stage is characterized by elongation of the formed fibril structures at long deformation times. The analysis of the debonding process at the different stages sustained by adhesives is based on the information gained from the stress-strain curves. During the probe tack test, the force was recorded as a function of time and distance. Force-time and force-distance curves can be found in the literature [13, 112] and they exhibit different shape for Newtonian, viscoelastic and elastic fluids. Fig. 3.5 shows representative stress-strain curves for copolymers with different M_w as measured with stainless steel substrates of three different roughnesses. On the diagram one can see, that stress peak is present in each of the obtained curves. In contrast, in a previous study [59] no nominal stress peak was observed when testing the polymer film with rough substrates. Strain-hardening polymer response rapid and elastic to a load applied to the system, and the stress goes through a maximum. Subsequently, the stress decreases until it eventually approaches a plateau. The existence of stress peaks indicates an internal or interfacial fracture in the adhesive film. For the studied acrylates, the plateau is more pronounced for the higher molecular weight copolymer. An explanation for this phenomenon can be found in the size of the polymer chain, which controls the elongational properties of the adhesive.

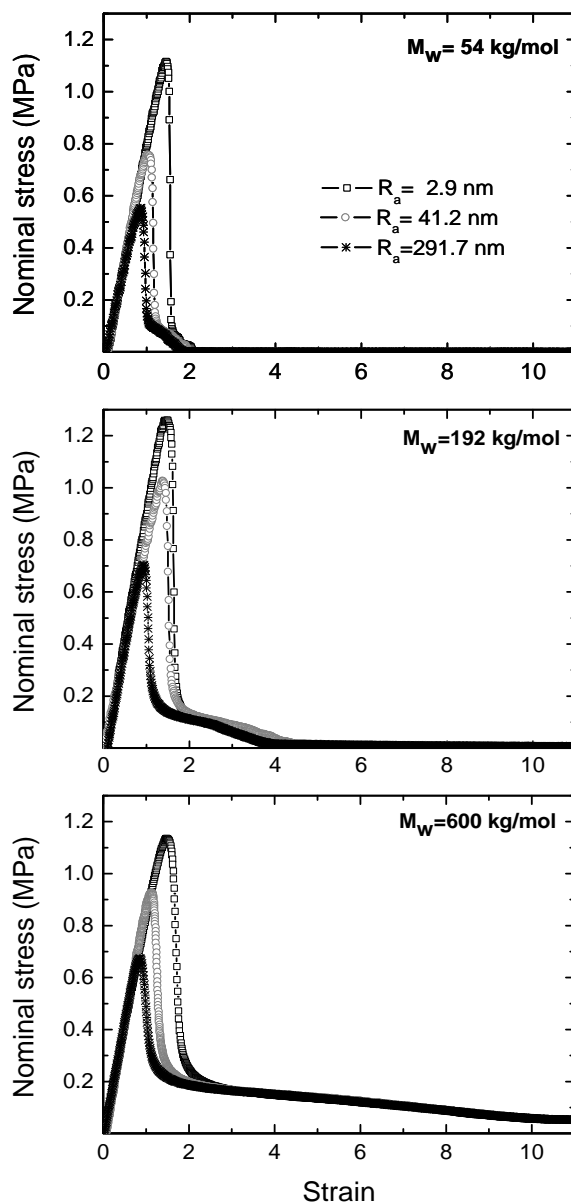


Figure 3.5. Representative nominal stress vs. strain curves for BA/MA PSAs of $M_w = 54$ kg/mol, $M_w = 192$ kg/mol, $M_w = 600$ kg/mol measured with substrate of different roughness: $R_a = 2.9$ nm, $R_a = 41.2$ nm and $R_a = 291.7$ nm.

After the maximum is reached, with increasing R_a the nominal stress drops due to the reduction in the lateral cavity expansion rate. The stress abatement proceeds for all polymers with similar speed. This observation represents another discrepancy with the previous study [59], where, after reaching its maximum, the nominal stress decreases distinctly faster by using the smooth probe, comparing with the tests with the rough probe, thus causing the stress-strain curves to cross. Here the characteristic difference in

the debonding behavior may presumably be related to the fact that uncrosslinked acrylic PSAs were used in this work, whereas SIS triblock copolymers and a hydrogenated resin were used in [59]. These distinctly different findings indicate that the cavitation process seems to be controlled by a delicate interplay between polymer composition and substrate roughness. The fibril formation during the debonding is more pronounced for copolymer with $M_w = 600$ kg/mol. Copolymers with higher M_w show higher deformation during debonding due to the larger size of the polymer molecules. Higher deformation of the walls between cavities, namely the formation and elongation of fibril structures, correspond to the amount of dissipated energy, which leads to increase in the work of adhesion.

- *Tack, stress peak and deformation at break*

Nominal stress peak, deformation at break and tack values are calculated from the stress-strain curves and shown in Fig. 3.6 as functions of the substrate roughness.

Stress peak value strongly decreases with increasing in roughness, and it appears earlier for the higher R_a i.e. cavities appear sooner (Fig. 3.6a). This result is in agreement with an earlier study, and can be rationalized in terms of an inhomogeneous stress distribution at the interface [66]. Local stresses can be higher than the average nominal stress at the nucleation sites on a rough surface. The deformation at break is independent of roughness, but increase strongly with increasing in molecular weight of the PSAs used here (Fig. 3.6b). These results can be explained considering the fact that the final plateau in nominal stress correspond to vertical growth of cavities i.e. stretching of the formed fibril structure.

This observation differs from the investigation of Hooker and co-worker [62] on SIS triblock with two steel probes with $R_a = 0.05$ and $1\mu\text{m}$, where the increasing the R_a resulting in a drop of the deformation at break. Authors explain the observed effect with incomplete relaxation of the adhesive during the time of contact.

The ability of the fibrils to be deformed, which characterize its stability, is mainly governed by the viscoelastic properties of the polymer material. Surface roughness does not influence this polymer deformation process. As a result, the tack values decreases with increasing roughness due to the contribution of the nominal stress peak Fig. 3.6c.

This decrease is only weak, since the tack value is dominated by the formation and elongation of fibrils and this process mostly depends on the viscoelastic properties of the PSAs. Within the range of molecular weights investigated here, the copolymers with the highest M_w have the highest tack due to the strong contribution of the filament stretching. Increase in the molecular weight corresponds to the increase in rheological moduli G' and G'' in the frequency range of the strain rate of tack measurements. The shear moduli in the frequency range corresponding to a characteristic debonding rate of tack test, as well as tack values are expected to level off as higher molecule weight as observed in [41].

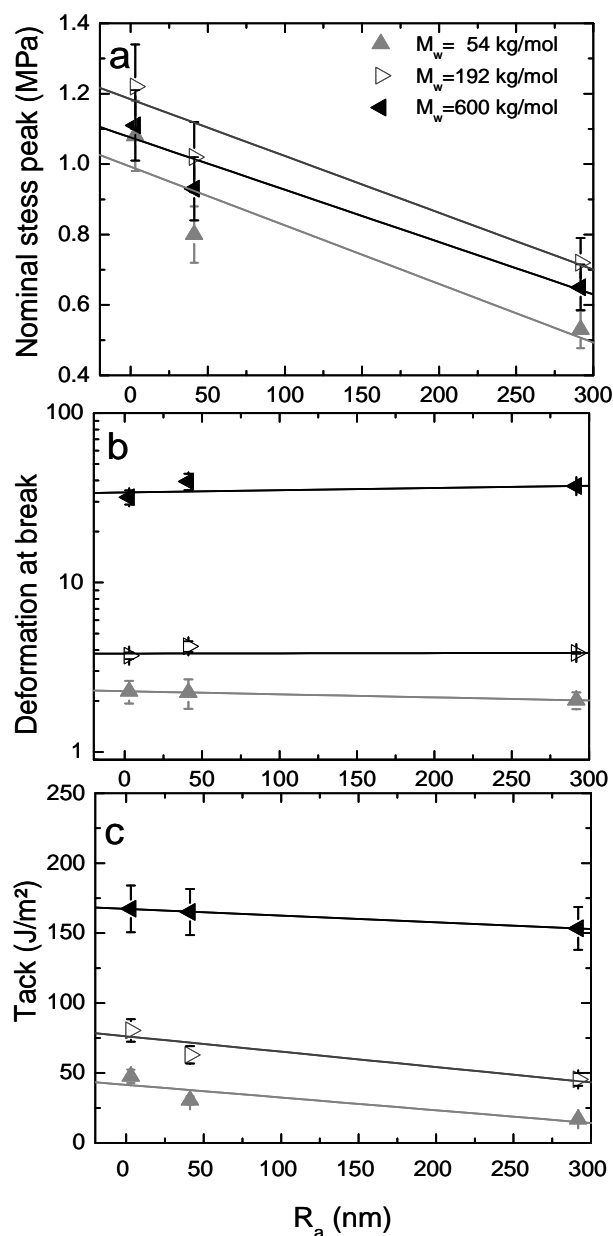


Figure 3.6. Nominal stress peak (a) , deformation at break (b) and tack (c) as a function of substrate roughness (R_a) for BA/MA PSAs of three molecular weight. Lines to show the tendency.

- Total number of cavities and final average cavity area

In order to understand the growth of cavities and the influence on the deformation and adhesion, it is necessary to observe the cavitations process in situ. The appearance of cavities changes the adhesive-free surface and influences the deformation process in the film. Surface roughness of the substrate R_a plays an important role in the number of

formed cavities and is expected to affect their growth velocity. Images of the contact area between the polymer film and the substrate were recorded simultaneously with the tack curves in order to evaluation of the effect of the surface substrate roughness on the adhesion of PSAs. Representative images of cavities taken in the moment, when their lateral growth is finished are shown in Fig. 3.7.

The video images recorded during debonding process show that the cavities appeared on the smooth surface are bigger and less circular, then those on the rough substrates. Additionally, the cavities formed on the smoother surface, display a dendritic shape, in agreement with earlier observation [30].

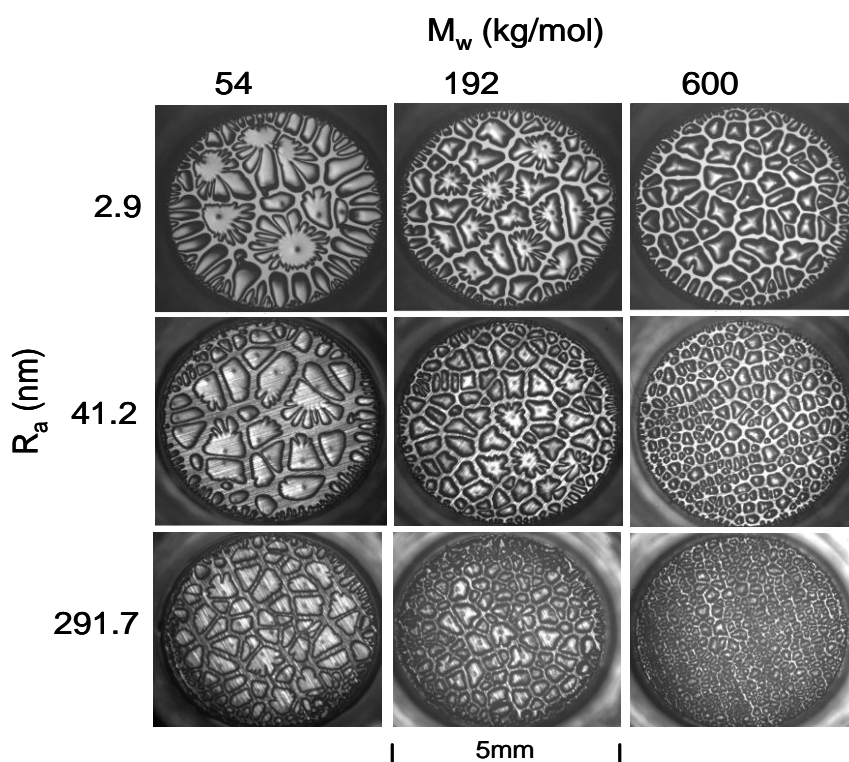


Figure 3.7. Representative images of contact area of the probes with three different average surface roughness for BA/MA PSAs of three molecular weights.

The total number of cavities and the average final cavity area were calculated from the images in Fig. 3.7, and are shown in Fig. 3.8 as function of the average substrate roughness. Surface roughness has a significant effect on the number of cavities and on their size. The number of cavities increases with increase in the substrate roughness. A fivefold increase of the average total number of cavities formed is observed, when increasing the surface roughness from 2.9 to 291.7 nm (Fig. 3.8a). The reason for this increase in the cavities number can be found in the larger amount of surface defects,

which act as germs for cavity formation. Accordingly, the final average size that the cavities can reach, reduces (Fig. 3.8b), the cavity size distribution (not shown in the graph) is much broader than then that in the smooth surface. In addition, cavity size is several orders of magnitude larger than the thickness of the adhesive film. Nevertheless, the viscoelastic properties of PASs have a comparable impact on the cavitation process. An increase in the molecular weight of the adhesives from 54 kg/mol to 600 kg/mol results in an average increase in the total number of cavities by a factor of 6 (Fig. 3.8a), and they appear later. Thus, in addition to the influence of contact defects, viscoelastic properties play an important role in cavity formation.

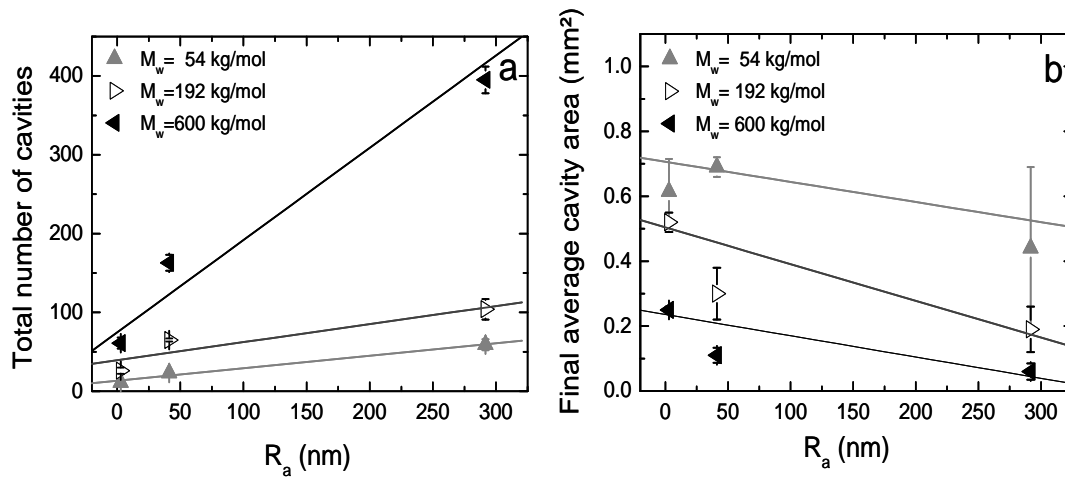


Figure 3.8. Total number of cavities and the final average cavity area vs. probe roughness, for BA/MA PSAs, with three different molecular weights. Lines show the tendency.

From Fig. 3.8b one can see, that the final average cavity area only lightly decreases with increasing roughness, while the effect of molecular weight is much more pronounced. When the molecular weight is high, for constant rough substrate surface, i.e. the viscosity is high, and this impairs the wetting process at the interface. As a result the number of cavities increases due to the higher amount of trapped air, which leads to reducing the load-bearing area. The maximum size, the cavities can reach, decreases due to the large amount of neighbors cavities, inhibiting their expansion in lateral direction. Similar prediction of the effect of M_w on the cavitation process was reported in an earlier study [21].

The influence of the surface roughness of the substrate and the adhesive film on the cavitation was investigated in a previous study [59]. The investigated model system

was a blend of systematic SIS and hydrogenated resin miscible with the isoprene. The case of smooth and rough adhesive film, both tested with smooth and rough substrate with roughness $R_a = 10$ nm and $R_a = 150$ nm, respectively, were analyzed in detail. Important qualitative differences were found between “rough” interface (rough adhesive film or substrate) and the “smooth” interface (smooth adhesive film or substrate), but almost similar results for rough film and rough substrate case. The authors claim that the cavity size and real density is insensitive to the interface, because the cavities grow in the bulk of the polymer film and their size is controlled by the elastic properties of the material used. From results shown in Fig. 3.9 one can see that although viscoelastic properties of PASs play a decisive role, the number of cavities and their size are very sensitive to the roughness of the substrate used.

The simultaneously recorded video sequences were analyzed quantitatively and the number and size of individual cavities were determined, depending on time to study the kinetics of cavity growth. The number of cavities as a function of time with synchronized stress against time curves, for copolymers with intermediate $M_w = 192$ kg/mol measured with substrates of three different roughness are shown in Fig. 3.10a. Similar results are obtained for the adhesives with $M_w=54$ kg/mol and $M_w=600$ kg/mol.

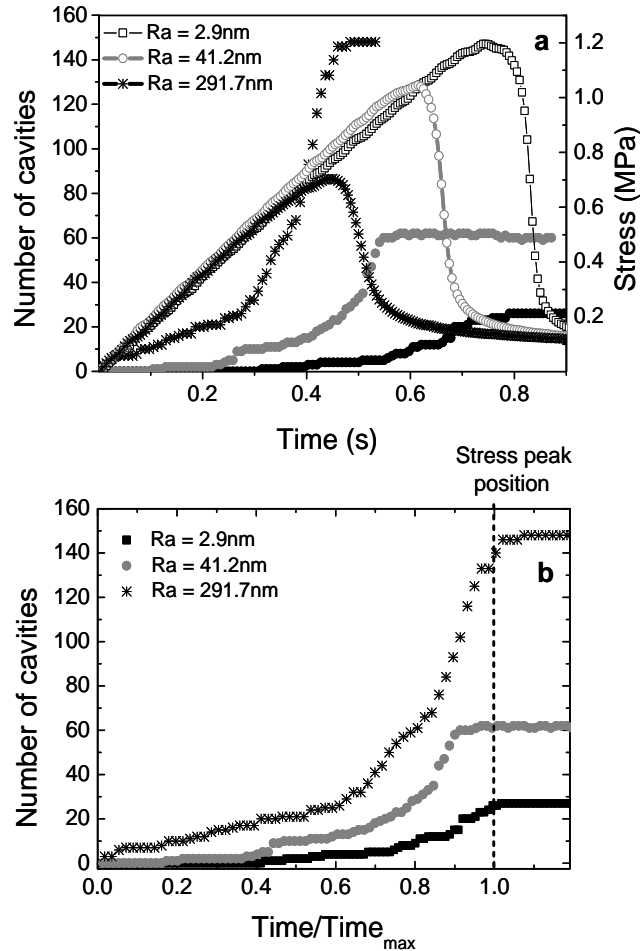


Figure 3.9. Number of cavities (closed symbols) and stress (open symbols) vs. time (a) and number of cavities vs. $Time/Time_{max}$ (b) for BA/MA PSAs with $M_w = 192$ kg/mol measured with substrates with different roughness.

The formation of the first cavities starts already long before the stress reaches its maximum value. The number of cavities increases slowly at the beginning of debonding and then grows rapidly with increase in the level of nominal stress and approaching the peak. It is important to mention that the increase in the substrate surface roughness leads to the result, that the maximum cavities density is reached faster and this results in earlier stress reduction in the adhesive bulk, and therefore the stress approaches its peak earlier and at the lower level. These results explained the decrease in the stress peak value with the increase in R_a , observed for all three M_w (Fig. 3.5), where a larger amount of contact defects on the interface, results in a nucleation of cavities, on a low nominal stress level. The value of maximal nominal stress is not only influenced by the rheological properties of the polymer but is affected by the size and

density of the initial defects present at the interface between substrate and adhesive [59].

Fig. 3.9b shows the number of cavities as a function of time divided by the time where the stress peak is reached. On the smooth surface no additional cavities appear after the nominal stress peak has been passed. On the rough surface and in case of adhesive with the highest molecular weight, few cavities occur even after the stress peak has been passed. Nevertheless, in all cases almost all of the cavities appear at the time interval until the stress peak is reached, and emergence of new cavities ceases before the stress starts to decay significantly and eventually reaches the characteristic plateau value.

Fig. 3.10 shows an example of stress vs. time curve and corresponding equivalent cavity radius vs. time curves. Additionally, images of the contact area are shown, taken at the time marked with vertical dashed lines on the diagrams. The measurements were performed using copolymer with the lowest molecular weight and the substrate with $R_a = 41.2$ nm. Time zero on both graphs corresponding to the zero crossing of the force-distance curve from tack measurements.

The series of typical curves cavity radius vs time illustrate that cavity growth continues almost until the characteristic plateau of the nominal stress curve is reached. Additionally, one can clearly distinguish two types of cavities. The cavities of the first type (filled symbols) occur at the beginning of debonding, long before the nominal stress approached its maximum value and their growth has two stages. On the first stage, when the stress value is low, cavities appear and then grow slowly with increasing the stress in the adhesive film. In the area of the nominal stress peak the cavities increase their growth rate (second stage). A similar behavior has been reported in earlier study [25].

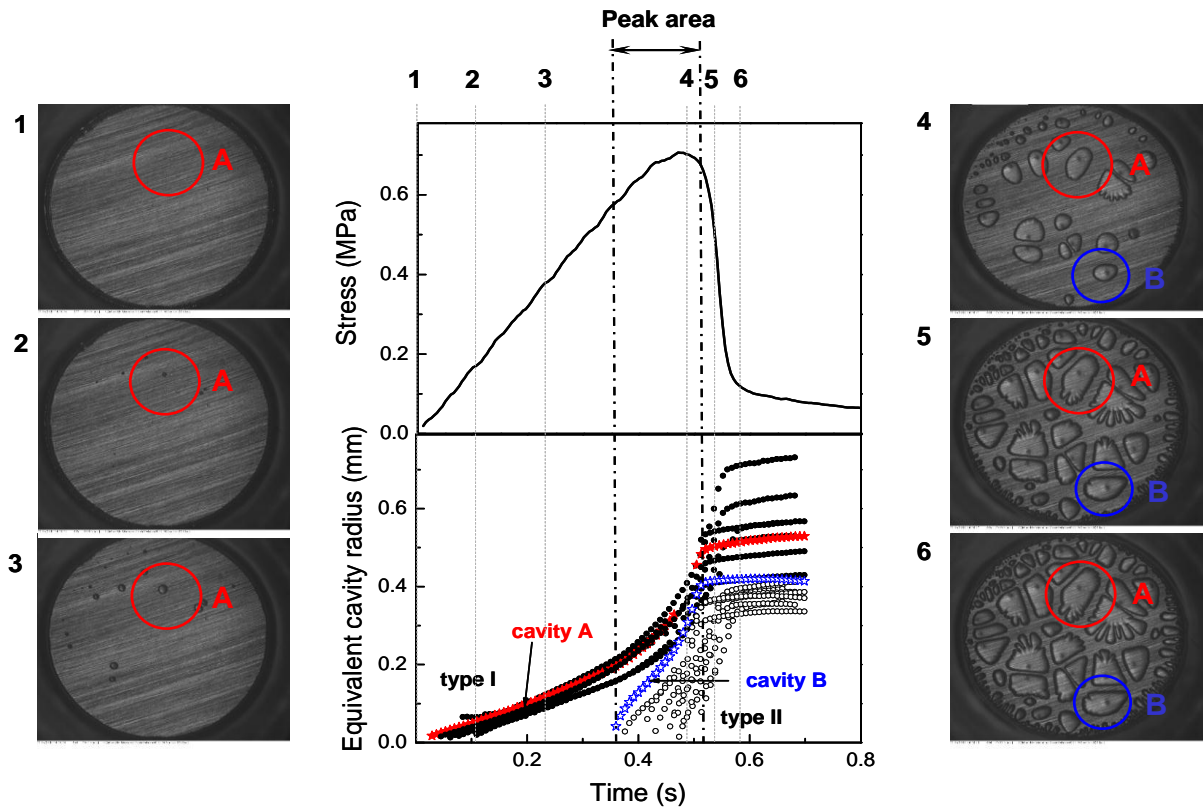


Figure 3.10. Typical nominal stress vs. time curve and corresponding equivalent cavity radius vs. time date measured using the substrate of $R_a = 41.2$ nm on the BA/MA PSAs of $M_w = 54$ kg/mol. In addition a sequence of images is shown illustrating the occurrence and growth of cavities of type I (A) and type II (B).

But in contrast to the exponential increase in cavity size observed there, the increase in growth velocity observed here, is much less pronounced. The cavities of the second type (open symbols) appear later, in the area of stress peak, and grow rapidly with a constant speed. The growth rate on the second stage of growth of the first type of cavities corresponds to the velocity of expansion of the second type of cavities. One can conclude that the main parameter, which governed the cavity growth rate here, is the level of stress at which the cavities appear.

- *Cavity growth rate*

Cavity growth rate was investigated in some earlier studies, but the knowledge about this phenomenon remains incomplete. Surface roughness of the substrate was expected to play an important role on cavity growth rate. The velocity of cavity growth was discussed in [59]. However, it was claimed there, that on the rough interface all cavities

expand simultaneously from contact defects, grow at the same rate and have similar size at any given time. On the smooth interface cavities occur sequentially and their growth rate increases with stress level, at which they appear. Cavities grow more rapidly, when they start to grow later, i.e. at higher stress level. In contrast, our experiments suggest that for all substrate roughness studied there are always two types of cavities, those appearing earlier and growing slowly, and those appearing later and growing with a higher rate.

Cavity growth rate as a function of the average roughness of the substrate for both types of cavities is shown in Fig. 3.11.

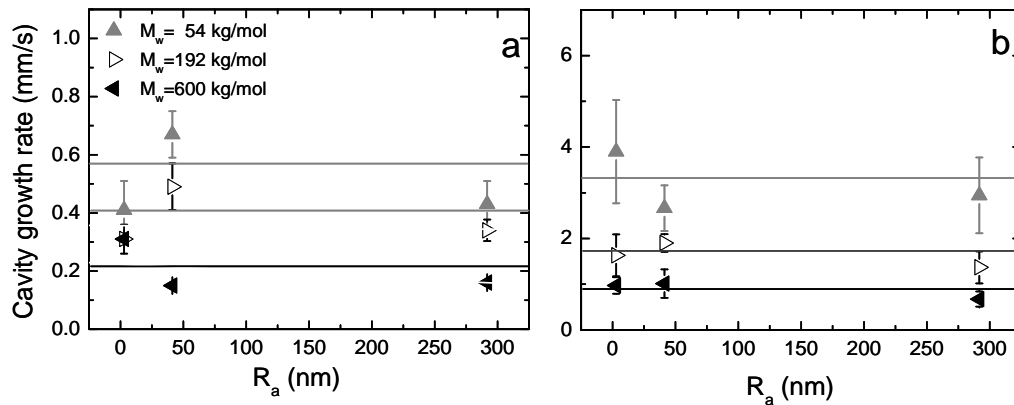


Figure 3.11. Cavity growth rate as a function of the substrate roughness for BA/MA PSAs with $M_w = 54$ kg/mol, $M_w = 192$ kg/mol, $M_w = 600$ kg/mol: (a) type I cavities occurring at the beginning of the debonding; (b) type II cavities occurring in the area of the stress peak.

Cavities of the second type grow approximately five times faster than the cavities of the first type. The surface roughness of the substrates has particularly no influence on the velocity of the cavity expansion for both types of cavities as shown in Fig. 3.11a, 3.11b. In contrast, in [66] where the investigated model system was acrylic latex PSA, based on EHA and measured with stainless steel substrate with R_a from 5 to 76 μm , it was speculated that rough surface slows down the growth of cavities. The authors observed that the slope of the strain-stress curves decreases with increasing R_a , just after the maximum stress is achieved, and this was interpreted as decrease of the lateral propagation rate of cavities. However, the experimental results in Fig. 3.6. show that for BA/MA PSAs the slope of representative stress vs. strain curves is essentially

independent of surface roughness and no influence of roughness on the cavity growth rate is seen (Fig. 3.11). The growth rate decreases significantly with increasing the molecular weight of the polymer. This demonstrates that, although surface roughness defect play a significant role in the cavitation process, the cavity growth rate is determined by the viscoelastic properties of the PSAs. Cavities appear at the interface from already existing defects, but they grow into the bulk polymer material; therefore their growth rate is insensitive to surface roughness.

However, different growth modes were observed on the smooth and rough substrates surface. The cavity growth rate is insensitive to the viscoelastic properties of the polymer (on the smooth substrate), and decrease with increasing the G' module (on the rough surface). This discrepancy in the mechanisms of debonding due to the different substrate surface roughness will be described in details in sec. 3.4.3 .

3.3.2. Surface energy of the substrate

The material of the probe (adherent) used in the tack test and its surface energy strongly influence the adhesion of PSAs.

To be able to make a prediction for the adhesion of the acrylate copolymers material on substrate made of various of materials, it is important to carry out systematical investigations of the influence of the surface energy on the adhesive process. Surface energy plays an important role in the process of bonding, namely influences the wetting of the adherent by the adhesive. An obstacle in the quantitative characterization of the substrate surface is the fact that surface energy is difficult to be determined, and there is a lack of such data, particularly in relation with tack experiments [108].

In an early study [71] the adhesion of model PSAs on low surface energy has been investigated. Typically used substrates with low surface energy were polypropylene (PP), polyethylene (PE) and silicone rubbers. The reported results, however, were contradictory and could not clarify the effect of the surface energy on the adhesion behavior of PSAs. In these earlier works there was an assumption that tack significantly decreases with decreasing the surface energy of the substrate to values well below the values of the surface energy of the polymer film. Recently there were several studies on

the adhesion of PSAs on different substrates [72-76], however in the majority of cases only two type of substrates were investigated, namely stainless steel and polyolefines (PE, PP). The substrate studied here are made of four different materials: stainless steel, polyethylene, silica wafer and glass (additionally hydrophobized) for better investigation of the influence of the substrate material on the adhesion of PSAs.

- *Stress-strain curve*

Fig. 3.12 shows the nominal stress as a function of strain for BA/MA PSAs with intermediate molecular weight measured with substrates of different materials: polyethylene PE, stainless steel, hydrophilic (Glass_{25°}) and hydrophobic glass (Glass_{100°}) and silica wafer. Here it is necessary to admit, that the preparation of substrate with identical surface roughness of $R_a \sim 2$ nm is important due to the strong influence of the roughness on the adhesion process. However, it was impossible to prepare polyethylene with surface roughness lower than $R_a \sim 45$ nm. Therefore, one can compare the results obtained using stainless steel and polyethylene substrates with $R_a \sim 45$ nm, and steel, hydrophilic glass, hydrophobic glass and silica wafer substrates with $R_a \sim 2$ nm. The glass substrate was additionally hydrophobized in order to obtain contact angle and surface energy values similar to the values for PE.

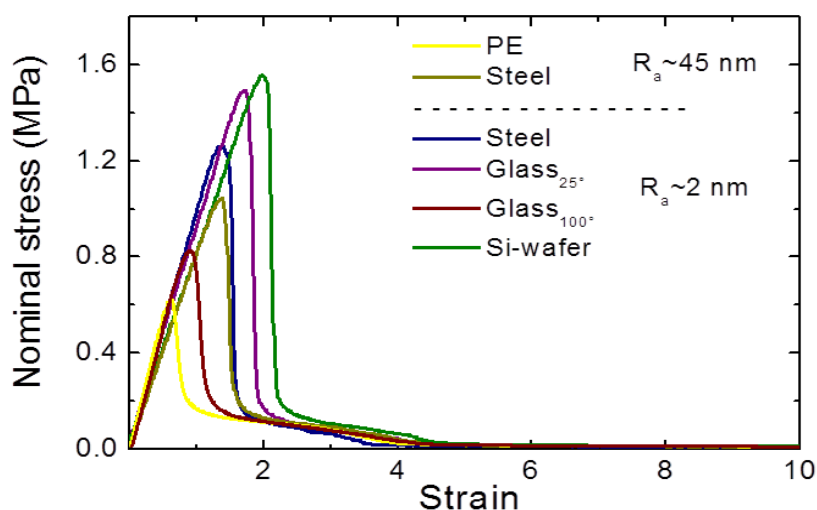


Figure 3.12. Nominal stress vs. strain for BA/MA PSAs ($M_w = 192$ kg/mol) measured with substrate made of PE (polyethylene), stainless steel, hydrophilic glass (Glass_{25°}), hydrophobic glass (Glass_{100°}), silica wafer and two roughness $R_a \sim 45$ nm and $R_a \sim 2$ nm.

Fig. 3.12 shows that, as expected, in case of the same polymer, on the initial stage of debonding, the stress increases with similar slope for all studied substrates. Tack curves measured with hydrophilic substrates, such as steel, glass_{25°} and silica wafer, exhibit high stress peak, corresponding to higher values of surface energy, while the curves measured with PE and hydrophobic glass show lower stress peak, due to their low values of surface energy.

- *Tack, stress peak and deformation at break*

Fig. 3.13 shows the values of parameters calculated from the stress-strain curves, namely stress peak, deformation at break and tack for BA/MA with intermediate molecular weight measured with substrates of different materials. As already mentioned, increasing the surface energy of the substrate results in increase in the stress peak and tack values. The explanation of this result can be found in the fact that during the bonding between the polymer and a substrate with higher surface energy, energy is gained by the establishing of the contact. Contact between substrate and polymer is preferred, compared to that between substrate and air, which leads to a promoting of the wetting process. The values of stress peak and tack are similar for stainless steel and hydrophilic glass substrates; the discrepancy is within the experimental error. Similar results have been observed earlier in [6] for random copolymer 2-ethylhexyl acrylate - acrylic acid (PEHA-AA) and homopolymer of poly (2-ethylhexyl acrylate) (PEHA) measured with stainless steel substrate with $R_a = 0.1 \mu\text{m}$ and glass probe with $R_a = 0.05 \mu\text{m}$.

The difference between substrates with high and low surface energy were analyzed in terms of the parameter G_c/E and reported in [113]. Three different cases of this ratio of the energy release rate G_c and the elastic modulus of the adhesive film were discussed. High value of G_c/E is accompanied with cavitation and fibrillation and is usually observed on steel and glass, which exhibit high values of the surface energy. In this case, the elongational properties of the fibrils are controlled by the rheological behavior of the adhesive, and not by the surface of the substrate. For a low G_c surface-adherent pair, and intermediate value of G_c/E , the maximal stress was found to be similar to the stress on steel, while the deformation at break was reduced. Authors conclude that the failure begins at the same stress level on high and low energy surface, but the lateral

growth of the appeared defects proceeds much faster in the low G_c situation. The failure occurs with cavitation and fibrillation, but the maximal expansion of the fibrils was controlled by the surface. For very low values of G_c/E , the initiation mechanisms were detected to be interfacial crack propagation. In this case, for the same hard elastic adhesive on steel and on low G_c surface-adherent pair, the nominal stress and deformation at break are significantly reduced for the substrate with low surface energy. Additionally, the cavities that appeared on low energy surface had a large irregular shape, whereas on steel substrate cavities were relatively small. Transition of intermediate value G_c/E to high value and accordingly bulk to interfacial failure appears by reducing the debonding rate. Because of the variation of the debonding velocity, a comparison between the results from these earlier studies and the results for the copolymers studied here is quite difficult. However, substrates made of different materials were used here, but the nominal stress peak and the corresponding tack decreases with decreasing the surface energy, while deformation was insensitive to the surface energy (Fig. 3.14). Although low surface energy reduces the G_c [31], for all substrates used here it was found that the failure is accompanied by cavitation and fibrillation and the maximal expansion of the fibrils is mainly controlled by the viscoelastic properties of the adhesive.

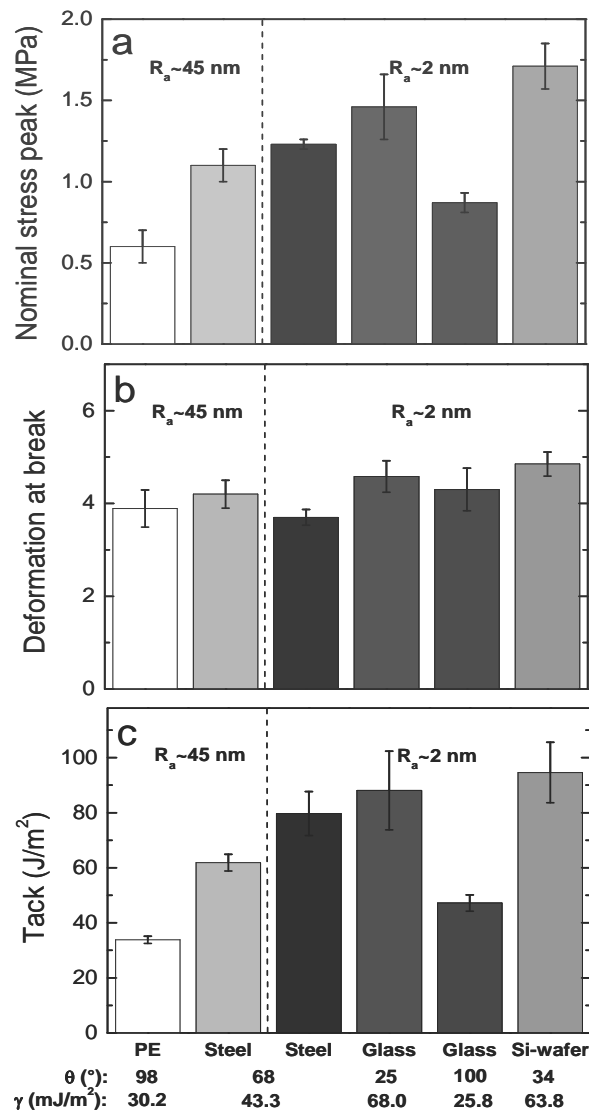


Figure 3.13. Nominal stress peak (a), deformation at break (b) and tack (c) for BA/MA PSA ($M_w = 192$ kg/mol) measured with substrates made of different materials with different surface energy γ_s (mJ/m^2) and two roughness $R_a \sim 45$ nm; $R_a \sim 2$ nm.

Therefore, one can assume that the surface energy of the substrate affects mainly the wetting and cavitation process and the correlated nominal stress peak.

Creton and et. al. [31], have investigated the elastic model system SIS and viscoelastic model system PEHA, measured with two types of stainless steel substrates, and hydrophilic modified steel with grafted monolayer poly (dimethylsiloxane) PDMS. The surface properties were described by a critical energy release rate G_c . The interfacial parameter influenced not only the value of the adhesion energy, but also mechanism of debonding, namely crack propagation and cavitation. It was found that for PEHA the maximum stress was insensitive to the substrate type, while for SIS the stress peak was

determined lower on the hydrophilic modified substrate. The authors interpret their results with the bulk cavitation for PEHA on both type of substrates, and crack propagation for SIS on PDMS-coated substrate. The different separation mechanism on hydrophobic modified substrate for the elastic system, the authors explained with the reduce in the critical energy release rate G_c , which results in an appearance of interfacial crack propagation, before the stress level reaches the critical values necessary for the expansion of cavities in the bulk of the polymer. In contrast, although the formation of cavities is also observed for the viscoelastic model system studied here on different substrates, the stress peak is markedly influenced by the substrate material (Fig. 3.13). Deformation at break is insensitive to the substrate material, as expected, since it is mainly controlled by the viscoelastic properties of the adhesive and substrate surface energy plays no role. In agreement with earlier studies [3, 66], stress peak and tack values decrease with decreasing the substrate surface energy. Toyama and co-worker have investigated the adhesion on polytetrafluoroethylene (Teflon), high-density polyethylene (PE), poly(methyl methacrylate) (PMMA) and poly(hexamethylene carboxamide) (Torey's Nylon 6) for acrylic adhesive copolymer ethyl acrylate and poly(ethyl vinyl ether) [70, 71]. The authors reported a maximum work of adhesion measured on substrates with values of surface energy near to the value of the polymer film, which differs from the results obtained for the substrates investigated here.

- *Total number of cavities and final average cavity area*

The effect of the substrate on the cavitation process is poorly investigated so far. Since the surface energy influences the wetting process, differences in the amount of cavities and eventually also in the velocity of cavity growth are expected.

The images of the contact area between the adhesive and substrate were recorded and the cavitation process was studied. For all substrates two types of cavities were observed: the cavities of the first type, which appear at the beginning of debonding, and the cavities of the second type, which appear later in the area of the stress peak. The images of the contact area, taken at the time when the lateral growth of cavities is finished are shown in Fig. 3.14.

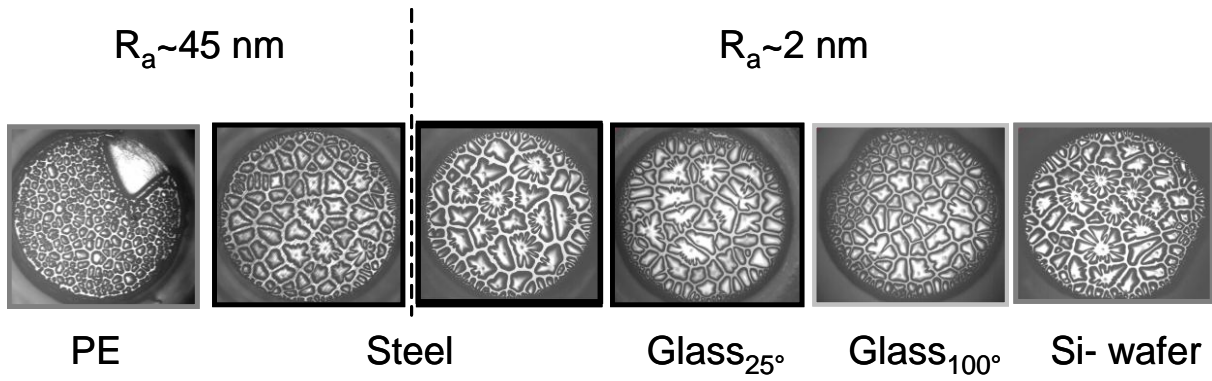


Figure 3.14. Representative images of contact area of the substrates made of different materials (different surface energy) and two roughness $R_a \sim 45 \text{ nm}$ and $R_a \sim 2 \text{ nm}$.

One can see, that in comparison to other substrates much more cavities appear on the PE surface and their size is smaller. This is due to worst wetting of PE substrate. The lower the substrate surface energy, the less round are the occurred cavities. Similar observation was reported in [6] where images of PEHA on polished stainless steel and spincoated polystyrene were recorded. However, the determined values of adhesion energy on the studied substrate surfaces was found to be quite comparable, the authors explained it with the lack of fibril structure formed during the debonding. This results confirm the conclusions made by the analysis of the role of the substrate surface roughness in the adhesion process, namely that there is a strong correlation between the bulk properties of the polymer and the substrate surface, which influence the cavitation process.

Fig. 3.15 shows the nominal stress vs. time and corresponding number of cavities vs. time, as well as the curves for number of cavities vs. time normalized to the time at which the stress reaches its maximum for BA/MA copolymers with intermediate molecular weight measured with substrates made of different materials.

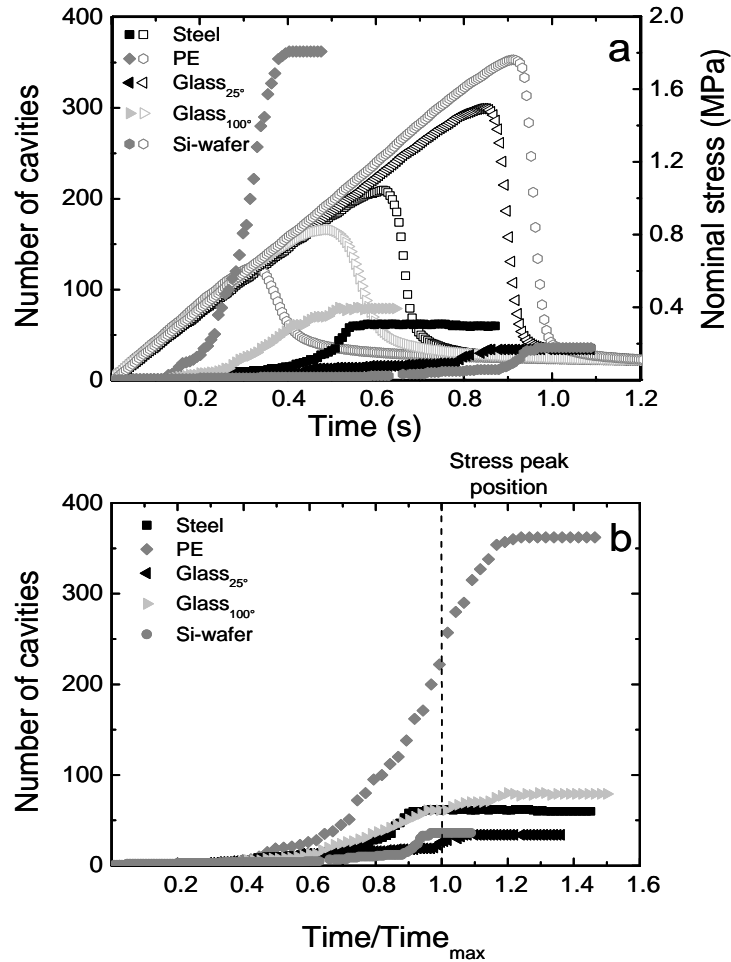


Figure 3.15. Number of cavities (closed symbols) and nominal stress (open symbols) as a function of time (a) and number of cavities vs. time/time_{max} (b) for BA/MA PSA with $M_w = 192$ kg/mol measured with substrates made of different materials and similar roughness $R_a \sim 2$ nm.

With increasing the surface energy of the substrate, the number of cavities decreases and, accordingly, their size increases due to better wetting (Fig. 3.16). In the case of hydrophilic probes, no additional cavities appear after the stress peak is reached, whereas, on the hydrophobic substrates, some additional cavities appear even after the maximum of the stress peak is passed.

- *Cavity growth rate*

Cavity growth rate on the substrates with different surface energy was studied and the results are shown in Fig. 3.16.

There is no clear influence of the substrate surface energy on the velocity of cavity expansion.

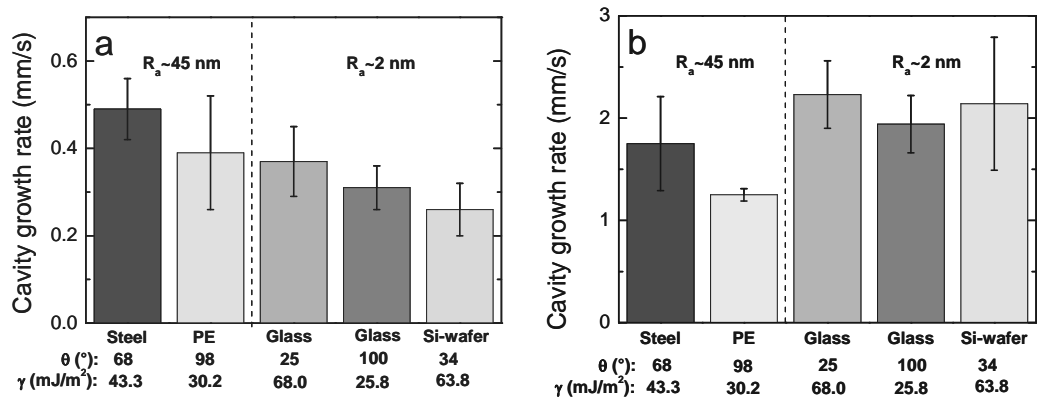


Figure 3.16. Cavity growth rate for substrates with different surface energy γ_s (mJ/m²) and two roughness $R_a \sim 45$ nm; $R_a \sim 2$ nm: (a) type I cavities occurring at the beginning of the debonding; (b) type II cavities occurring in the area of the stress peak.

It can be summarized that the substrate properties such as surface roughness and surface energy play an important role on the adhesion process. Both properties influence the nominal stress peak and correlated tack values, as well as the amount of the appeared cavities, due to the discrepancy in the wetting process. Deformation at break is mainly controlled by the viscoelastic properties of the adhesive film, and not by the characteristics of the substrate surface. Cavity growth rate is found to be insensitive to the surface roughness and surface energy of the substrates.

3.4. Influence of the polymer film modifications on the adhesion of PSAs.

3.4.1. Chemical composition of the polymer

According to the earlier studies [7, 52] changes in the monomer composition of the adherent often results in change of both bulk properties and surface characteristics of the polymer film. This leads to change in the adhesion performance of PSAs. For the investigation of the effect of the incorporated functional comonomer and its polarity on the adhesion of PSAs, copolymers with different composition and the same molecular weight were used. An important question is if the influence of the incorporated polar comonomer results from the modified bulk properties like T_g or rather through interfacial interactions.

Fig. 3.17 shows refractive index profiles of the near-surface region extracted from X-ray reflectivity data.

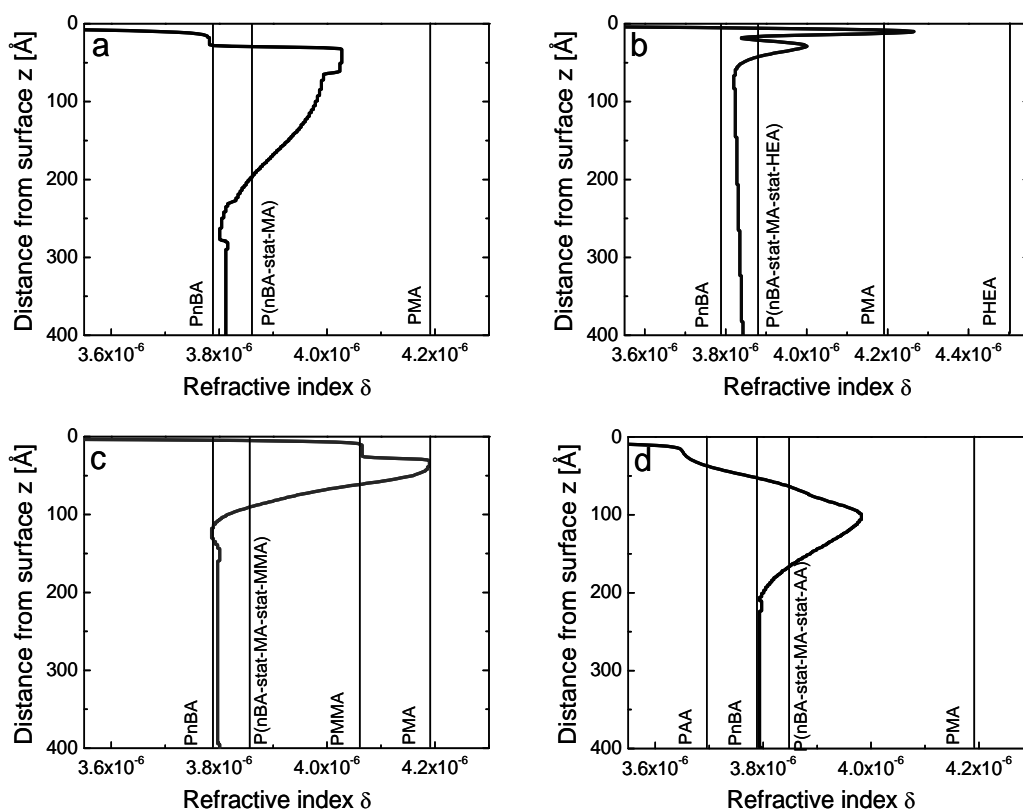


Figure 3.17. Refractive index profiles of the near-surface region extracted from X-ray reflectivity data of BA/MA (a), BA/MA/HEA (b), BA/MA/MMA(c) and BA/MA/AA films. The measurement were performed by Alexander Diethert – University of Munich and published in [114].

The vertical lines mark the values of the refractive index of the statistical copolymer and the related homopolymer as shown by the labels and the depth $z = 0$ denotes the sample surface.

- *Surface enrichment of the adhesive film*

The composition of the PSA films near the surface differs from the composition in the bulk film. Fig. 3.18 shows the refractive index profiles for a distance from the sample surface between $0 < z < 400 \text{ \AA}$ in order to emphasize the near-surface composition. At $z > 400 \text{ \AA}$ the composition of the film in all cases converge to the average composition of the statistical polymers. The surface of BA/MA copolymers is enriched with BA, while the surface of the other copolymers is not enriched with BA. While it is not possible to calculate the composition of a ternary system directly one can clearly see that the

surface of BA/MA/AA film is enriched with AA. For BA/MA/HEA and BA/MA/MMA films the results are ambiguous, and it can be conclude that in both cases the surface in not enriched with BA. In the BA/MA/MMA film, there is an MA enriched region close to the surface. On the other hand integration of the additional comonomer does not change the surface energy of the copolymers (Tab.2.5). Table 3.3. shows the surface energy of polymer films measured as well as the literature values of their homopolymers.

Table 3.1. Surface energy values of polymer films and literature values of their homopolymers [114, 115, 116].

type	Surface energy γ (mJ/m ²)
BA/MA	31.8 ± 6.0
BA/MA/HEA	31.4 ± 5.9
BA/MA/MMA	32.1 ± 6.1
BA/MA/AA	30.3 ± 6.1
PBA	30.7
PMA	41
PHEA	37
PMMA	35

The surface energy values of BA/MA and BA/MA/AA copolymers are close to surface energy values of PBA while is the major component of the PAA. Here could be assumed that the incorporation of polar comonomer in the polymer chain does not change the surface tension of the adhesive film. In contrast, Li and co-worker [38] reported that acrylic acid content in studied PSA-LNs (acrylic acid copolymerized with 2-ethyl hexyl acrylate and 1,6-hexane diol diacrylate) increases the surface energy measured according to JKR-based contact mechanisms. The discrepancy found between our study and the previous one, eventually results from the different adhesives and different methods for surface energy determination used.

Even the enrichment of PMA and PHEA close to the surface has no effect on polymer surface energy although the surface energy of these polymers is significantly higher than that of the major component PBA. Obviously the macroscopic wetting

experiments average the vdW interactions over a length scale larger than that analyzed in the x-ray reflection experiments.

- *Stress-strain curves*

Fig. 3.18 shows the stress-strain curves for BA/MA and BA/MA with incorporated functional comonomers AA, MMA and HEA with similar molecular weight, and measured with stainless steel substrate with two different roughnesses. The effect of roughness is characterized by approximately twofold decrease in the nominal stress peak and corresponding tack values at lower roughness. Therefore, the stress-strain curves increase with different slope at the initial stage of debonding, which correspond to different elastic modulus E by the different composition on the smooth surface.

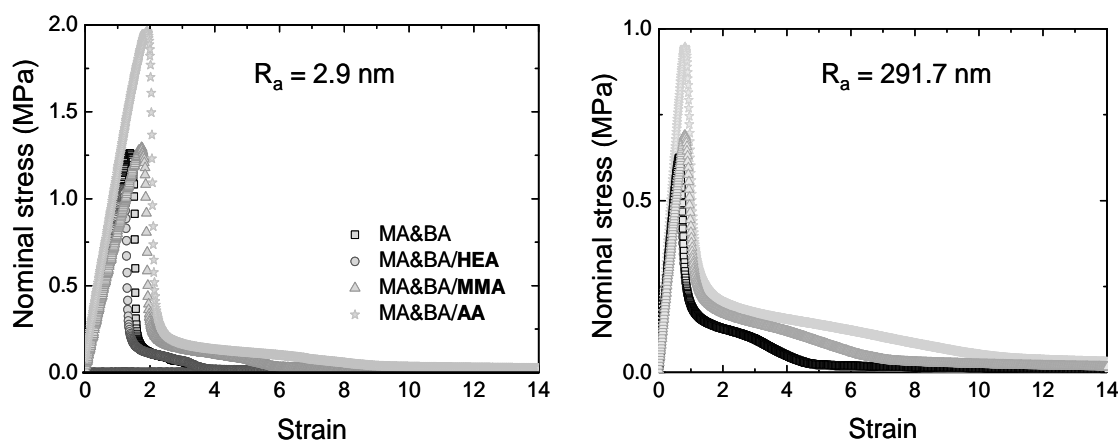


Figure 3.18. Nominal stress vs. strain curves for adhesives with different composition measured with stainless steel substrates with different roughness.

From the stress-strain curves one can clearly see, that copolymer with incorporated small amount of acrylic acid exhibit the highest stress peak. The nominal stress peak value of BA/MA/AA is approximately 1.5 times higher as of BA/MA. As expected, the characteristic plateau, which corresponds to the deformation of the formed fibrils, increase with increasing the polarity and the rheological moduli of the functional monomer. Variation in the monomer composition of the copolymer, leads to change in the viscoelastic properties which results in different elongation ability of the fibril structures. Note, that the stress-strain curves for BA/MA and BA/MA/HEA are almost identical due to similar G' and G'' values (Fig. 3.1).

- Tack, nominal stress peak and deformation

Fig. 3.19 shows the values of stress peak, deformation at break and tack, calculated from stress-strain curves for PSAs with different composition measured with stainless steel substrate with two different R_a . As was already shown above (see section 3.3.1) and can be seen in Fig. 3.19, the roughness of the substrates has no effect on the deformation at break, it is controlled only by the viscoelastical properties of PSA.

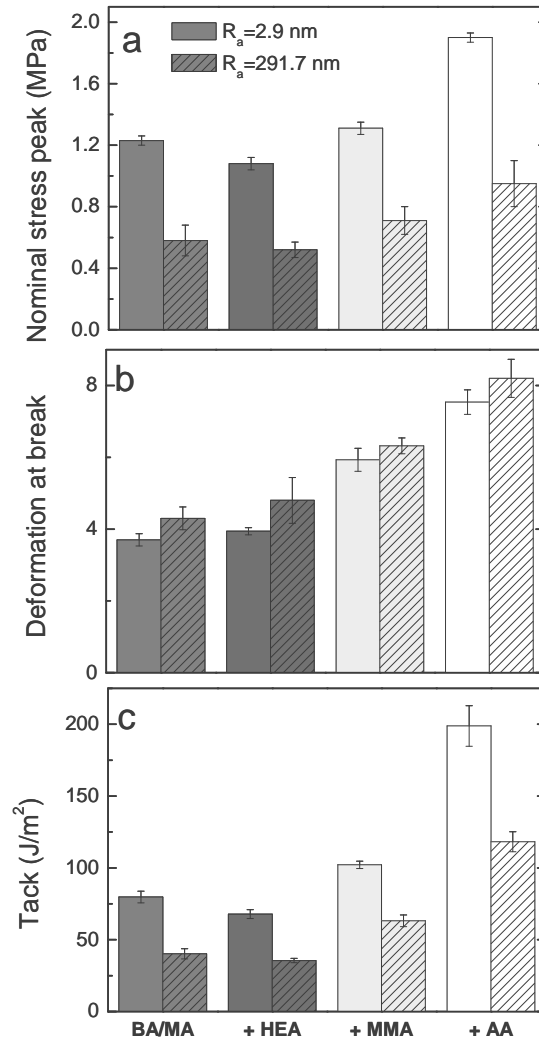


Figure 3.19. Nominal stress peak (a), deformation at break(b) and tack(c) for BA/MA and BA/MA with additional functional monomer: HEA; MMA and AA measured with steel surface of two different roughness $R_a = 2.9$ nm and $R_a = 291.7$ nm.

In case of a rough substrate, which goes deep into the PSA film during the tack test, the bulk properties of PSA play the decisive role in adhesion. In contrast, in case of a smooth probe, the surface composition i.e. surface properties are assumed to determine the adhesion behavior of PSA. For both substrates the value of stress peak, deformation

at break and tack increase with increasing polarity of the functional comonomer (Fig. 3.19). The copolymer containing AA exhibits the high values for the tack parameters, which could be related to the additional hydrogen bonds between the carboxylic groups, acting as physical cross-linking. Incorporating a small amount of AA increases the tack values more than a factor of 2 for both substrate roughness. Similar results were obtained in an earlier study [7] where AA copolymerized with poly (butyl acrylate) was used. The authors estimated that the presence of 10% by weight of copolymerized acrylic acid increases the thermodynamic work of adhesion by a factor of about 1.5. Chan and co-worker [52] investigated the adhesive performance of ethyl acrylate copolymerized with polar comonomers AA, MMA, HEA and acrylonitrile (AN) and found out that incorporation of a small amount of polar monomer results in an increase in tack values up to a maximum beyond which it drops for all cases. However, they observed that the failure mode was apparently interfacial in all cases. Nevertheless, the authors conclude that at low levels of polar comonomer the adhesion is influenced by the improved interfacial interaction with the substrate, rather than by the bulk properties, while at the higher polar contents the hardening of the polymer is sufficient to decrease the tack strength.

Due to the fact that the surface energy of the polymer was not changed after copolymerization with a polar monomer, one can surmise that the change of adhesive properties of the acrylic polymers, studied here, are influenced by the modification of the viscoelastic properties and not of the surface energy of the adhesive films. Furthermore, the values of the stress peak, deformation at break and tack also increase with increasing shear modulus. One can assume that the viscoelastic properties of the PSA, especially on the rough surface, mainly influence its tack.

- *Number of cavities and cavity growth rate*

Images of the contact areas polymer/substrate recorded at the time where the lateral growth is finished are shown in Fig. 3.20. The cavities for BA/MA/AA on a smooth surface (Fig. 3.20a₄) are rounder due to the predominant elastic behavior of this sample. On a rough substrate surface this discrepancy in the cavity shape vanishes, because of the higher amount of appeared cavities.

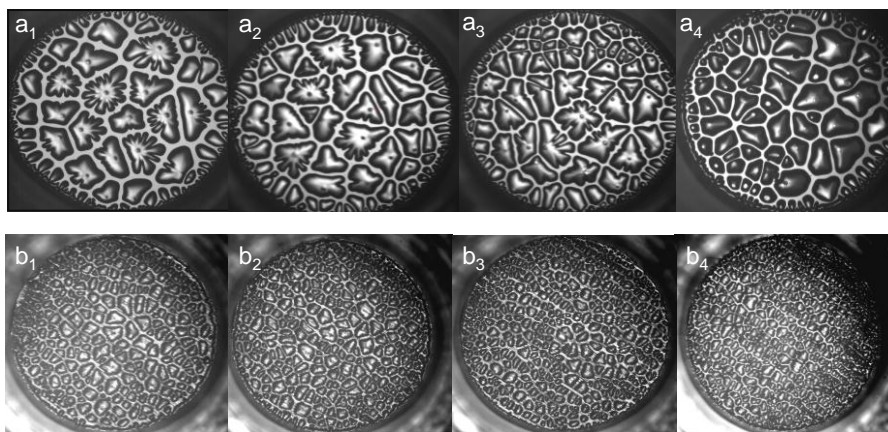


Figure 3.20. Representative images for (1) BA/MA; (2) BA/MA/HEA; (3) BA/MA/MMA and (4) BA/MA/AA obtained with (a) smooth $R_a = 2.9\text{nm}$ and (b) rough substrate $R_a = 291.7\text{nm}$.

Number of cavities vs. time and corresponding stress-time curves, as well as number of cavities vs. time normalized to the time at which the stress reaches its maximum are shown in Fig. 3.21. With increasing the polarity and viscoelasticity, the maximum stress occurs later in time. Additionally, only few additional cavities occur after the maximum stress is reached. From the curves for the number of cavities vs. time one can see that increasing the polarity and viscoelasticity of the polymer results in an increase in the number of cavities at the beginning of debonding, apparently due to worst wetting. In contrast to the effect of the substrate surface roughness, the highest number of cavities corresponds to the highest stress peak. One can conclude that the influence of the bulk properties is greater than the effect of the surface characteristics.

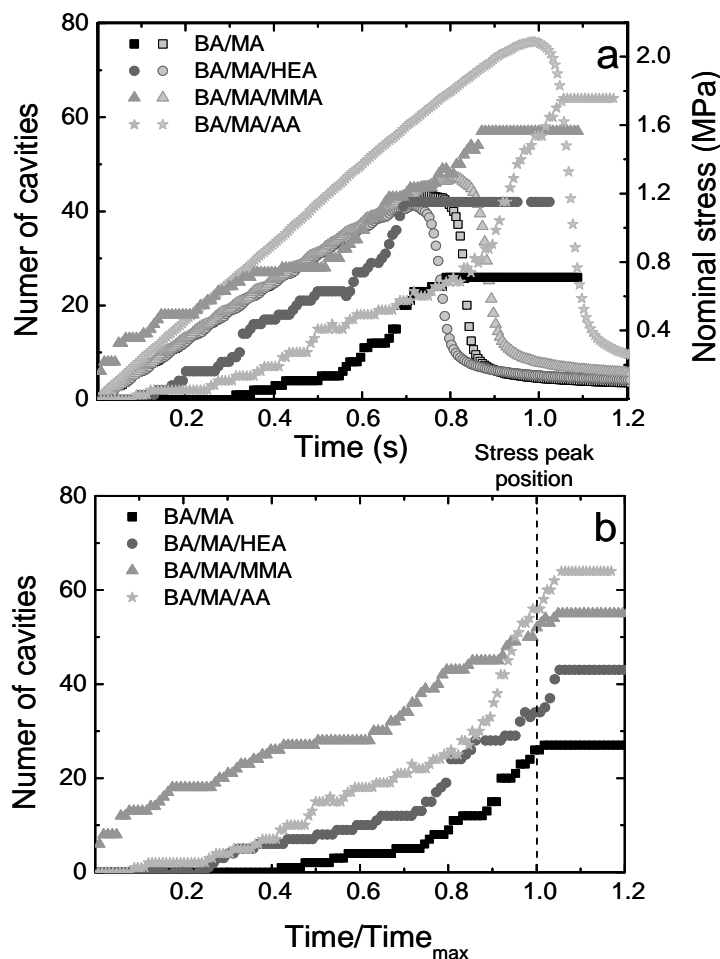


Figure 3.21. Number of cavities (dark symbols) and nominal stress (light symbols) as a function of time (a) and number of cavities vs. time/time_{max} (b) for BA/MA PSA with $M_w = 192 \text{ kg/mol}$ measured with steel substrates with roughness $R_a \sim 2 \text{ nm}$.

The total number of cavities calculated from the images of the contact area of the substrate with PSA is shown in Fig. 3.22. The cavitation process is influenced by the polarity of incorporated comonomer, increasing comonomer polarity leads to an increase in the number of cavities, with the PSA containing AA having the highest number of cavities. This effect is even more pronounced in the case of a smooth substrate, due to its AA enriched surface, which may be attributed to the poor wetting of the substrate with the AA containing copolymer (Fig. 3.17). Thus, experiments with substrate of different roughness demonstrate that inferior wetting results in a larger number of cavities. This is not only interfacial effect due to the high polarity of the AA-enriched surface layer, but decrease wetting is also caused by an increase in the modulus for the PSA including AA. An additional consequence of the enhanced

modulus is the high stress peak observed despite the poor wetting mentioned above. Thus, bulk properties play the decisive role in the adhesion.

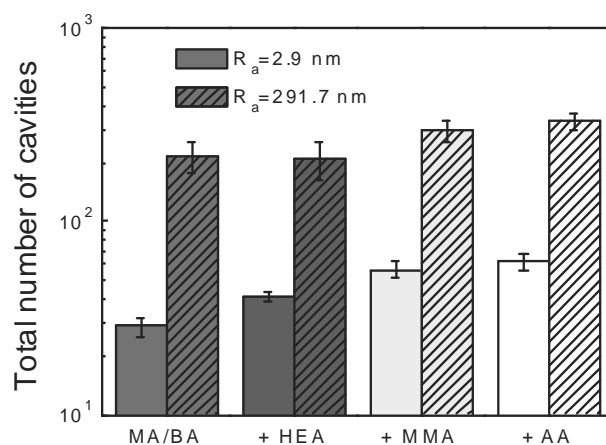


Figure 3.22. Total number of cavities for BA/MA and BA/MA with additional functional monomer: HEA; MMA and AA measured with steel substrate of surface roughness $R_a = 2.9 \text{ nm}$ and $R_a = 291.7 \text{ nm}$.

Debonding of BA/MA PSAs with an incorporated comonomer is also accompanied by the presence of two types of cavities (see sections 3.3.1 and 3.3.2). Fig. 3.23 shows the cavity growth rates for copolymers with different compositions.

On the rough surface, the growth rate is determined by the viscoelastic properties of PSA, i.e. an increase in the modulus leads to a reduction in cavity growth rate. On the smooth surface, there is no dependence on the composition of copolymers and their viscoelastic properties; in this case, the cavities grow on the surface and not in the bulk as will be discussed in detail in sec. 3.4.3.

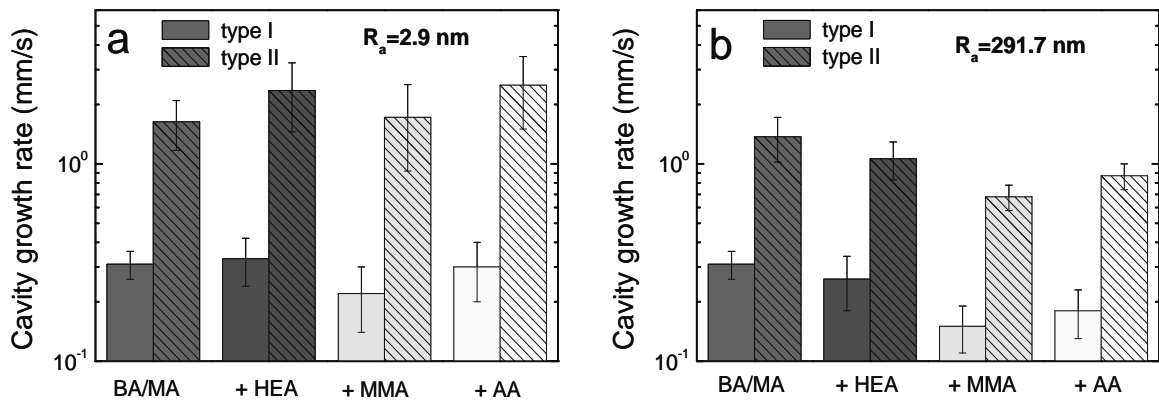


Figure 3.23. Cavity growth rate for the two type of cavities (I type, occurring in the beginning of debonding and II type, occurring at the region of the stress maximum and growing faster) for BA/MA and BA/MA with additional functional monomer: HEA; MMA and AA measured with steel substrate with roughness (a) $R_a = 2.9$ nm and (b) $R_a = 291.7$ nm.

- Adherent surface energy and adhesive with additional functional comonomer

As discussed above the substrate surface roughness has similar effect on adhesion irrespective of the monomer composition of the PSAs. Further, it is interesting to compare the influence of the substrate surface energy on the adhesion of BA/MA copolymer with and without additional functional comonomer. For this purpose, BA/MA/AA PSAs were measured with hydrophilic and hydrophobic glass substrate. This substrates were chosen, due to their identical R_a and different surface energies; hydrophilic glass with $\gamma_s = 68$ mJ/m² and hydrophobic glass with $\gamma_s = 25.8$ mJ/m².

Fig. 3.24 shows the nominal stress vs. strain curves for BA/MA/AA measured with hydrophilic and hydrophobic glass substrate.

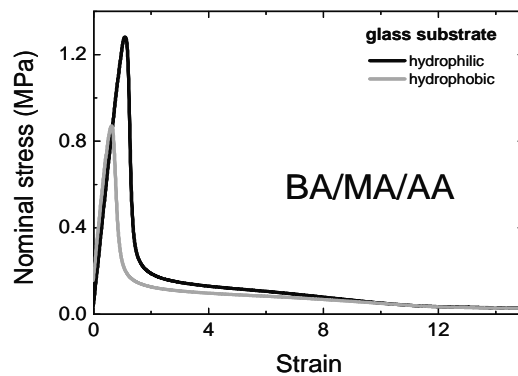


Figure 3.24. Nominal stress vs. strain for BA/MA with incorporated functional monomer AA measured with hydrophilic and hydrophobic glass substrates.

One can see that increasing the substrate surface energy results in an increase of stress peak value by a factor of about 1.5; similar result was obtained for BA/MA PSA measured with hydrophilic and hydrophobic substrates (Fig. 3.12).

The values of stress peak, deformation at break and tack, calculated from the stress-strain curves for BA/MA and BA/MA/AA and measured with glass substrates with different surface energy, are shown in Fig. 3.25.

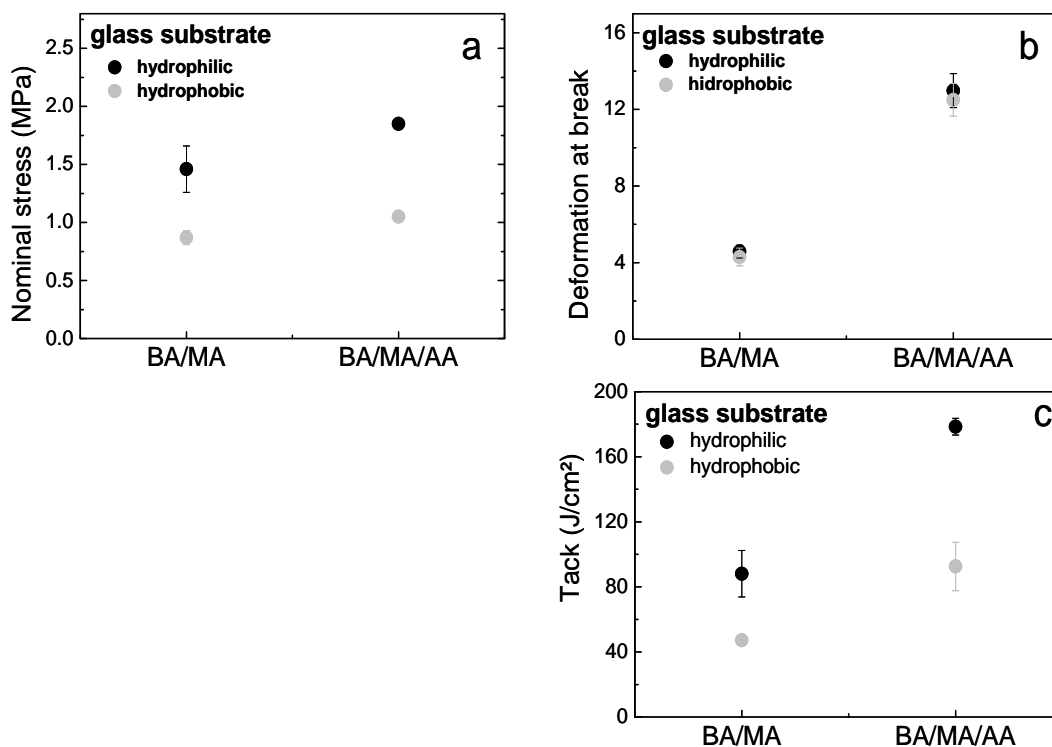


Figure 3.25. Nominal stress (a); deformation at break (b) and tack (c) for BA/MA and BA/MA/AA with incorporated functional monomer AA measured with hydrophilic and hydrophobic glass substrates.

Polymer with incorporated AA comonomer exhibit higher stress maximum and tack, as already mentioned, but the influence of the substrate surface energy on the adhesion performance is almost identical for BA/MA and BA/MA/AA. One can assume that the viscoelastic properties of the polymer have more pronounced effect, than the surface energy of the substrate. Furthermore, the surface properties of substrate do not influence the deformation at break neither for BA/MA, nor for BA/MA/AA. However, in an earlier study [117], the carboxyl group concentration were observed by incorporation of carboxylic groups into a polymer. It was found that the additional small amount of carboxyl groups markedly increase the bond strength on polar

substrate as glass. However, since the influence of the viscoelastic properties of the polymer film is significant, it is difficult to separate the effect of the bulk and interface characteristics on the adhesion performance of PSAs.

Fig. 3.26. shows the images of the contact area of polymer and substrate recorded at the time when the lateral cavity growth finished and obtained on glass substrates with different surface energy.

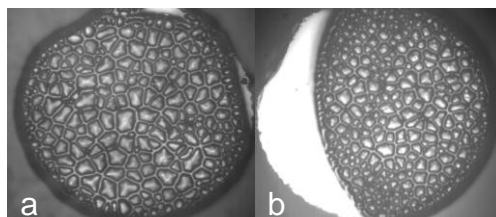


Figure 3.26. Representative images of contact area for BA/MA/AA obtained using hydrophilic (a) and hydrophobic (b) glass.

Number of cavities calculated from the images: 141.5 ± 5.3 on hydrophilic glass and 307.9 ± 8.4 on hydrophobic glass for BA/MA/AA. The number of cavities increases with decreasing surface energy in case of BA/MA/AA similarly to the increase of the number of cavities for BA/MA.

Similarly to the results obtained for BA/MA, no clear influence of the surface energy on the cavity growth rate was found for BA/MA/AA.

One can conclude that for polymer films with different chemical composition, there is similar effect of the substrate surface characteristics on the adhesive performance. Finally we conclude, that the results obtained for the substrates with different surface roughness and surface energy can be used for other system in order to establish an universal model of the effect of the interfacial phenomenon on the adhesive behavior of PSAs.

3.4.2. Crosslinking

The degree of crosslinking after exposure to ultra violet light (UV) strongly influences the performance of PSAs. This is a unique property of the polymers used here, since they include a small amount of photoinitiator. With crosslinking of acrylate copolymers, one can vary their adhesive properties in a wide range. The increase in

crosslink density results in transition from tacky performance to cohesive behavior, and the optimum in the adhesive performance was found to be near the gel point ($G' \approx G''$) in the broad frequency range, i.e. the transition range from uncrosslinked to crosslinked behavior [8]. The crosslinking below the gel point affects the fibril stability and elongation flow by applied load. Therefore, the deformation ability of the fibrils increased, which leads also to an increase in the tack energy value. In case of crosslinking above the gel point, strain hardening occurs during the elongation process. However, due to significant strain hardening an earlier detachment from the substrate can be observed.

The motivation for the study of crosslinked acrylate copolymers in this work is based on the fact that when these materials are uncrosslinked or crosslinked only by hydrogen bonds, they exhibit insufficiently thermomechanical stability and are practically useless as PSAs [118].

- *Variation of the UV dose*

Fig. 3.27 shows stress-strain curves for BA/MA crosslinked with different UV dose.

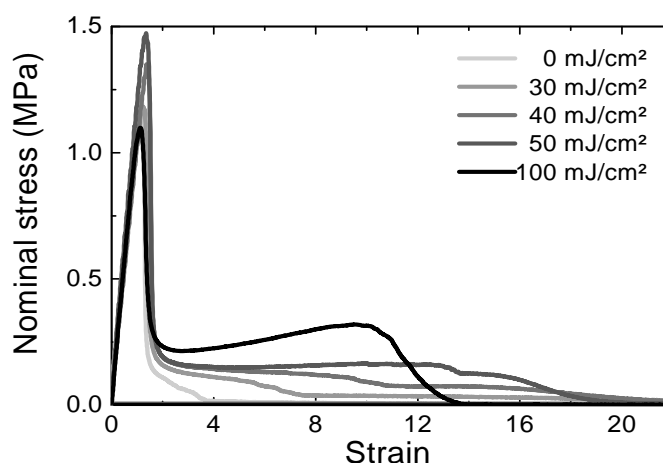


Figure 3.27. Nominal stress vs. strain for BA/MA PSAs with $M_w = 192$ kg/mol crosslinked with different UV doses.

One can see that for all copolymers (uncrosslinked and crosslinked) the stress strongly increases at the beginning of the deformation, then goes through the maximum and finally drops to a characteristic plateau region. With increasing the UV dose and, accordingly, crosslink density, the plateau becomes more pronounced. This observation is in agreement with earlier studies [13]. The increase in the UV dose results in slight

increasing the maximum of nominal stress. When UV dose increases from 50 to 100 mJ/cm², a drop in the stress peak is observed. This observation can be attributed to the fact that during the crosslinking process, chemical bonding of the polymer network is established, leading to an increase in the cohesion strength of the adhesive and a reduction in the chain mobility. The higher the internal strength of the polymer, the higher is the resistance to flow, and longer is the deformation at break. Copolymer crosslinked with UV dose = 100 mJ/cm² shows an increase in the force in the plateau region corresponding to a strain hardening and, subsequently, earlier detachment of the adhesive from the adherent is observed. Therefore, the samples crosslinked with UV dose = 30, 40 and 50 mJ/cm² are below the gel point, while the sample, which was crosslinked with 100 mJ/cm² is over the gel point.

- *Tack, nominal stress peak and deformation at break*

The tack parameter, as stress peak, deformation at break, plateau stress and tack, calculated from the stress-strain curves for crosslinked copolymers BA/MA with intermediate M_w with different UV doses, are plotted on Fig. 3.28. With increasing the UV doses the nominal stress slightly increase and then decrease for dose of 100mJ/cm², as already explained (Fig. 3.28a), while the deformation at break significantly increases by approximately a factor of 20 between uncrosslinked and crosslinked with dose of 30 mJ/cm² samples (Fig.3.28b). After an almost constant level between 30 and 50 mJ/cm² doses, the deformation at break drops dramatically. Plateau stress constantly increases with the UV doses with the highest value measured at 100 mJ/cm² (Fig.3.28c). Tack values show an strong increase from uncrosslinked sample to crosslinked with 50mJ/cm² dose after which exhibit an constant value for a UV dose of 100mJ/cm² (Fig.3.28d). Plateau stress and deformation at break have the biggest contribution to the work of adhesive. However, Zosel reported in [13] that the crosslinking to different degrees beyond the gel point, for PnBA, shows that with increasing the crosslinks density deformation at break decrease while stress peak and the height of the plateau remain more or less constant.

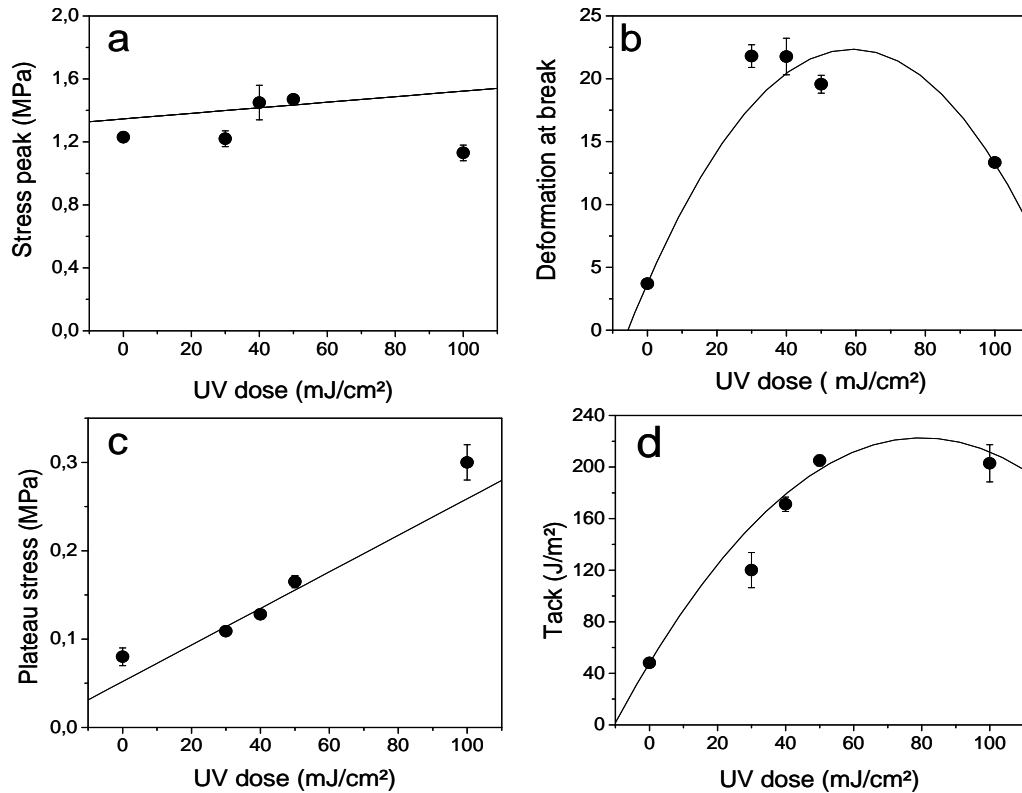


Figure 3.28. Stress peak (a), deformation at break (b), plateau stress (c) and tack (d) as a function of UV doses for crosslinked BA/MA PSAs with $M_w=192$ kg/mol. Lines are to guide the eye.

Additionally, Zosel has investigated crosslinking of poly(dimethylsiloxane) (PDMS) and measured a maximum tack energy for degree of crosslinking slightly above the gel point [45].

Because of the tendency of tack to decrease with further increasing the UV dose, the maximum UV dose used in this study for crosslinking was 100 mJ/cm². This tendency is also confirmed in recent studies [47, 48], where it was observed that the tack is significantly reduced by high UV dose for acrylic PSA and photoinitiator-grafted polystyrene-block-polybutadiene-block-polystyrene.

- *Number of cavities and cavity growth rate*

The images of the contact area polymer/substrate recorded simultaneously with the tack curves are shown in Fig. 3.29 a-e. One can see that the shape of cavities in case of copolymers crosslinked with UV dose from 0 to 50 mJ/cm² and UV dose of 100 mJ/cm² is different. For the sample cured with UV dose = 100 mJ/cm² the cavities are rounder

and smaller. The reason for this difference in the cavity forms could be related to the increase in the cohesive strength, which is very well pronounced in a case of sample cured with maximal UV dose used here.

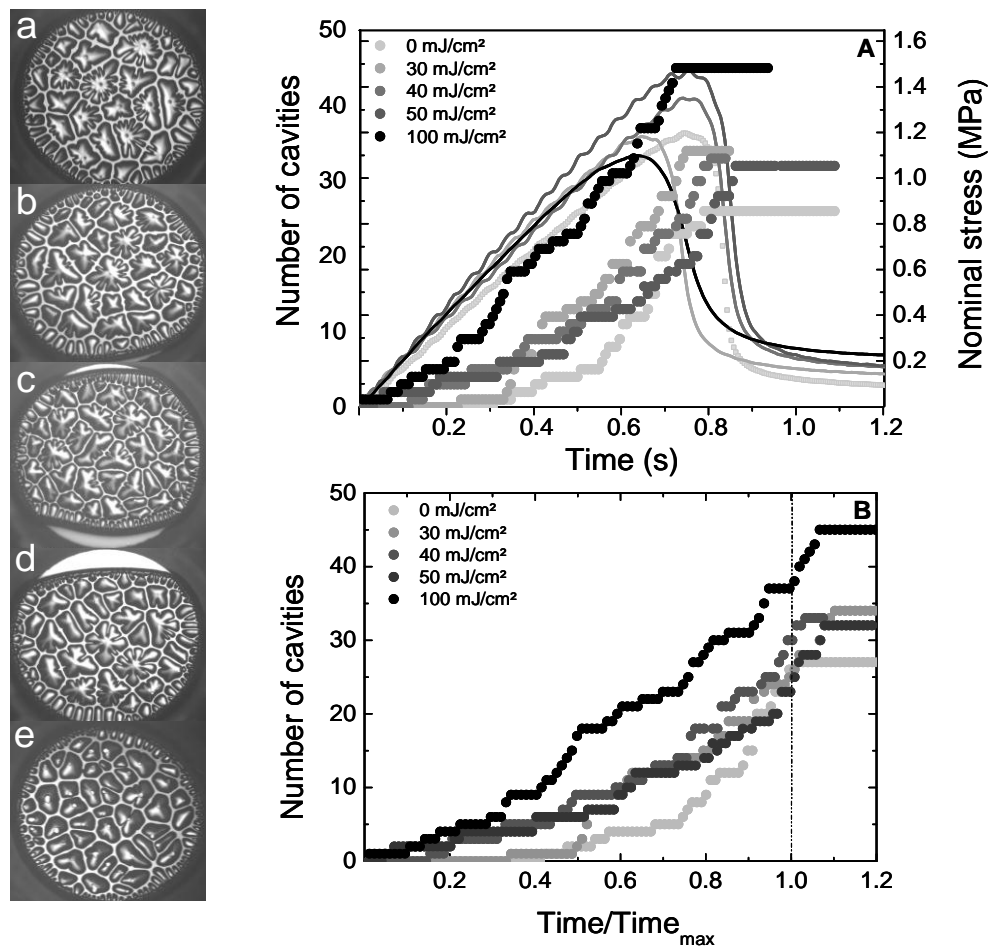


Figure 3.29. Number of cavities (circles) and nominal stress (lines) vs. time (A) and number of cavities vs. time/time_{max} (B) for BA/MA PSAs with $M_w=192$ kg/mol and crosslinked with different UV doses, and representative images of contact area: (a) 0 mJ/cm²; (b) 30 mJ/cm²; (c) 40 mJ/cm²; (d) 50 mJ/cm² and (e) 100 mJ/cm².

Moreover, the cohesive failure observed by uncrosslinked and crosslinked with dose from 30 to 50 mJ/cm² samples changes to adhesive failure for the sample cured with UV dose of 100 mJ/cm².

With increasing the crosslink density, the number of cavities slightly increases, as shown in Fig. 3.29. Higher crosslink density corresponds to higher viscoelasticity, which results in worse wetting. The number of cavities vs. time, and the corresponding nominal stress curves vs. time for BA/MA PSAs with intermediate molecular weight are shown in Fig. 3.29A. The initial slopes of the stress curves for uncrosslinked

samples and maximal crosslinked samples differ from those cured with UV doses from 20 to 50 mJ/cm^2 , which means that the elastic modulus is different. The curves shown in Fig. 3.29B have also different shapes for uncrosslinked and maximal crosslinked samples and almost identical for the samples cured with UV doses from 30 to 50 mJ/cm^2 . This again indicates the discrepancy in the number of cavities and their appearance with time caused by different crosslink density. Similar density leads to similar separation mechanism.

The minimal number of cavities and corresponding maximal final average cavity size are observed for uncrosslinked copolymer, while the maximal cavity amount and minimal final average cavity area are obtained for maximal crosslinked sample (Fig. 3.30).

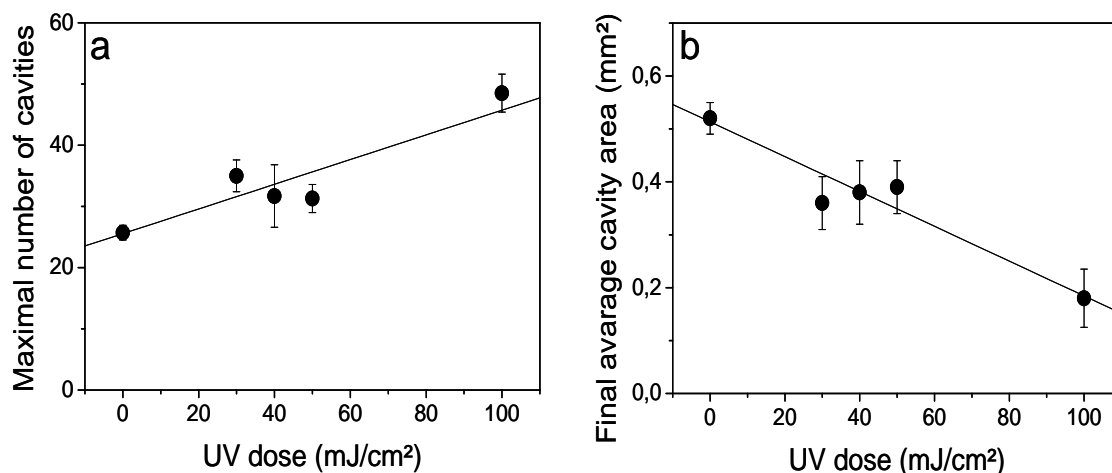


Figure 3.30. Maximal number of cavities (a) and final average cavity area (b) as a function of UV dose for BA/MA with $M_w = 192 \text{ kg/mol}$ measured with smooth steel substrate.

The cavity growth rate for both cavity types for uncrosslinked and crosslinked with different UV doses samples measured with smooth stainless steel substrate is shown in Fig. 3.31. For the first type of cavities one can see that the cavity growth rate decreases with increasing the crosslink density, while the cavities of the second type are insensitive to the crosslink density. Thus, there is no clear dependence of the velocity of cavity expansion on degree of crosslinking.

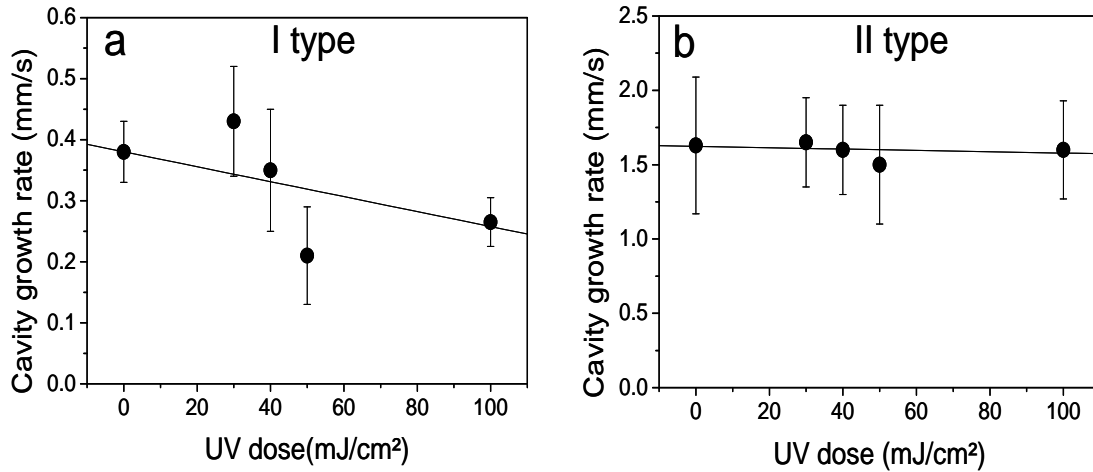


Figure 3.31. Cavity growth rate vs. UV dose for (a) cavity of type I / and (b) cavities of type II.

- Crosslinked polymer and rough substrate

In order to investigate the influence of the surface roughness on the adhesion of crosslinked samples, tack measurements with BA/MA copolymer crosslinked with UV doses of 0, 30, 40 and 50 mJ/cm², were performed additionally with stainless steel substrate with $R_a = 291.7$ nm (Fig. 3.32).

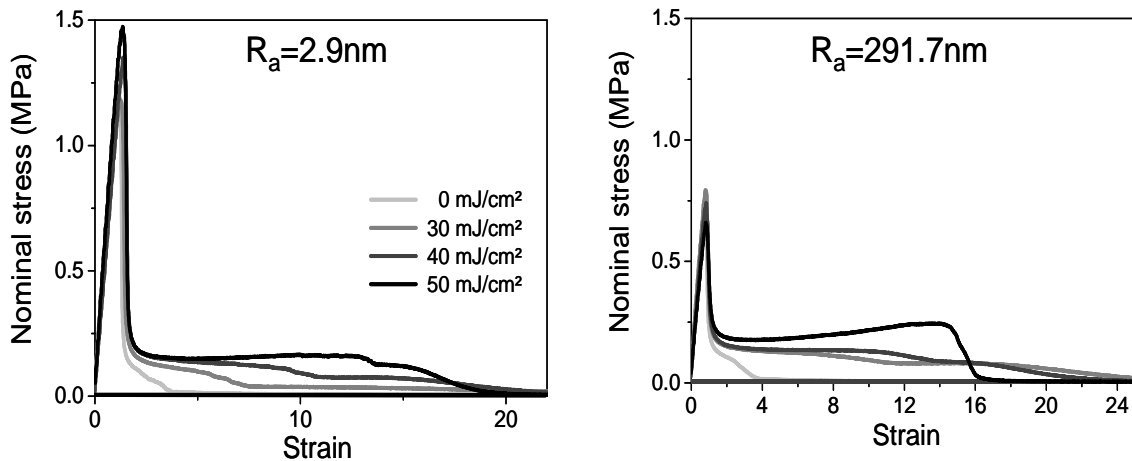


Figure 3.32. Nominal stress vs. strain curves for BA/MA with $M_w=192$ kg/mol crosslinked with different UV doses, measured with stainless steel substrate of $R_a=2.9$ nm and $R_a=291.7$ nm.

One can see that with increasing the roughness of the substrate the value of the stress peak decreases by a factor of around 2. Similar influence of R_a was observed for BA/MA with incorporated functional monomer. The deformation at break is roughness independent and controlled only by the viscoelastic properties of the polymer. The

height of plateau also seems to be insensitive to the roughness. Plateau region as well as the deformation at break are insensitive to the substrate R_a both for uncrosslinked and crosslinked BA/MA. But the roughness of the substrate affects negative the stress peak and the corresponding tack values.

Fig. 3.33. shows the tack values for uncrosslinked and crosslinked with different UV doses BA/MA measured using the probes of three different roughness $R_a = 2.9$ nm, 41.2 nm and 291.7 nm.

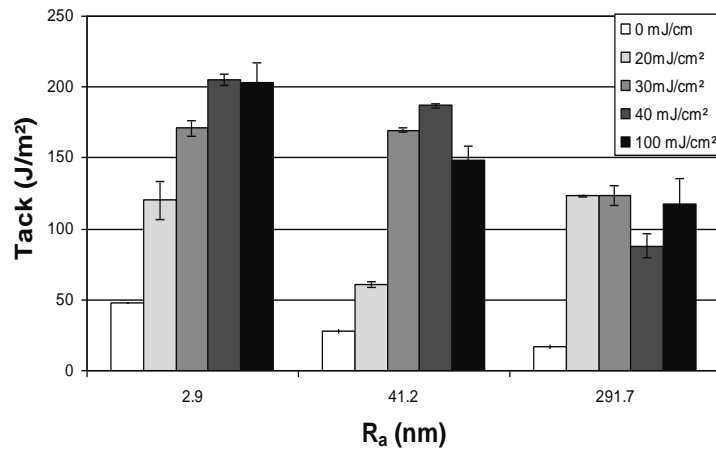


Figure 3.33. Tack for BA/MA, uncrosslinked and crosslinked with different UV doses, measured with steel substrates of different surface roughness.

Tack value increases with increasing the crosslink density caused by the increased UV doses, for all studied substrates. Additionally, tack decreases with increasing the substrate roughness. The change in the tack values with increasing the crosslink density is much stronger in case of smooth ($R_a = 2.9$ nm) surface. On the rough surface ($R_a = 291.7$ nm) the samples crosslinked with different UV dose show higher values of tack than uncrosslinked copolymer, however, these values are almost insensitive to the crosslink density. A possible explanation is the worst wetting, caused both by an increase in the viscoelastic modulus and the substrate roughness, which leads to incomplete contact between polymer and substrate.

Fig. 3.34 shows the nominal stress-strain curves, as well as the parameters calculated from these curves, as a function of the substrate surface roughness R_a for uncrosslinked and crosslinked with UV dose = 100 mJ/cm² BA/MA ($M_w = 192$ kg/mol). One can clearly see the typical shoulder (Fig. 3.34a) on the curves of crosslinked samples, which

along with the increased deformation at break (Fig. 3.34c) leads to higher tack values (Fig. 3.34d). Stress peak shows a very small decrease with crosslinking of the polymer. The influence of the substrate surface roughness is similar for uncrosslinked and crosslinked samples. The influence of the viscoelastic properties is much more pronounced.

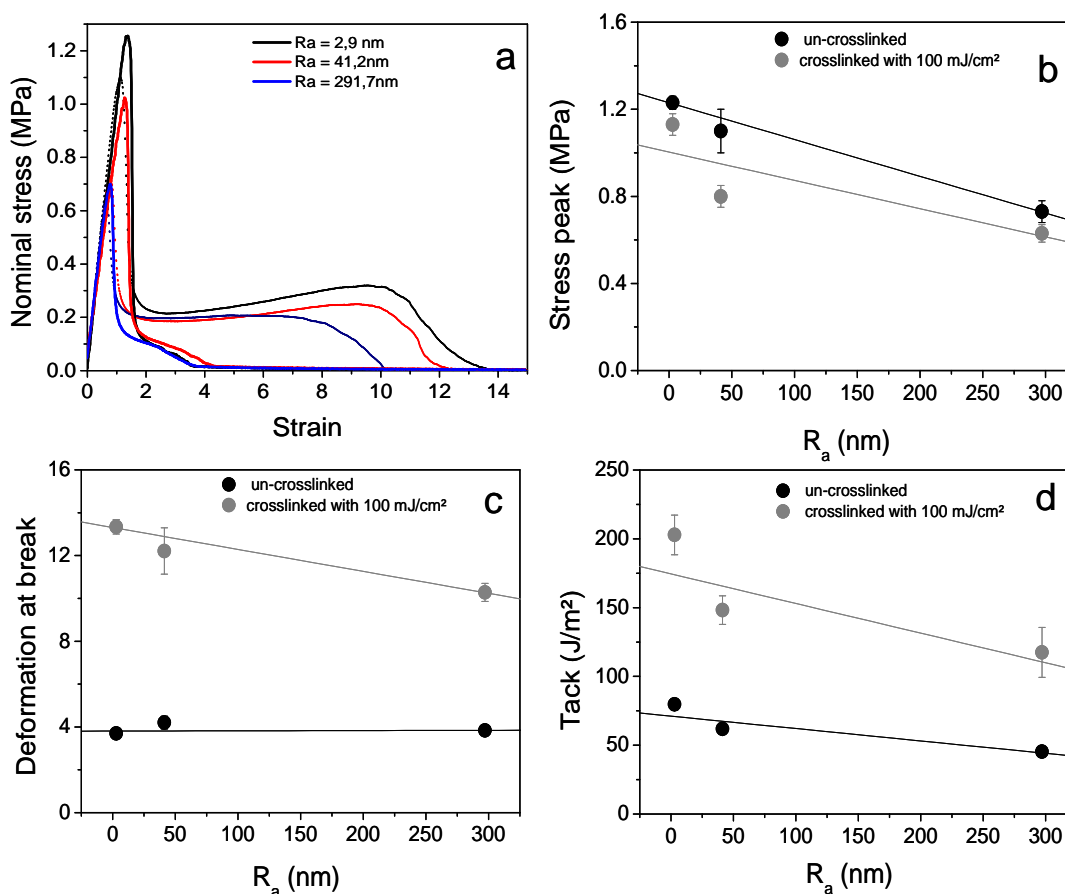


Figure 3.34. a) Nominal stress-strain curves for uncrosslinked and crosslinked with UV dose = 100 mJ/cm^2 BA/MA with $M_w=192$ kg/mol measured with steel substrate of different surface roughness, b) stress peak, c) deformation at break and d) tack.

Fig. 3.35 shows the number of cavities and stress vs. time, as well as the number of cavities vs. time normalized to the time in the stress maximum for crosslinked UV dose = 100 mJ/cm^2 BA/MA PSAs measured with substrate of different R_a and representative images of the area of contact. Comparing the number of cavities for uncrosslinked BA/MA (Fig. 3.9) with crosslinked with UV dose = 100 mJ/cm^2 BA/MA (Fig. 3.35) one can see, that the number of cavities increases by a factor of 2 after curing. Moreover, the influence of the substrate surface roughness on the number of appeared cavities is

similar for both uncrosslinked and crosslinked samples. With increasing the roughness, the number of cavities increases and stress maximum decreases. No additional cavities appeared after stress passes its maximum value.

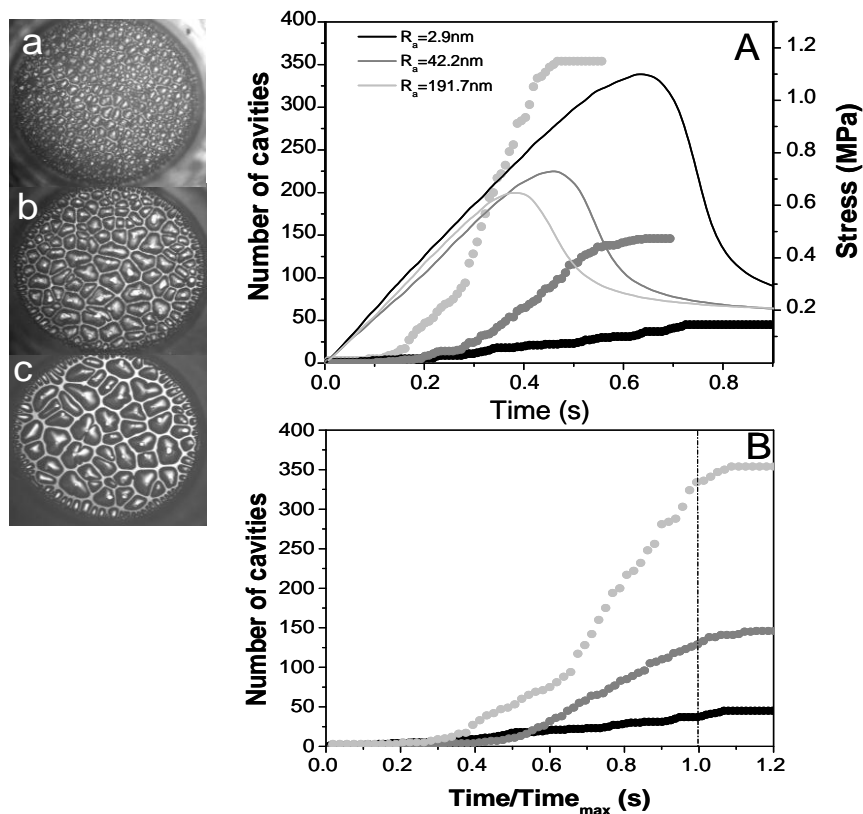


Figure 3.35. Number of cavities (circles) and nominal stress (lines) vs. time (A) and number of cavities vs. time/time_{max} (B) for crosslinked with UV dose = 100 mJ/cm² BA/MA PSAs with $M_w = 192 \text{ kg/mol}$, and representative images of contact area: (a) with substrate $R_a = 291.7 \text{ nm}$; (b) $R_a = 41.2 \text{ nm}$; (c) $R_a = 2.9 \text{ nm}$.

The cavity growth rate, for crosslinked BA/MA, shows no clear dependence on the substrate surface roughness, the same result was obtained for uncrosslinked BA/MA (Fig. 3.11). However, the copolymer curing leads to a decrease in the cavity growth rate.

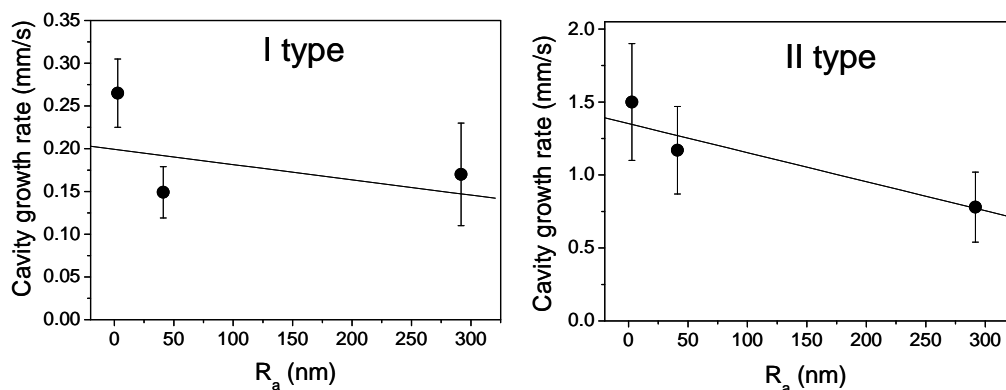


Figure 3.36. Cavity growth rate vs. R_a for crosslinked with UV dose = 100 mJ/cm^2 BA/MA PSAs with $M_w=192 \text{ kg/mol}$: (a) cavity of type I and (b) cavities of type II

- Adherent surface roughness and adhesive with additional functional comonomer crosslinked with UV dose = 100 mJ/cm^2 .

Fig. 3.37a illustrates the nominal stress-strain curves for BA/MA/AA crosslinked with UV dose = 100 mJ/cm^2 and measured using substrates with different R_a , as well as the parameters calculated from the curves, i.e. stress peak (Fig. 3.37b), deformation at break (Fig. 3.37c) and tack (Fig. 3.37d) as a function of the substrate surface roughness.

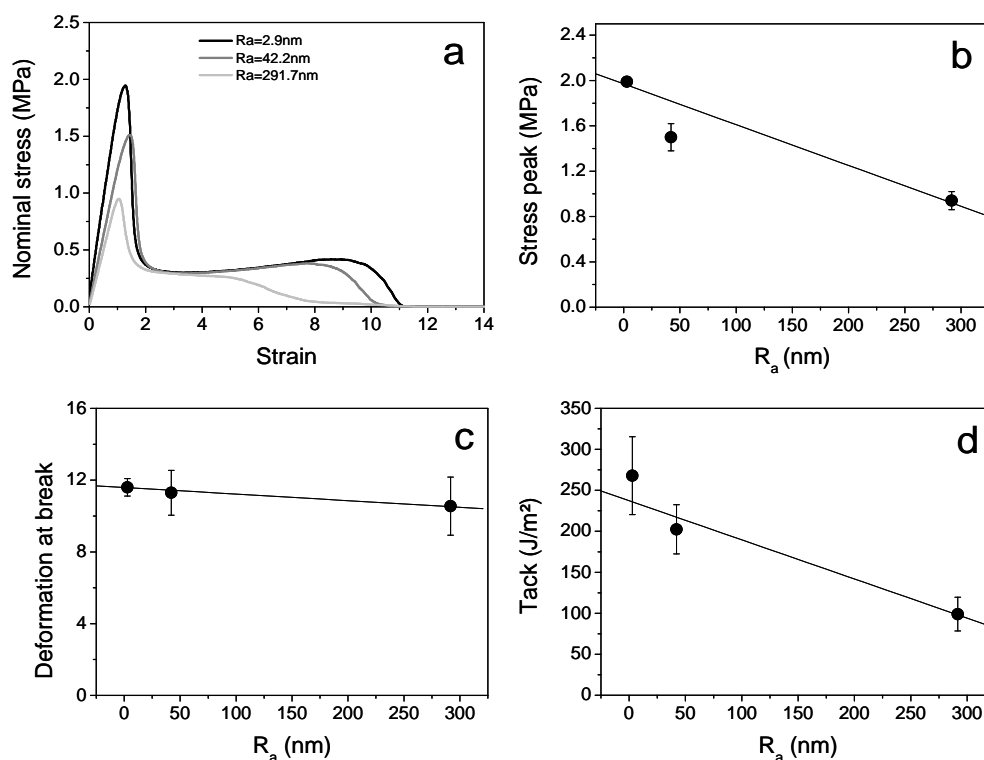


Figure 3.37. Nominal stress vs. strain curves (a) and stress peak (b); deformation at break (c) and tack (d) vs. substrate surface roughness R_a for BA/MA/AA crosslinked with UV dose of 100 mJ/cm^2 .

Similar effect of the substrate surface roughness on the shape of the stress-strain curves is observed for crosslinked BA/MA and crosslinked BA/MA/AA. Crosslinking leads to appearance of characteristic plateau region and increase in the tack values, while the value of the nominal stress peak is insensitive to degree of crosslinking (see Fig. 3.28). The increase in roughness leads to decrease in nominal stress peak and corresponding tack values of crosslinked BA/MA/AA in similar way as for both uncrosslinked and crosslinked BA/MA (see Fig. 3.34). The number of cavities and cavity growth rate of crosslinked BA/MA/AA (Fig. 3.38) shows also similar dependence on R_a , as for uncrosslinked (Fig. 3.9) and crosslinked (Fig. 3.35) BA/MA.

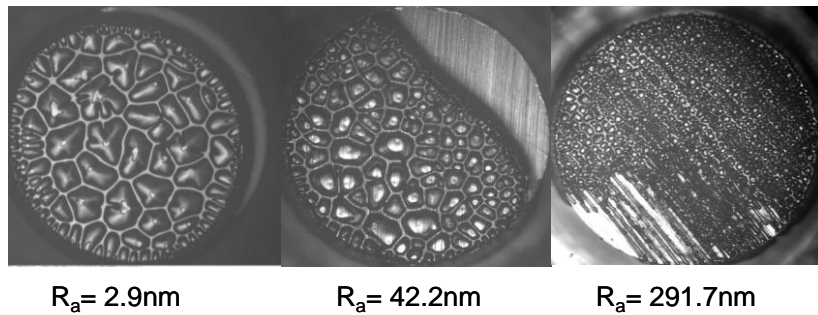


Figure 3.38. Representative images of contact area for BA/MA/AA crosslinked with UV dose = 100 mJ/cm² obtained with substrates of different roughness.

Nevertheless, no clear influence of R_a on the cavity growth rate in case of BA/MA/AA, crosslinked with UV dose = 100 mJ/cm², was observed.

One can suggest that the influence of the substrate roughness, studied here, is always present for acrylates independently of the viscoelastic properties of the polymer film.

- *Cohesive vs. adhesive failure*

In an earlier study [119] a transition from liquid-like cohesive failure to solid-like adhesive failure when increasing the deformation rate above some critical value has been observed. Additionally, Shull and Creton have assumed that at the cohesion-adhesion transition, the fibril extension reaches its maximum [22]. Moreover, the authors observed that at low deformation rates the fibril extension was limited by a cohesive failure at the center of the fibrils, while at high deformation rates fibril extension was limited by adhesive failure of much less extended fibrils, as a result of the large elastic stresses. Therefore, it is worthwhile to investigate if the change in the

failure mechanisms plays some role on the cavitation process during debonding of acrylate copolymers.

Tack tests for PSAs demonstrating different failure mechanisms were performed with constant debonding rate (0.1 mm/s). Uncrosslinked and crosslinked with UV doses from 30 to 50 mJ/cm² copolymers show cohesive failure, under the experimental conditions chosen for the tack test here. The crosslinking of polymers changes their viscoelastic properties in addition to the mechanism of debonding. Crosslinking with UV dose = 100 mJ/cm² switches the failure mechanisms to adhesive.

Fig. 3.39 shows stress-strain curves measured with a steel substrate of $R_a = 291.7$ nm for uncrosslinked and crosslinked copolymers and Fig. 3.41 shows the dependence of the parameters calculated from the tack curves as a function of R_a for the same systems.

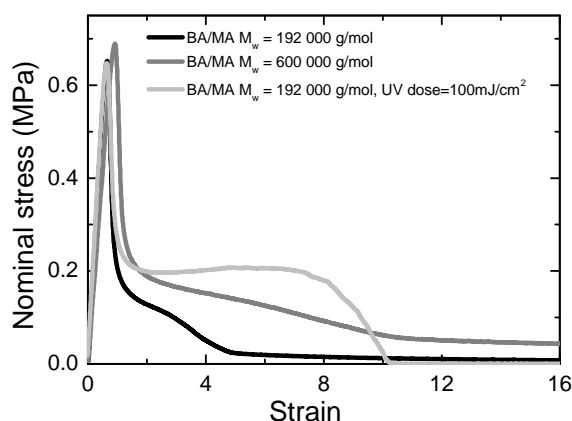


Figure 3.39. Nominal stress vs. strain curves for uncrosslinked BA/MA with $M_w=192$ kg/mol and $M_w=600$ kg/mol and crosslinked BA/MA with $M_w=192$ kg/mol (UV dose=100 mJ/cm²) measured with stainless steel probe of $R_a=291.7$ nm.

In agreement with earlier studies, crosslinking shows very little effect on stress peak values, but strongly increases the stress plateau and correspondingly the tack. The tack values for high molecular weight PSA are similar to the values for crosslinked one.

Deformation at break increases with crosslinking, but is always lower than for high molecular weight PSA. This is attributed to the different viscoelastic properties with respect to the terminal flow regime. Finally, the failure was cohesive in the case of the uncrosslinked copolymers, but adhesive in the case of the crosslinked polymers under the test conditions here. Images of the contact area were recorded simultaneously with the tack curves

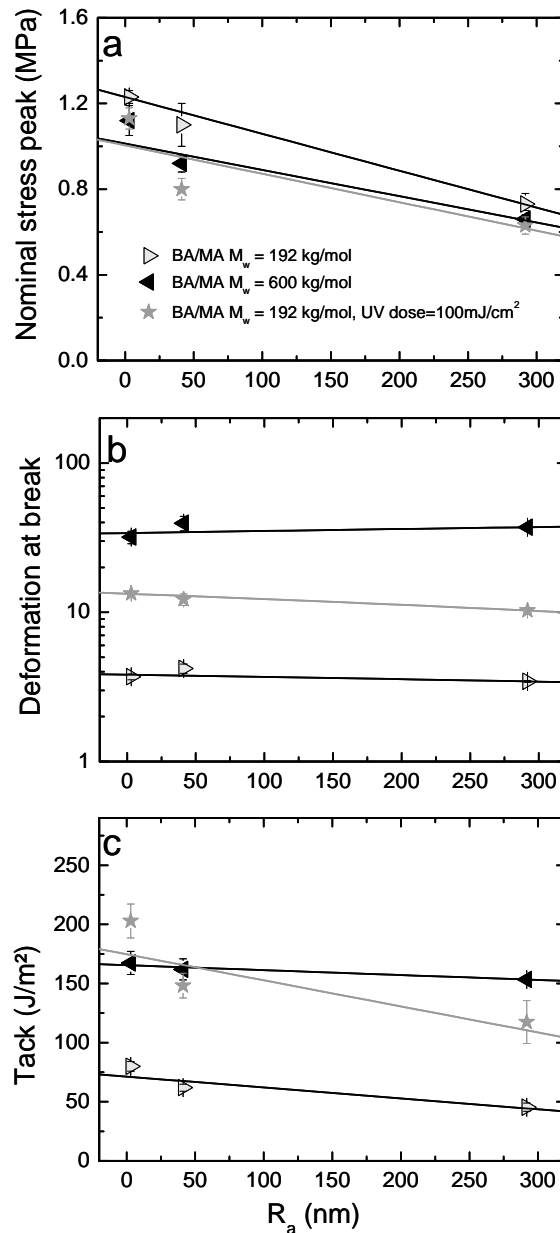


Figure 3.40. Nominal stress (a), deformation at break(b) and tack(c) for uncrosslinked BA/MA and crosslinked (100 mJ/cm²) PSAs with $M_w=192$ kg/mol and uncrosslinked with $M_w=600$ kg/mol.

Fig. 3.41 shows the number of cavities and the stress as a function of time for uncrosslinked and crosslinked polymers. The corresponding images are also given. The formation of the first cavities, in all cases, starts at times long before the stress reaches the maximum value. The number of cavities increases slowly at the beginning of debonding and then grows rapidly as the stress peak is approached. For the BA/MA film with $M_w = 192$ kg/mol, new cavities do not appear after the stress peak is approached. It can be conclude that for crosslinked copolymers, the stress peak appears

much earlier than for uncrosslinked ones, in the case of high molecular weight PSA and crosslinked PSAs, additional cavities appear even after the stress peak is reached.

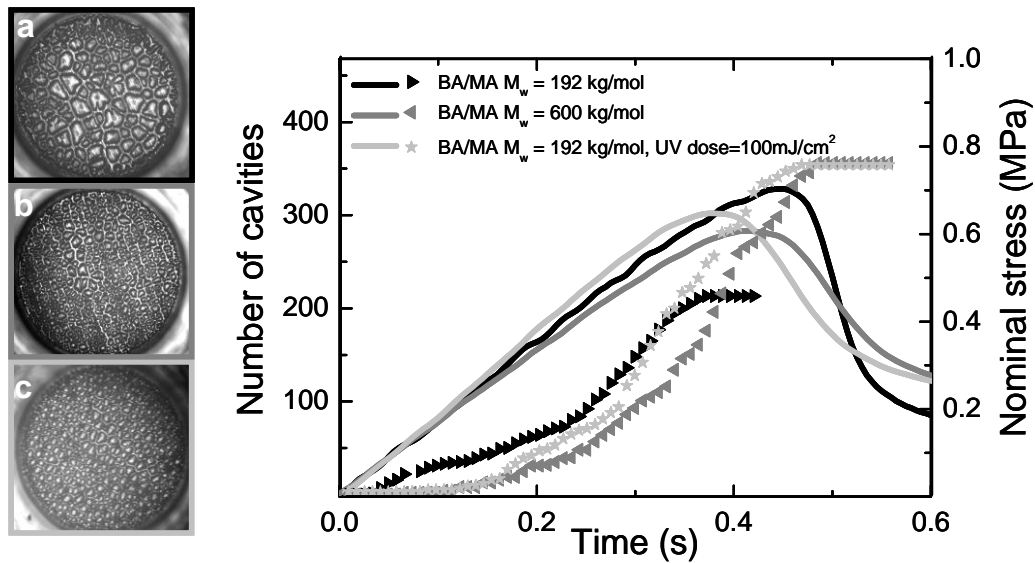


Figure 3.41. Number of cavities (symbols) and nominal stress (lines) as a function of time for uncrosslinked BA/MA and crosslinked (100mJ/cm²) with $M_w = 192$ kg/mol, and $M_w = 600$ kg/mol and representative images of contact areas: (a) uncrosslinked BA/MA with $M_w = 192$ kg/mol; (b) uncrosslinked BA/MA with $M_w = 600$ kg/mol, and (c) crosslinked BA/MA with $M_w = 192$ kg/mol.

Nevertheless, the final number of cavities for the high molecular weight and crosslinked PSAs is practically identical. Thus, cavitation is determined by the viscoelastic properties of the PSA regardless of the debonding mechanism, cohesive or adhesive.

Fig. 3.42 shows the cavity growth rate for BA/MA PSA on the steel substrates as a function of the substrate surface roughness for both types of cavities. Uncrosslinked BA/MA with intermediate and high molecular weight, was compared with BA/MA with $M_w = 192$ kg/mol crosslinked with UV dose = 100 mJ/cm². It should be noted that the shear modulus increase with increasing molecular weight. Crosslinked BA/MA with $M_w = 192$ kg/mol and BA/MA with $M_w = 600$ kg/mol exhibit a similar shear modulus, as already shown above (Section 3.1.1, Fig. 3.2). Moreover, for the probes of all surface roughnesses studied, the cavity growth rate decreases with increasing M_w and degree of crosslinking of the polymers, and for the crosslinked BA/MA with

intermediate molecular weight and crosslinked BA/MA with the highest molecular weight the cavities extend with similar velocity.

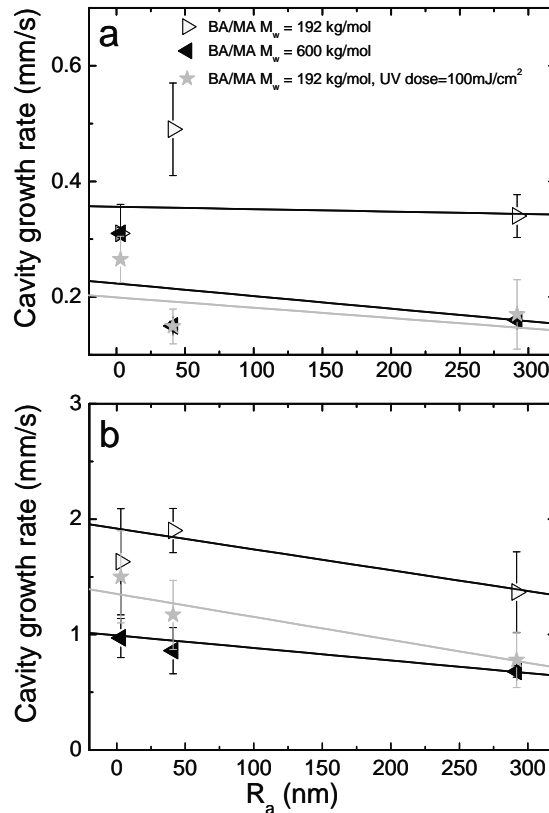


Figure 3.42. Cavity growth rate vs. roughness for uncrosslinked and crosslinked with UV dose = 100 mJ/cm^2 BA/MA with $M_w = 192 \text{ kg/mol}$ and uncrosslinked BA/MA with $M_w = 600 \text{ kg/mol}$: (a) cavities of type I, appearing at the beginning of debonding, and (b) cavities of type II, appearing at the area of stress peak.

The cavity growth rate for both uncrosslinked and crosslinked adhesives is insensitive to the substrate roughness and is mainly controlled by the viscoelastic properties of the copolymer films. Mechanism of failure plays no role in the expansion velocity of the cavities appearing during the debonding.

3.4.3. Cavity growth modes

According to the previous study [108] it is not easy to determine whether rupture is adhesive i.e. at the interface or cohesive, within the material. Especially for viscoelastic system, it is not so clear whether failure is in the bulk or at the interface. The different modes of failure are: edge-crack propagation, internal-crack propagation, cavitation and bulk fingering. In this study both interfacial and bulk failure were observed.

In order to compare and analyze the influence of the interfacial factors on the growth rate of both types of cavities, all results for different PSA systems on the steel probe of two different roughness, were plotted on Fig. 3.43.

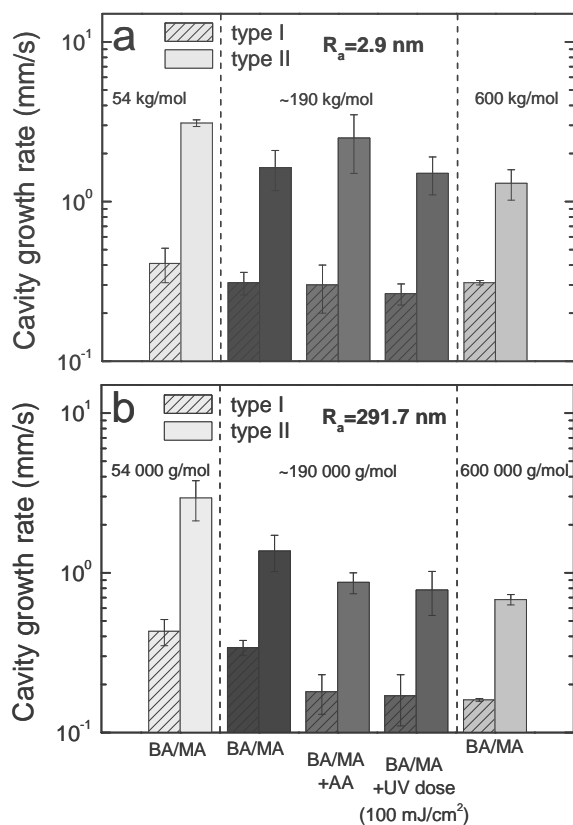


Figure 3.43. Cavity growth rate for uncrosslinked BA/MA with different M_w and with incorporated AA monomer and crosslinked BA/MA with $M_w = 192$ kg/mol measured with a steel substrate of surface roughness $R_a = 2.9$ nm and $R_a = 291.7$ nm.

Uncrosslinked BA/MA PSAs with different molecular weights were compared with crosslinked BA/MA and BA/MA/AA with intermediate molecular weight. On the smooth surface the cavity growth rate is insensitive to the change in the molecular weight, incorporation of functional monomer or crosslinking. In contrast, on the rough surface, the cavities of the PSA with the lowest molecular weight grow faster, than the cavities of BA/MA with the highest M_w , crosslinked BA/MA and BA/MA/AA.

Fig. 3.44 shows the growth rate for both types of cavities for BA/MA with different molecular weights, BA/MA with intermediate M_w additionally crosslinked with UV dose = 100mJ/cm² and with incorporated AA, MMA, HEA comonomers as a function of the shear modulus measured with substrates of two different roughnesses.

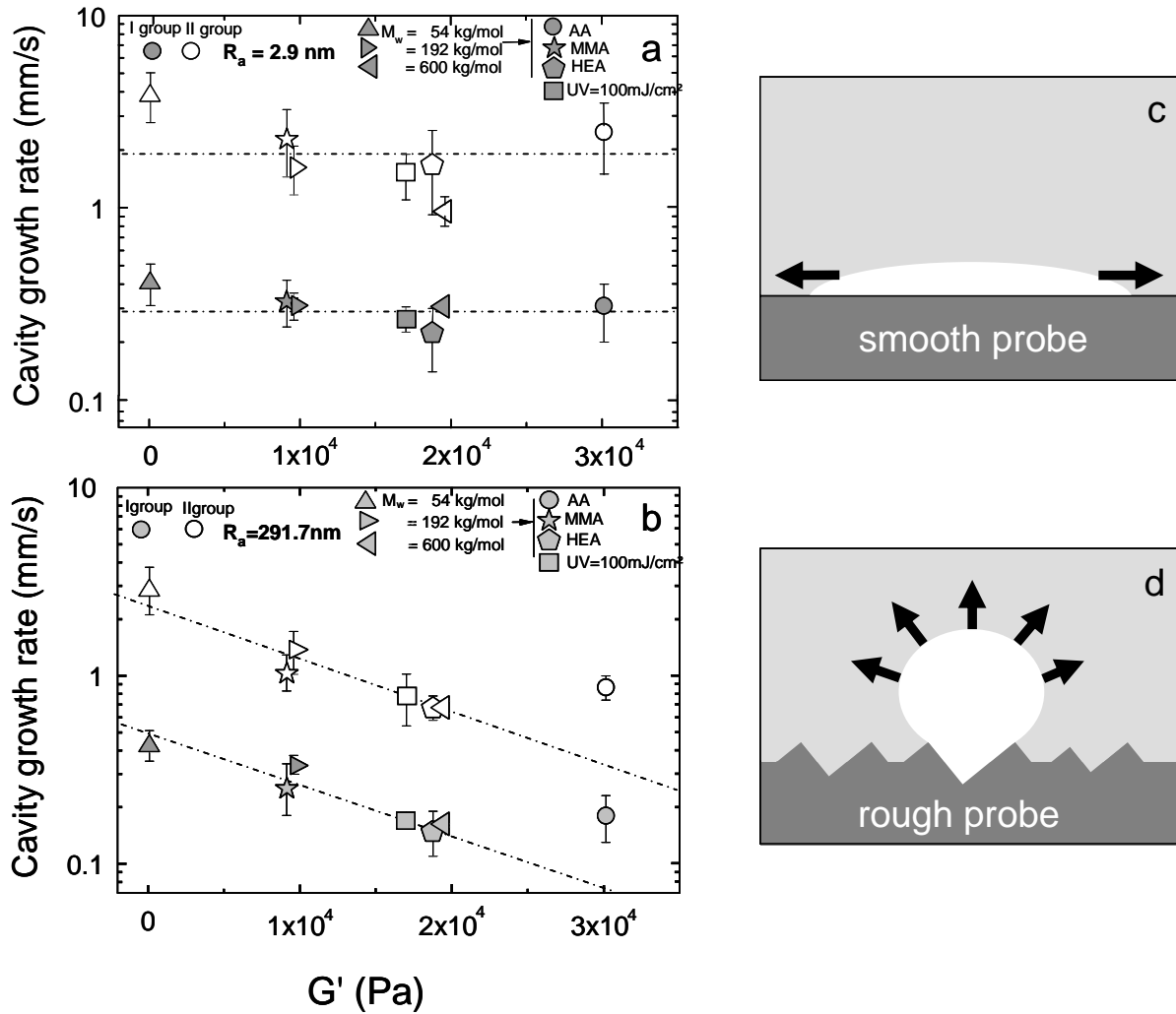


Figure 3.44. Cavity growth rate for BA/MA PSAs ($M_w = 54$ kg/mol, $M_w = 192$ kg/mol, $M_w = 600$ kg/mol and $M_w = 192$ kg/mol cured with UV dose = 100 mJ/cm²) and for BA/MA/AA, BA/MA/HEA and BA/MA/MMA PSA, measured with steel probe of $R_a = 2.9$ (a) and $R_a = 291.7$ nm (b). The corresponding schemes of the cavity growth on the smooth (c) and on the rough (d) surface are also given.

On the smooth surface (Fig. 3.44a), there is no clear influence of PSA modulus on the cavity growth rate with cavities growing presumably on the surface. In contrast, on the rough surface (Fig. 3.44b), the cavity growth rate is controlled by the viscoelastic properties of PSA independently of the debonding mechanism (cohesive or adhesive), and it decreases significantly with increasing shear modulus. Therefore, one can conclude that cavities grow laterally along the smooth substrate (Fig. 3.44c), but they grow omnidirectionally into the polymer film in case of rough substrates (Fig. 3.44d). Lateral and vertical cavity growth have been observed in earlier studies [18, 26]. In contrast to our investigation, the appearance of different mode of cavity expansion was not caused by the substrate roughness, but was provoked by the viscoelastic properties

of the adhesive film. Leger and Creton [18] have analyzed two different mechanisms of cavity growth depending on the ratio of the critical energy release rate G_c , which related to the interfacial structure, and the bulk elastic modulus E of the adhesive layer. If G_c/E is high, the cavities will grow in the bulk of the polymer, while low G_c/E values lead to interfacial propagation. Yamaguchi and co-workers [26] have investigated the height and width of the cavities as a function of time for 2-ethylhexylacrylate/ethylacrylate/acrylic acid tri-block and they detected that increasing the crosslink density results in decrease in the cavity height, while the width increases. The authors conclude that the cavities in highly crosslinked samples expand laterally, rather than in the bulk of the polymer.

3.4.4. Surface enrichment

The internal reorganization and subsequently enrichment of one component from binary system at the polymer-air interface were observed for different polymers such as blends of polystyrene/polybromostyrene [120], polystyrene/deuterated polystyrene [121], polystyrene/polyvinyl methyl ether [122]. The reorganization and the appearance of the enrichment layer is a result of the chain mobility. This process was observed for statistical copolymers and documented in a recent study [68].

For the investigation of the surface enrichment for statistical copolymers, 90% ethylhexyl acrylate (EHA) copolymerized with 10% styrene (S), maleic acid anhydride (MAA), a methylmethacrylate (MMA) were used. Cleaned glass microscope slides were coated with solution of the statistical polymer dissolved in toluene. The coated slides were dried for 24 h at room temperature. The film thickness of all polymer films were determined from the tack curves, as described in "Materials and Methods".

- *Near-surface component enrichment*

Fig. 3.45 shows stress-strain curves for EHA/MAA, EHA/S and EHA/MMA obtained with stainless steel substrate of $R_a = 5.1$ nm, as well as the values of nominal stress peak, deformation at break and tack, calculated from this curves.

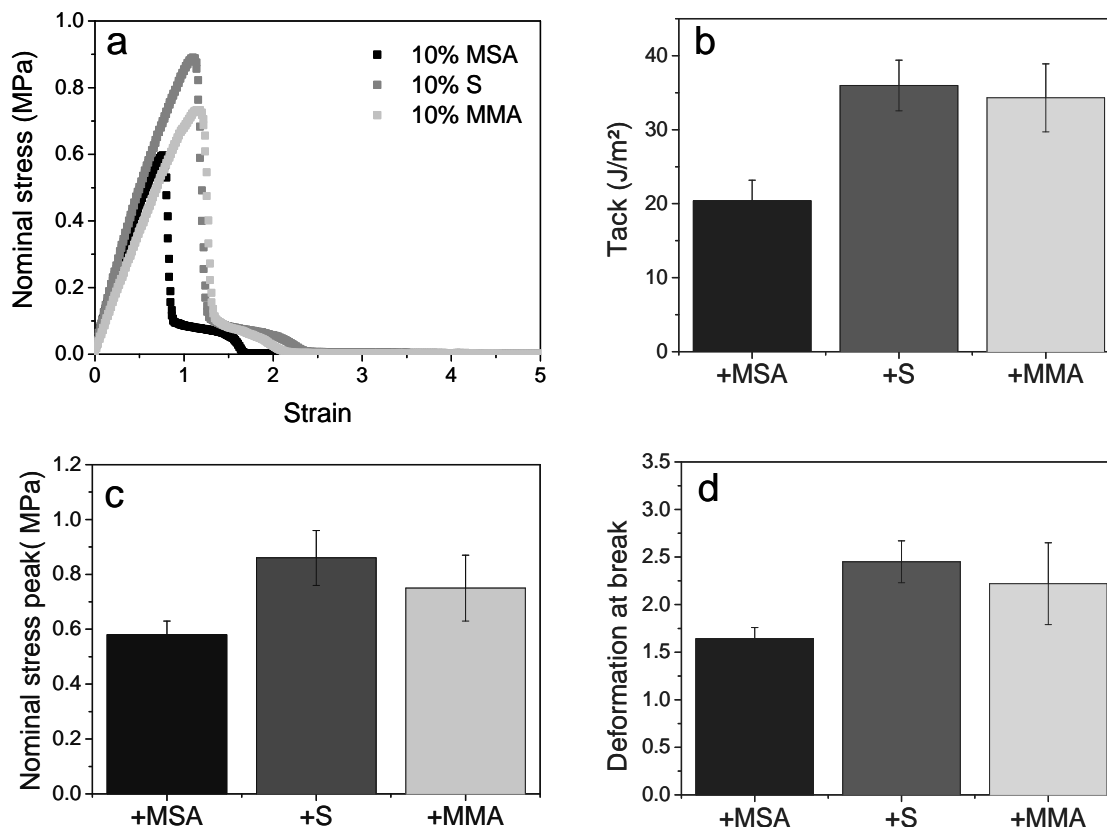


Figure 3.45 (a) Representative stress vs. strain curves for EHA/MAA, EHA/S and EHA/MMA; (b) tack energy; (c) stress peak; and (d) deformation at break [68].

One can see that nominal stress peak and corresponding tack values are similar for EHA/S and EHA/MMA, whereas the values for EHA/MAA are significantly lower. Additionally, for copolymers containing MAA and MMA, the rheological measurements show similar values for the storage and loss modulus (Fig. 3.46). Therefore, the differences in the tack values cannot be attributed to the viscoelastic properties of the polymer films. Similar shape of stress-strain curve was observed also for the plateau region, which occurred after the stress passes its maximum. This plateau region characterizes the deformation ability of the fibril structure and is mainly controlled by the rheological properties of the adhesive. Therefore, the different tack of the copolymers has to be related to an interfacial phenomenon, and not to the variation in the bulk properties.

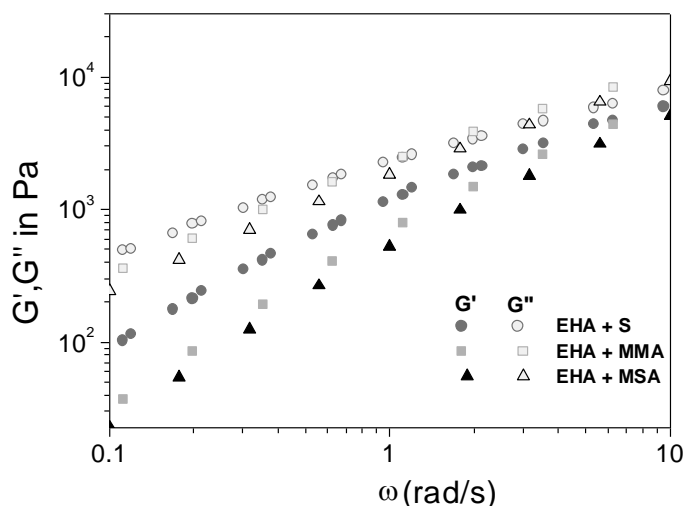


Figure 3.46. Storage G' and loss G'' moduli as a function of angular frequency for EHA/S, EHA/MMA and EHA/MSA measured at room temperature.

The number of cavities as a function of the time, normalized to the time of the maximum stress for EHA/S, EHA/MSA and EHA/MMA and corresponding images of the contact area substrate/polymer are shown in Fig. 3.48.

The observed higher amount of formed cavities for EHA/MSA is a result of worse wetting of the surface substrate and leads to decrease in the nominal stress peak.

The X-ray measurements, performed in Technical University of Munich [68], show similar behavior of EHA/S and EHA/MMA. The surface was enriched with majority component EHA. Underneath the surface enrichment, the enrichment with the minority component has maximum at a shallow depth of $z = 5.9$ nm for EHA/S; $z = 5.4$ nm for EHA/MSA and the monomers ratio in this position was found to be 100% for PS and 61.3% for PMAA. In contrast to these systems, EHA/MMA enriched the surface layer with maximum contribution of 97.6% in a depth of $z = 1.2$ nm. As a possible explanation of this reorganization of the adhesives is the different solubility of the polymer chains. Chains containing higher amount of that monomer, which exhibits better solubility, are brought to the surface during the evaporation of the solvent. After integration over the substrate roughness of the substrate $R_a = 5.2$ nm, the total minority component content in the region $0 < z < 5.1$ nm were: 42.1% MAA for EHA/MSA, 66.4% S for EHA/S and 49.8% MMA for EHA/MMA [68].

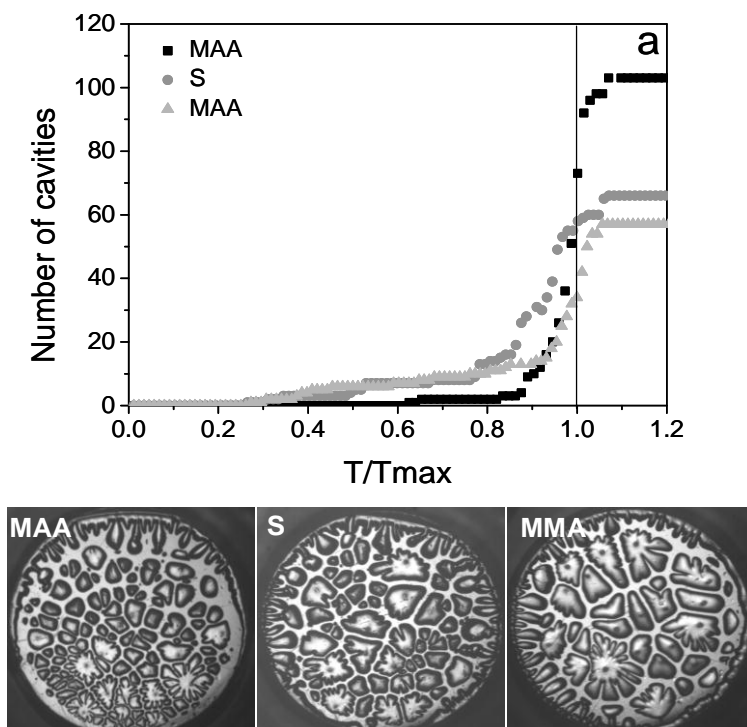


Figure 3.47. (a) number of cavities as a function of the time normalized to the time at the maximum stress, and the representative images of the contact area polymer/substrate for EHA/MAA, EHA/S and EHA/MMA.

It can be assumed that reduce in the content of MAA in the surface region leads to different cavitation process and low values for the adhesion energy. It could be concluded that there is a correlation between the enrichment of the surface layer and the adhesive properties of the polymer film. Such a correlation was detected in the aging experiment

- *Aging effect*

A. Diethert and Prof. Müller-Bushbaum (TU Munich) observed that the composition profiles extracted from the X-ray measurements, change strongly with time. The aging effect is characterized by enrichment of fresh sample with minority component and occurrence of two well distinguished layers of PEHA and PMMA, while with time PEHA moves to the surface leading to a collapse of the separated layers [68]. In contrast, during the tack measurements we found no clear change in the samples adhesive properties with time. Fig. 3.48 shows stress-strain curves and calculated from them parameters for copolymer containing 80% of EHA and 20% of MMA measured 4, 142, 408, 696 and 1176 hours after preparation of the polymer film.

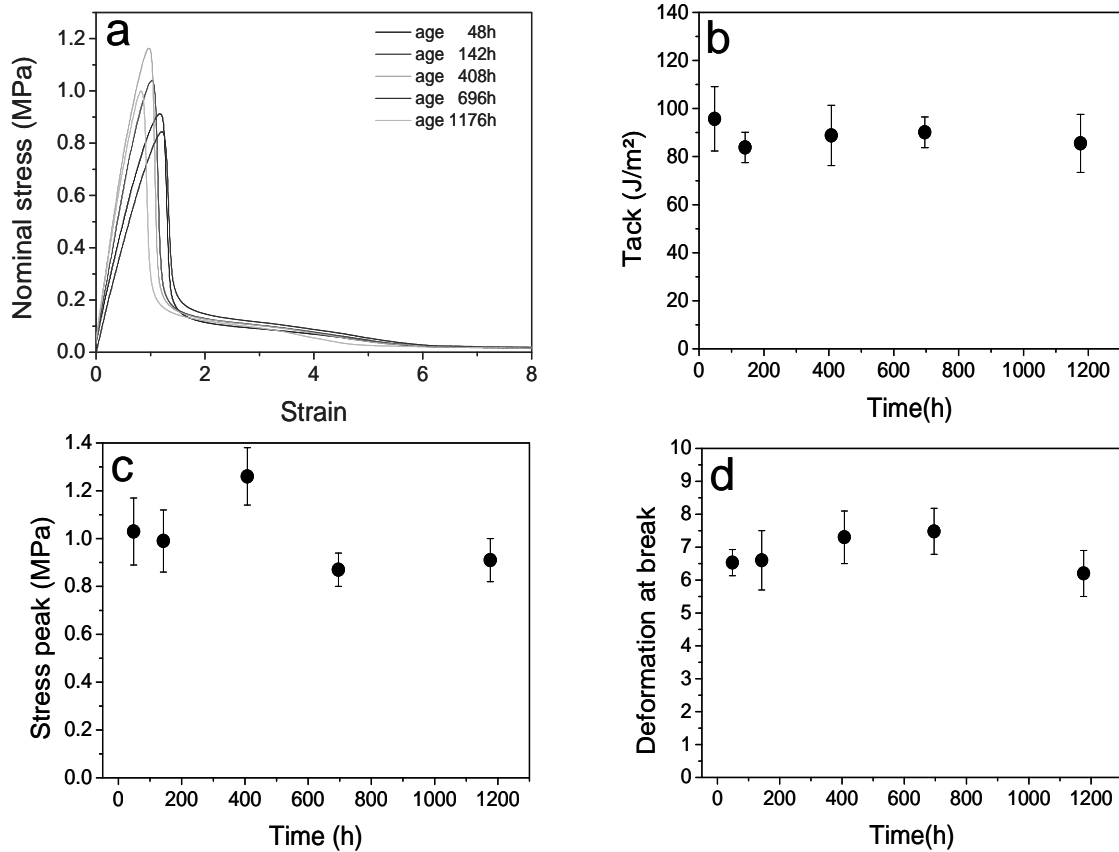


Figure 3.48. (a) Stress-strain curves for films of different sample age, (b) tack energy, (c) stress peak and (d) deformation at break as a function of time. Smooth probe roughness is 5.1nm.

- Effect of the relative humidity (RH).

A correlation between air humidity, enrichment of the surface with the minority component and mechanical properties has been investigated in detail for 80% EHA/20% MMA PSAs. An increase in the stress peak and corresponding tack values was observed with increasing the enrichment with PMMA at the near-surface region (Fig. 3.49). Increasing of the PMMA concentration at near-surface layer is a result of increase in the RH from 2 to 85%.

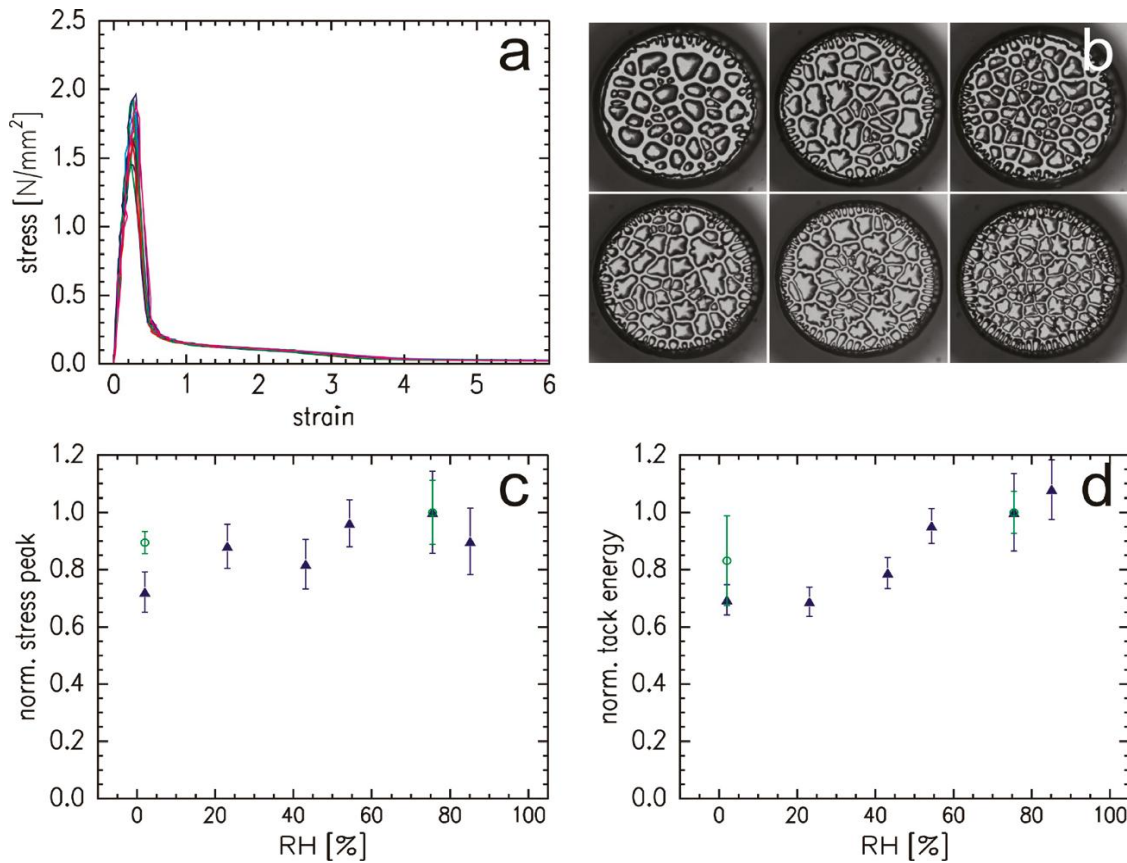


Figure 3.49. (a) Stress-strain curves for the measurements under dry conditions
 (b) Representative video images for each sample of the humidity series
 (c) Stress peak as a function of RH normalized to the value at a RH normalized to the value at a RH of 75%. Filled triangles correspond to data obtained with a steel substrate (measured in TU Munich) and open circles are data measured with silicon substrate (measured in KIT).
 (d) Tack energy as a function of RH in analogy to panel c. [69].

It should be noticed that PMMA is the less mobile component. Therefore, the number of cavities also increases with increasing the RH and correspondingly PMMA concentration. In summary, the change in the RH influences the molecular structure and the adhesion properties of PSAs [69].

III. Summary and Outlook

The influence of the interface phenomena on the debonding mechanisms of pressure sensitive adhesives was systematically studied in this work. The statistical acrylate copolymers used as model systems were investigated using a probe tack test in combination with video-optical observation of the cavitation process. The high speed camera allowed for in situ observation of the cavitation and the qualitative analysis of the video sequence expanded the information about the cavity nucleation mechanisms and their growth. The cylindrical form of the substrate chosen here provides uniform pressure distribution along the entire diameter of the surface while establishing a contact with the adherent, which results in a uniform distribution of the contact defects. The debonding of acrylate copolymers used here is accompanied by the cavitation. Since the cavitation is an interface phenomenon, analyzing the cavitation process and the factors that influenced it, expand the existing knowledge about the separation of adhesive and adherent.

The existence of two types of cavities was confirmed for all polymers investigated here. The first type of cavities appears at the very beginning of the debonding of the adherent from the adhesive. They grow slowly at the beginning and then, near the stress peak, they increase their expansion velocity. The second type of cavities occurs later, at the region of the stress maximum and they grow five times faster than the cavities of the first type, but with a constant speed.

The rheological properties of all model copolymers were studied using oscillation tests. All samples exhibit a storage modulus G' below 3.3×10^5 at 1 Hz and according to the Dahlquist criterion they can be used as pressure sensitive adhesives. The increase in the molecular weight of one polymer leads to increase in the storage G' and loss G'' moduli at low frequency, while at high frequency, they show no difference. It was also observed that incorporating of a polar comonomer results in an increase of shear

III. Summary and Outlook

modulus, due to the additional secondary bonds between the functional groups of the different polymers. Both increasing the length of the polymer chain and crosslinking the polymer leads to an increase of G' and G'' due to the augmentation of the entanglement density and corresponding cohesive strength. Adjusting the viscoelastic properties for all samples equally using crosslinking, was found to be difficult to manage, because crosslinking changed not only the moduli, but also the longest relaxation times.

Interfacial factors such as surface roughness and surface energy of the substrates used, as well as the chemical composition and crosslinking of the polymers, markedly influence the debonding process of PSAs.

It was observed in this work, that the increase of the substrate surface roughness in nanometer scale (between 3 and 300 nm) leads to a drop of the value of the stress peak. The height of the plateau on the tack curves as well as the deformation at break were found to be insensitive to the change in the substrate roughness and increased with increasing of the length of the polymer chain. This observation was expected since the elongation properties of the fibril structures formed are mainly controlled by the viscoelastic properties of the polymers. The work of adhesion decreases with increasing substrate surface roughness and, accordingly, the contribution of the stress peak. The effect of the surface roughness on the adhesion decreases with increasing molecular weight of the polymers, due to the fact that the plateau region in tack curves starts to dominate. The crucial role of the surface roughness on the nucleation and growth of the cavities was detected by detailed analysis of the recorded video images during the cavitation process. The number of cavities increases slowly with time at the beginning of debonding and then rapidly increases as the stress peak is approached. The final number of cavities is reached later on the rough surfaces and in some cases additional cavities are formed even after the stress peak has been passed. Cavity growth stops when the plateau of the nominal stress is reached. For both types of cavities, the surface roughness of the substrate did not play any role in the velocity of expansion, but the growth rate increased markedly with increase of the polymer molecular weight, implying that the viscoelastic properties has greater influence on the rate of the cavity growth. In this work, it was for the first time observed that for acrylate copolymers

III. Summary and Outlook

with different viscoelastic properties the effect of surface roughness is similar. It could be expected, that the surface roughness has a similar effect for other PSAs. Additional experiments with other type adherents are imperative and can further confirm or reject this hypothesis.

In this work, it was detected that the surface energy of the substrate also affects the adhesion properties with respect to the cavitation process of acrylate copolymers. On lower surface energy substrates, the cavities occur earlier, at corresponding lower stress levels. The increase in the surface energy of the substrate results in an increase in the stress peak value and the corresponding work of adhesion, because the number of cavities decreases. The decrease in cavity number indicates improved wetting of the substrate surface. Deformation at break, as expected, is insensitive to the substrate surface energy and is governed by the bulk properties of the polymer film.

Incorporated comonomer increases the shear modulus, which resulted in an increase in the polymer strength, i.e., an increase in the peak stress, deformation at break, the corresponding tack values, as well as the number of cavities. The latter indicates inferior interfacial wetting. Although the higher amount of cavities leads to a reduction in the stress peak and work of adhesion, the beneficial effect of the increased shear modulus is more pronounced and counteracts the detrimental influence of the diminished wetting. No clear influence of the surface energy on the cavity growth rate was detected. The incorporation of a polar comonomer was expected to modify the surface energy of the polymer film. However, the measured surface energies of copolymers were found to be unaffected by the incorporation of comonomers with different surface energy, although, the near-surface composition was changed in a non-trivial manner.

Crosslinking of the acrylate copolymers results in an increase of the work of adhesion. Crosslinked and high molecular weight samples show the best adhesion. The change in the modulus seems to be the primary factor producing the observed changes in wetting and adhesion. The failure mode changes from cohesive to adhesive due to a high stress peak level during the stretching of the fibrils. However, when comparing crosslinked and uncrosslinked samples with similar shear modulus levels, it was observed that

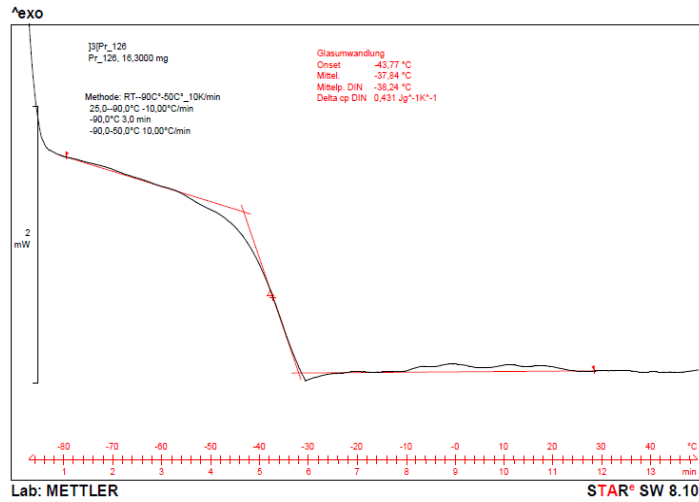
III. Summary and Outlook

crosslinking does not affect the cavitation process. This is important to notice, since essentially all commercial PSAs are crosslinked to a certain degree.

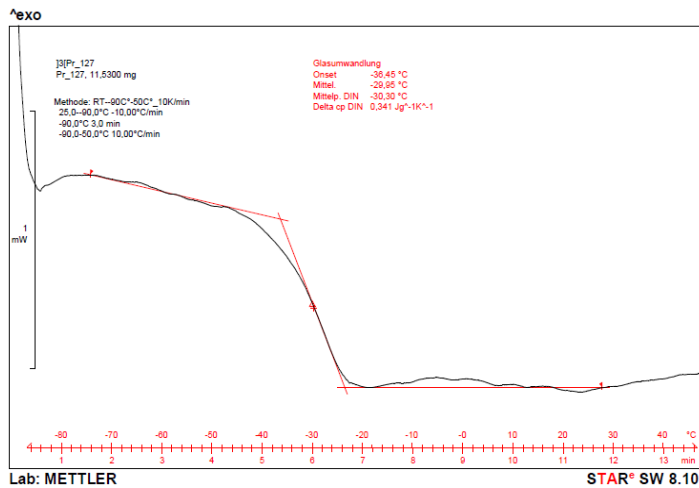
Independently of the type of failure in case of rough substrate surfaces, the cavity expansion velocity significantly decreases with an increasing shear modulus of PSA, while on smooth substrate surfaces, this characteristic quantity is insensitive to the bulk properties of the polymer film. Using a variety of PSA including uncrosslinked copolymer with different molecular weights, crosslinked adhesive, and polymer with an incorporated functional comonomer reveals that the cavity growth rate decreases with increasing modulus on the rough substrate, but is independent of the modulus on the smooth substrate. For the first time, two different modes of cavity growth have been postulated in this work: lateral growth along the interface on a smooth substrate and omnidirectional growth into the polymer film on a rough substrate. Further modification on the tack apparatus in order to allow 3D observation of the cavitation process, recently reported in [26] could be useful in confirming the existence of the different modes of cavity growth.

IV. Appendix

A Data for T_g of acrylate co-polymers measured with DSC



FigureA.1: T_g data for BA/MA measured with DSC.



FigureA.2.: T_g data for BA/MA/AA measured with DSC.

IV. Appendix

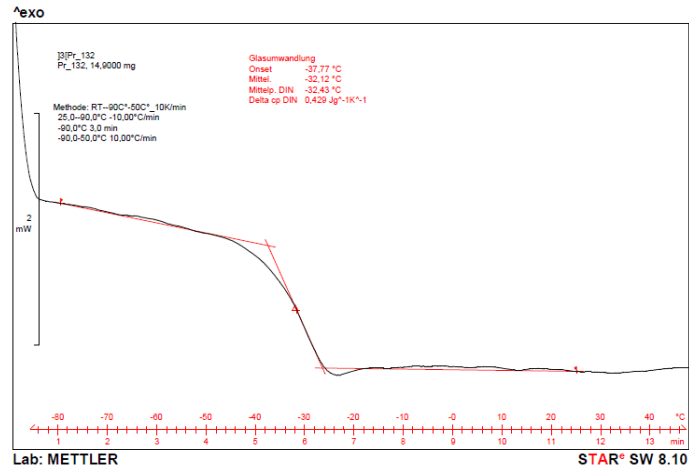


Figure A.3.: Tg data for BA/MA/MMA measured with DSC

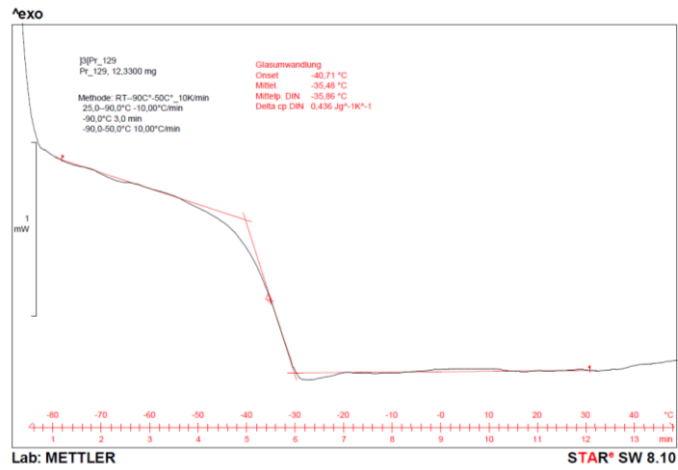
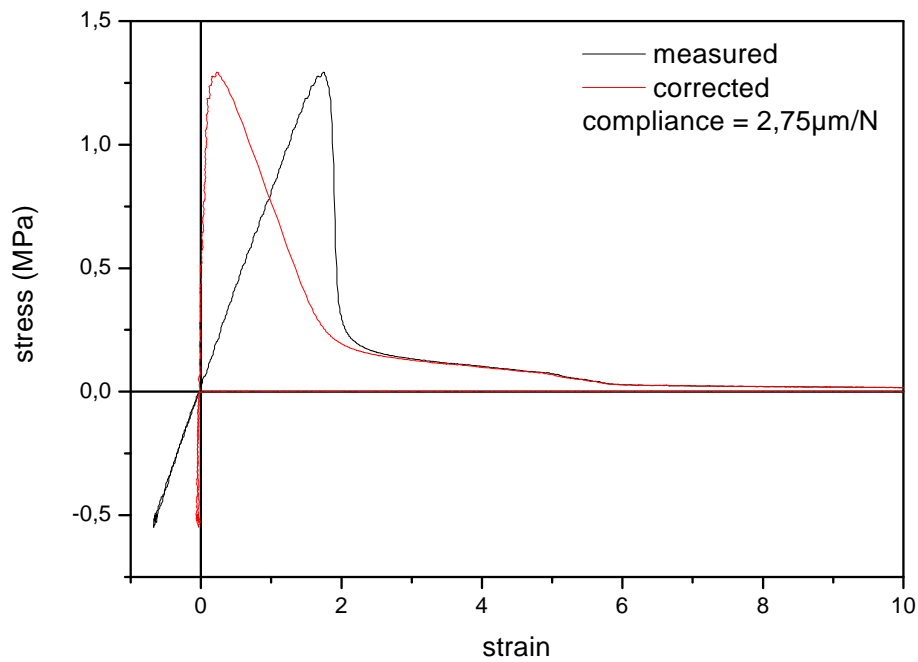


Figure A.4.: Tg data for BA/MA/HEA measured with DSC

B Correction of the tack curves of acrylate co-polymers (example: BA/MA/MMA) according to the compliance of the tack devices.



$$D = d - (2,75 \mu\text{m}/\text{N}) * \text{forceN},$$

where d = apparent gap [123]

C Abbreviations and symbols

1. Abbreviation

Compounds

AA	acrylic acid
AN	acrylonitrile
BA	butyl acrylate
EA	ethylene acrylate
HEA	hydroxy ethylacrylate
MA	methyl acrylate
MAA	maleic acid anhydride
MEK	methyl ethylketone
MMA	methyl methacrylate
LDPE	low density polyethylene
PDMS	poly (dimethylsiloxane)
PE	poly (ethylene)
PEHA	poly (ethylhexyl acrylate)
PIB	poly (isobutylene)
PP	polypropylene
S	styrene
SBS	styrene-butadiene-styrene
SIS	styrene-isoprene-styrene triblock
Si-wafer	silicon wafer
StA	stearyl acrylate
TMCS	trimethylchlorosilane

terms

DSC	differential scanning calorimeter
IPS	image processing system

IV. Appendix

PSA	pressure sensitive adhesives
PDI	polydispersity index
RH	relative humidity
ROIs	regions of interest
LVE	linear viscoelastic region
UV light	ultra violet light
SEC	size exclusion chromatography
SPM	scanning probe microscope
TTS	time temperature superposition

2. Symbols

Latin

A	contact area
a	contact probe radius
a_m	molecular size
a_0	initial probe radius
a_c	radius of crack
a_T	shift factor
C_1, C_2	material constants
De	Deborah number
E	Young's modulus
$F (F_A)$	force
G	crack driving force
G_0	plateau modulus
G'	storage modulus
G''	loss modulus
G_{edge}	bulk crack propagation
G_c	critical energy release rate
G_{cavity}	interfacial crack propagation

IV. Appendix

G_l	limiting value energy release rate
h	film thickness
h_0	initial film thickness
h_c	height of cavity
$h(R)$	gap
L	length of the sample
l	displacement by elongation
M	torsional moment
M_c	molecular weight between crosslinks
M_e	molecular weight between entanglements
M_n	number average molecular weight
M_w	molecule weight
R	ideal gas constant
R_a	average roughness
R_c	radius of the cavity
R_d	debonding area of cavity
R_p	initial projected radius of cavity on the substrate surface
r	distance along the radial direction
T	temperature
t_c	contact time
T_g	glass transition temperature
T_{ref}	reference temperature
V_{deb}	debonding rate
W	adhesion energy
W_a	thermodynamic work of adhesion
W_i	weight fraction of monomer spies i
Greek	
α	cone-angle

IV. Appendix

γ	deformation
$\dot{\gamma}$	shear rate
γ_0	deformation amplitude
γ_l	surface energy of the liquid (polymer)
γ_{LV}	Surface tension between liquid and vapor
γ_s	surface energy of the substrate
γ_{SL}	interfacial tension between solid and liquid
γ_{SL}^d	disperse part of the interfacial tension
γ_{SL}^p	polar part of the interfacial tension
γ_{sl}	interfacial energy
γ_{SV}	surface tension between solid and vapor
δ	phase shift
ε	elongation (strain)
$\dot{\varepsilon}$	strain rate
$\dot{\varepsilon}_H$	Hencky strain rate
ε_{\max}	maximum elongation
$\eta_E^+(t)$	tensile stress growth function
Θ	contact angle
Θ_e	contact angle in equilibrium
π	mathematical constant
ρ	density
$\sigma (\tau)$	stress
$\sigma_0 (\tau_0)$	stress amplitude
τ_r	relaxation time of the adhesive
$\Omega(\omega)$	angular frequency
v	crack velocity
v_{deb}	debonding velocity

References

- [1] DAHLQUIST, C.A. Pressure-Sensitive Adhesives in Adhesion and Adhesives, ed.by Patrick R.1969,vol.2, 219-258.
- [2] CRETON C., FARBE P., Tack in Adhesion Science and Engineering,vol.I: The Mechanics of Adhesion, Dillar D.A. and Pocius A.V. 2002, Elsevier, Amsterdam cap.14.
- [3] ZOSEL A., Adhesion and Tack of Polymers: Influence of Mechanical Properties and Surface Tensions. Colloid. Polym. Sci. 1985; 263, 541-553.
- [4] BENEDEK I., FELDSTEIN M.M. vol.3. Application of Pressure-Sensitivity.,eds. Taylor & Francis, Boca. 2009.
- [5] URBAN D:and TAKAMURA K. Polymer Dispersions and Their Industrial Applications . 2002, Wiley-VCH Verlag GmbH & Co. KGaA
- [6] LAKROUT H., SERGOT P., CRETON C., Direct Observation of Cavitation and Fibrillation in a Probe Tack Experiment on Model Acrylic Pressure-Sensitive-Adhesives, J. Adhes. 1999, 69, 307-359.
- [7] AUBREY D.W., GINOSATIS S. Peel Adhesion Behavior of Carboxylic Elastomers. J. Adhes. 1981,12, 189-198.
- [8] ZOSEL A, BARWICH J. Mechanical Properties and Adhesion Performance of UV Crosslinkable Hot Melt Pressure Sensitive Adhesives. PSTC Pressure Sensitive Adhesive Tape. Conference proceedings Orlando 3rd-5th May. 1995, 175-87.
- [9] CRETON C. Material Science of Adhesives: How to Bond Things Together. Mrs Bulletin. 2003, 419-423.
- [10] HABENICHT G. Kleben, 1997, Springer.
- [11] BENEDEK I., FELDSTEIN M.M. vol.1. Fundamentals of Pressure-Sensitivity.,eds. Taylor & Francis, Boca. 2009.

References

- [12] CRETON C. and SHULL K.R. Probe Tack in Adhesion Science and Engineering, vol.I: The Mechanics of Adhesion, Dillar D.A. and Pocius A.V., Elsevier, Amsterdam cap.6, 2002.
- [13] ZOSEL A. Adhesive Failure and Deformation Behavior of Polymers. *J. Adhesion*. 1989, 30, 135-149.
- [14] ZOSEL A. Fracture Energy and Tack of Pressure Sensitive Adhesives. In: Satas D, editor. *Advances in Pressure Sensitive Adhesives Technology*, 1992, vol.1. Warwick, RI: Satas & Associates, 92-127.
- [15] DAHLQUIST, C.A. Tack, in *Adhesion Fundamentals and Practice.*, London : Mc Laren, 1966.
- [16] GAY C. Stickiness-Some Fundamentals of Adhesion, *Integr. Comp. Biol.* 2002, 42, 1123-1126.
- [17] VAN OSS C.J., CHAUDHURY M.K.,GOOD R.J. Interfacial Lifshitz - van der Waals and Polar Interactions in Macroscopic Systems.*Chem.Rev.*1988, 88, 927-941.
- [18] LEGER L., CRETON C. Adhesion Mechanisms at Soft Polymer Interfaces, *Phil.Trans.R.Soc.A.* 2007, 366, 1425-1442.
- [19] SHULL K.R., AHN D., CHEN W.-L., FLANIGAN C.M., CROSBY A.J. Axisymmetric Adhesion Tests of Soft Materials. *Macromol. Chem. Phys.* 1998, 199, 489-511.
- [20] TIRUMKUDULU M., RUSSEL W. On the Measurement of „Tack“ for Adhesives. 2003, vol.15 (6), 1588-1605.
- [21] GAY C., LEIBLER L. On Stickiness. *Phys.Today.* 1999, 52, 48-52.
- [22] SHULL K.R., CRETON C. Deformation Behavior of Thin, Compliant Layers Under Tensile Loading Conditions. *J. Polym. Sci. Part B: Polym. Physic.* 2004, vol. 42, 4023-4043.
- [23] CHICINA I., GAY C. Cavitation in Adhesives. *Phys. Rev. Lett.* 2000, 85, 4546-49.
- [24] BROWN K., CRETON C. Nucleation and Growth of Cavities in Soft Viscoelastic Layers under Tensile Stress, *Eur. Phys. J. E: Soft Matter Biol. Phys.* 2002, 9, 35-40.
- [25] NASE J., CRETON C., RAMOS O., SONNENBERG L.,YAMAGUCHI T., LINDNER A. Measurement of the Receding Contact Angle at the Interface between a Viscoelastic Material and a Rigid Surface. *Soft Mater.* 2010, 6, 2685-2691.

References

- [26] YAMAGUCHI T., KOIKE K., DOI M. In Situ Observation of Stereoscopic Shapes of Cavities in Soft Adhesives. *Europhys. Lett.*, 2007, 5 (11), 64002.
- [27] SAFFMAN P.G., TAYLOR G. The Penetration of a Fluid into a Porous Medium or Hele-Shaw Cell Containing a more Viscous Liquid, *Proceedings of The Royal Society A Mathematical Physical and Engineering Sciences*. 1958, 245, 312.
- [28] GENT A.N., WANG C. Fracture Mechanics and Cavitation in Rubber-Like Solids. *J. Mat. Sci.* 1991, 26, 3392-3395.
- [29] BROWN K., HOOKER J.C., CRETON C. Micromechanisms of Tack of Soft Adhesives Based on Styrenic Block Copolymers. *Macromol.Mater.Eng.* 2002, 287, 163-179.
- [30] CROSBY A.J., SHULL K. Deformation and Failure Modes of Adhesively Bonded Elastic Layers, *J. Appl. Phys.* 2000, vol. 88 (5), 2956-2966.
- [31] CRETON C., HOOKER J., SHULL K.R. Bulk and Interfacial Contributions to the Debonding Mechanisms of Soft Adhesives: Extension to Large Strains. *Langmuir* 2001, 17, 4948-4954.
- [32] SHULL K.R., AHN D., CHEN W-L., Flanigan c.M.,Crosby A. Axisymmetric Adhesion Test of Soft Materials. 1998, 199, 489-511.
- [33] URAHAMA Y. Effect of Peel Load on Stringiness Phenomena and Peel Speed of Pressure-Sensitive Adhesive Tape, *J.Adhes.* 1989, 31, 47-58.
- [34] ANDREWS E.H., KINLOCH A.J. Mechanics of Adhesive Failure I, *Proc.R.Soc. Lond.* 1973, 332, 385-399.
- [35] ANDREWS E.H., KINLOCH A.J. Mechanics of Adhesive Failure II, *Proc.R. Soc. Lond.*1973, 332, 401- 414.
- [36] GENT A.N., SCHULTZ J., Effect of Wetting Liquids on the Strength of Adhesion of Viscoelastic Materials. *J.Adhes.* 1971, vol.3, 281-294.
- [37] MAUGIS D., BARQUIS M., Fracture Mechanics and the Adherence of the Viscoelastic Bodies, *J.Phys.D; Appl.Phys.*1978, 11, 1989-2023.
- [38] LI L., TIRRELL M., KORBA G., POCIUS A.V.Surface Energy and Adhesion Studies on Acrylic Pressure Sensitive Adhesives. 2001, 76, 307-334.
- [39] FOREMAN P.B. Acrylic Adhesives in Thechnology of Pressure Sensitive Adhesives and Products. Benedek I, Feldstein M.M.,eds. Taylor & Francis, Boca. 2009, vol.2, cap.5.
- [40] KRENCESKI M.A., JOHNSON J.F. Shear, Tack, and Peel of Polyisobutylene: Effect of Molecular Weight and Molecular Weight Distribution. *Polym. Eng. Sci.* 1989, 29, 36-43.

References

- [41] O'CONNOR A.E., WILLENBACHER N. The Effect of Molecular Weight and Temperature on Tack Properties of Model Polyisobutylenes. *Int. J. Adhes. Adhes.* 2004, 24, 335-346.
- [42] FELDSTEIN M. M. Molecular Nature of Pressure-Sensitive Adhesives, in: *Fundamentals of Pressure-Sensitivity*. Benedek I, Feldstein M.M., eds. Taylor & Francis, Boca. 2009, vol.1, cap.10.
- [43] CRETON C., *Processing of Polymers*, 1997, 15, 709-741.
- [44] CZECH Z. Synthesis and Cross-linking of Acrylic PSA Systems. *J. Adhes. Sci. Technol.* 2007, 21, 625-35.
- [45] ZOSEL A. Effect of cross-linking on tack and peel strength of polymers. *J Adhes* 1991, 34, 201-209.
- [46] ZOSEL A. The Effect of Fibrillation on the Tack of Pressure Sensitive Adhesives. *Int. J. Adhes. Adhes.* 1998, 18, 265-71.
- [47] DO H.S., Park Y.J., Kim H.J. Preparation and Adhesion Performance of UV-Crosslinkable Acrylic Pressure Sensitive Adhesives. *J. Adhes. Sci. Technol.* 2006, 20, 1529-1545.
- [48] WU G.L., JIANG Y., YE L., ZENG S.J., YU P.R., XU W. J. A novel UV-Crosslinked Pressure-Sensitive Adhesive based on Photoinitiator-grafted SBS. *Int. J. Adhes. Adhes.* 2010, 30, 43-46.
- [49] GOWER M.D., SHANKS R.A., Comparison of Styrene with Methyl Methacrylate Copolymers on the Adhesive Performance and Peeling Master Curves of Acrylate Pressure Sensitive Adhesives. *Macromol. Chem. Phys.* 2005, 206,1015-27.
- [50] GOWER M.D., SHANKS R.A. The Effect of Varied Monomer Composition on Adhesive Performance and Peeling Master Curves for Acrylic Pressure-Sensitive Adhesives. *J. Appl. Polym. Sci.* 2004, 93, 2909-2917.
- [51] LAKROUT H., CRETON C., AHN D., SHULL K.R. Influence of Molecular Features on the Tackiness of Acrylic Polymer Melts. *Macromolecules*; 2001, 34, 7448-7458.
- [52] CHAN H.K., HOWARD G.J. Structure-Property Relationships in Acrylic Adhesives. *J. Adhes.* 1978, 9, 279-304.
- [53] AHN D., SHULL K.R. Effects of Methylation and Neutralization of Carboxylated Poly(n-Butyl Acrylate) on the Interfacial and Bulk Contributions to Adhesion. *Langmuir.* 1998, 14, 3637-3645.

References

- [54] LINDNER A., LESTRIEZ B., MARIOT S., CRETON C., MAEVIS T., LUHMANN B., BRUMMER R. Adhesive and Rheological Properties of Lightly Crosslinked Model Acrylic Networks. *J. Adhes.* 2006, 82, 267-310.
- [55] KRAUS G., ROLLMANN K.W., GRAY R.A. Tack and Viscoelasticity of Block Copolymer Based Adhesives. 1979, 10, 221.
- [56] DAHLQUIST, C.A., in *Treatise on Adhesion and Adhesives*, vol.2, Patrick R.L. ed., Dekkar, 1969, New York, 2, 219-258.
- [57] SHARPE L.H., SCHONHORN H., in *Contact Angle, Wettability and Adhesion*, Adv.Chem.Series 43, American Chemical Society, Washington, D.C. 1964, 189.
- [58] DIMITROVA T.D., JOHANNSMANN D., WILLENBACHER N., PFAU A. Mesoscopic Fibrillation Properties of Pressure Sensitive Adhesives Based on Latex Films. 2003, 19, 5748-5755.
- [59] CHICHE A., DOLLHOFER J., CRETON C. Cavity Growth in Soft Adhesives. *Eur. Phys. J. E: Soft Matter Biol. Phys.* 2005, 17, 389-401.
- [60] ZOSEL A., The Effect of Bond Formation on the Tack of Polymers, *J. Adhes. Sci. Technol.* 1997; 11, 1447-1457.
- [61] PERSSON B.N.J. and TOSATTI E. The Effect of Surface Roughness on the Adhesion of Elastic Solids. *J. Chem. Phys.*, 2001, vol. 115, No. 12.
- [62] CRETON C, LEIBLER L. How does Tack Depend on Time of Contact and Contact Pressure? *J. Polym. Sci. Part B: Polym. Phys.* 1996, 34, 545-554.
- [63] HUI C.Y., LIN Y.Y., BANEY J.M., The Mechanics of Tack: Viscoelastic Contact on a Rough Surface, *J. Polym. Sci., Part B: Polym. Phys.* 2000, 38, 1485-1495.
- [64] HUI C.Y., LIN Y.Y., BANEY J.M., KRAMER E.J., The Mechanics of Contact and Adhesion of Periodically Rough Surfaces, *J. Polym. Sci., Part B: Polym. Phys.* 2001, 39, 1195-1214.
- [65] HOOKER J., CRETON C., SHULL K.R., TORDJEMANN P. Surface Effects on the Microscopic Adhesion Mechanisms of SIS + Resin PSA's. In: *Proceedings of the 22nd Annual Meeting of The Adhesion Society*, 1999, Panama City Beach, USA.
- [66] CHICHE A., PAREIGE P., CRETON C. Role of Surface Roughness in Controlling the Adhesion of a Soft Adhesive on a Hard Surface. *C. R. Phys.* 2000, 1, 1197-1204.
- [67] POCIUS A.V. *Adhesion and Adhesive Technology*. 2002. Carl Hanser, München.
- [68] DIETHERT A., PEYKOVA Y., WILLENBACHER N., MÜLLER-BUSCHBAUM P. Near-surface Composition Profiles and the Adhesive Properties of Statistical

References

Copolymer Films being Model Systems of Pressure Sensitive Adhesive Films. ACS Appl Mater Interfaces. 2010, 2, 2060-2068.

[69] DIETHERT A., ECKER K., PEYKOVA Y., WILLENBACHER N., MÜLLER-BUSCHBAUM P. Tailoring the Near-surface Composition Profiles of Pressure-Sensitive Adhesive Films and the Resulting Mechanical Properties. ACS Appl. Mater Interfaces 2011, Vol.3 (6), 2012-2021.

[70] TOYAMA M., ITO T., MORIGUCHI H. Studies on Tack of Pressure-Sensitive Adhesive Tapes. J. Appl. Polym. Sci. 1970, 14, 2039-2048.

[71] TOYAMA M., ITO T., NUKATSUKA H., IKEDA M. Studies on Tack of Pressure-Sensitive Adhesive Tapes: On the Relationship between Pressure-Sensitive Adhesion and Surface Energy of Adherends. J. Appl. Polym. Sci. 1973, 17, 3495-3502.

[72] AGIRRE A., NASE J., CRETON C., ASUA J.M. Adhesives for Low-energy Surfaces. Macromol. Symp. 2009, 281, 181-190.

[73] JOVANOVIĆ R., DUBE M.A. Screening Experiments for Butyl Acrylate/Vinyl Acetate Pressure-Sensitive Adhesives. Ind. Eng. Chem. Res. 2005, 44, 6668-6675.

[74] CARELLI C., DEPLACE F., BOISSONNET L., CRETON C. Effect of a Gradient in Viscoelastic Properties on the Debonding Mechanisms of Soft Adhesives. J. Adhes. 2007, 83, 491 - 505.

[75] DEPLACE F., CARELLI C., MARIOT S., RETSOS H., CHATEAUMINOIS A., OUZINEB K., CRETON C. Fine Tuning the Adhesive Properties of a Soft Nanostructured Adhesive with Rheological Measurements. J. Adhes. 2009, 85, 18 - 54.

[76] DEPLACE F., RABJOHNS M.A., YAMAGUCHI T., FOSTER A.B., CARELLI C., LEI C.H., OUZINEB K., KEDDIE J.L., LOVELL P.A., CRETON C. Deformation and Adhesion of a Periodic Soft-Soft Nanocomposite Designed with Structured Polymer Colloid Particles. Soft Matter. 2009, 5, 1440-1447.

[77] KAELBLE D.H. Rheology of Adhesion. J. Macromol. Sci.- Revs. Macromol. Chem., C. 1971; 6(1), 85-112.

[78] MARIN G., DERRAIL C. Rheology and Adherence of Pressure-Sensitive Adhesives. J. Adhes. 2006, 82, 469-485.

[79] CHANG E.P. Viscoelastic Windows of Pressure-Sensitive Adhesives. J. Adhes. 1991, vol.34, 189-200.

[80] ROOS A., CRETON C. Linear Viscoelasticity and Non-Linear Elasticity of Block Copolymer Blends Used as Soft Adhesives. Macromol. Symp. 2004, 214, 147-156.

[81] REINER M. The Deborah Number. Physics Today. 1964, 17(1), 62.

References

- [82] FERRY J.D., *Viscoelastic Properties of Polymers*; 3ed ed.; Wiley, 1980, vol.1.
- [83] FERGUSON J., HUDSON N.E. The Shear and Extensional Flow Properties of S1. *J. Non-Newtonian Fluid Mech.* 1994, vol. 52(2), 121-135.
- [84] JONES W.M., HUDSON N.E., FERGUSON J. The Extensional-Properties of M1 Obtained from the Stretching of a Filament by a Falling Pendant drop. *Non-Newtonian Fluid Mech.* 1990, 35, 263-276.
- [85] MEISSNER J. Int. Workshop of Extensional Flows, Paper 4, Mulhouse-la Bresse, France, 1980.
- [86] MUNSTEDT H., LAUN H.M. Elongational Properties and Molecular Structure of Polyethylene Melts. *Rheolog. Acta*, 1981, 20, 211-221.
- [87] OOI Y.W., SRIDHARD T. Extensional Rheometry of Fluid S1. *J. Non-newtonian Fluid Mech.* 1994, 52, 153-162.
- [88] FERGUSON J., REILY B., GRANVILLE N. Extensional and Adhesion Characteristics of a Pressure Sensitive Adhesive. *Polymer* 1997, vol. 38 (4), 795-800.
- [89] SENTMANAT M.L., WANG B.N., Mc KINLEY G.H., Measurement the Transient Extensional Rheology Universal Testing Platform, *J. Rheol.* 2005, 49, 585-606.
- [90] FOX H. W., ZISMAN W. A. The Spreading of Liquids on Low Energy Surfaces 1. Polytetrafluoroethylene. *J. colloid Sci.* 1950, 514-531.
- [91] ELLISON A.H., FOX H.W., ZISMAN W.A., Wetting of Fluorinated Solids by Hydrogen-Bonding Liquids. *J. Phis.Chem.* 1953, 57, 622-627.
- [92] FOX, H.W., HARE, E.F., ZISMAN W.A. Wetting Properties of Organic Liquids on High Energy Surfaces. *J. Phya. Chem.*, 1955, 59, 1097-1106.
- [93] LANGMUIR I. J. The Constitution and Fundamental Properties of Solids and Liquids. Part I. Solids, *Amer.Chem.Soc.* 1916, 38(2), 2221-2295.
- [94] SHUTTLEWORTH R. and BAILEY G.L.J. The Spreading of a Liquid over a Rough Solid. *Discussions of the Faraday Society.* 1948, vol. 3, 16-22.
- [95] SHYR F.-S. An approximate method to determine the surface tension from a sessile drop. *J. Material Sci. Letters*, 1991, 10, 946-948.
- [96] SENTMANAT M.L. Dual Wind up Extensional Rheometer, US Patent No. 6578413, 2003.
- [97] SENTMANAT M.L. Miniature Universal Testingplatform: from Extensional Solid-state Deformation Behavior, *Rheol. Acta*, 2004, vol.43, 657-669.

References

- [98] PETR F. Various Aspects of Measurement of Uniaxial Elongational Viscosity of Polymer Melts Institute of Hydrodynamics, Acad.Sci.Czech Rep., Pod Patankou 5,166 12 Prague 6, CZECH
- [99] PARRATT L.G. Surface Studies of Solids by Total Reflection of X-rays. *Phys. Rev.*1954, 95, 359-369.
- [100] FORNY L., PEZRON I., SALEH K., GUIGON P., KOMUNJER L. Peculiar Absorption of Water by Hydrophobized Glass Beads. *Colloids. Surf. A.* 2005, 270-271, 263-69.
- [101] FUJI M., FUJIMORI H., TAKEI T., WATANABE T., CHIKAZAWA M. Wettability of Glass-bead Surface Modified by Trimethylchlorosilane. *J. Phys. Chem. B.* 1998, 102, 10498-10504.
- [102] PEYKOVA Y., GURIYANOVA S., LEBEDEVA O.V., DIETHERT A., MÜLLER-BUSCHBAUM P., WILLENBACHER N. The Effect of Surface Roughness on Adhesive Properties of Acrylic Copolymers. *Int. J. Adhes. Adhes.* 2010, 30, 245-254.
- [103] LAVI B., MARMUR A. The Exponential Power Law: Partial Wetting Kinetics and Dynamic Contact Angles. *Colloids. Surf., A: Physicochem. Eng. Asp.* 2004, 250, 409-414.
- [104] OWENS D.K., WENDT R.C. Estimation of the surface free energy of polymers. *J.App. Polym. Sci.* 1969, 13, 1741-1747.
- [105] FOWKES F.M. Attractive Forces at Interfaces. *Ind. Eng. Chem.* 1964, 56(12), 40.
- [106] VAN OSS C.J. *Interfacial Forces in Aqueous Media.* M.Dekker, New York, 1999.
- [107] CHU S-G. In: *Dynamic Mechanical Properties of Pressure-Sensitive Adhesives;* Lee L-H, editor. Adhesive Bonding. New York: Plenum press: 1991, 97-137.
- [108] VERDIER C., PIAU J-M. Effect of Nonlinear Viscoelastic Properties on Tack. *J. Polym. Sci: Part B: Polym. Phys.* 2003, vol. 41, 3139-3149.
- [109] FERGUSON J. and REILLY B. Extensional and Adhesion Characteristics of a Pressure Sensitive Adhesive. *Polymer.* 1997, vol. 38(4), 795-800.
- [110] TORDJEMAN P., PAPON E., VILLENAVE J-J. J. Tack Properties of Pressure-Sensitive Adhesives. *Polym. Sci., Part. B: Polym.Phys.* 2000, 38, 1202-1208.
- [111] FULLER K.N.G., TABOR D. Effect of Surface-Roughness on Adhesion of Elastic Solids. *Proc. Roy. Soc. London.* 1975, vol. 345 (1642), 327-342.
- [112] CROSBY A. J., SHULL K.R. Debonding Mechanisms of PSAs. *Adhes. Age.* 1999, vol. 42 (7), 28-33.

References

- [113] CRETON C., SHULL K.R. Deformation Behavior of Thin, Compliant Layers under Tensile Loading Conditions. *J. Polym.Sci. Part B-Polym.Phys.* 2004, vol.42 (22), 4023-4043.
- [114] PEYKOVA Y., LEBEDEVA O. V., DIETHERT A., MÜLLER-BUSCHBAUM P., WILLENBACHER N. *Int. J. Adh.Adh.* , 2012, 34,107-116.
- [115] BRANDRUP J., IMMERGUT E.H., GRULKE E.A. editors. *Polymer Handbook (4th Edition): VI.Solid state properties: John Wiley & Sons, 1999, 521-541.*
- [116] FRIEDSAM C., DEL CAMPO BECARES A., JONAS U., SEITZ M., GAUB H.E. Adsorption of Polyacrylic Acid on Self-assembled Monolayers Investigated by Single-Molecul Force Spectroscopy. *New J. Phys.*, 2004, 6, 9.
- [117] HOFRICHTER C.B., McLAREN A.D. Temperature Dependence of the Adhesion of High Polymers to Cellulose. *Ind. Eng. Chem.*1948, vol.40(2), 329-331.
- [118] CZECH Z. Crosslinking of Pressure Sensitive Adhesive based on Water-borne Acrylate. *Polym. Int.* 2003, 52, 347-357.
- [119] BENYAHIA, L., VERDIER C. PIAU J.M. The Mechanisms of Peeling of Uncross-linked Pressure Sensitive Adhesives. *Int. J. Adhes.* 1997, vol. 62 (1-4), 45-73.
- [120] SCHWARZ S.A., WILKENS B.J., PUDENSKI M.A.A., RAFAILOVICH M.N., SOKOLOV J., ZHAO W., ZHENG X, RUSSEL T.P., JONES R.A.L. Studies of Surface and Interface Segregation in Polymer Blends by Secondary Ion Mass-Spectrometry. *Molec. Phys.*1992, vol. 76(4), 937-950.
- [121] JONES R.A.L., KRAMER E.J., RAFAILOVICH M.H., SOKOLOV J., SCHWARZ S.A. Surface Enrichment in an Isotropic Polymer Blend. *Phys. Rev. Lett.* 1989, vol. 62(3), 280-283.
- [122] EL-MABROUK K., BELAICHE M., BOUSMINA M. Phase Separation in Ps/PVME Thin and Thick Films. *J. Coll. and Interf. Sci.* 2007, 306 (2), 354-367.
- [123] JOSSE G., SERGOT P., DORGET M. and CRETON C"Measuring interfacial adhesion between a soft viscoelastic layer and a rigid surface using a probe method." *Journal of Adhesion*: 2004; 80 (1-2), 87-118.

Part of this work was published in the following articles:

Y.Peykova, O.Lebedeva, A.Diethert, P.Müller-Buschbaum, N.Willenbacher: Adhesion Properties of Acrylate Copolymers: Effect of the Nature of the Substrate and Copolymer Functionality, *International Journal of Adhesion & Adhesives* - in progress.

A.Diethert, K.Ecker, Y.Peykova, N.Willenbacher and P.Müller-Buschbaum: Tailoring the near-Surface Composition Profiles of Pressure-Sensitive Adhesive Films and the Resulting Mechanical Properties, *Applied. Materials & Interfaces* 2011, 3, 2012-2021(2011).

Y.Peykova, S.Guriyanova, O.Lebedeva, A.Diethert, P.Müller-Buschbaum, N.Willenbacher: The effect of surface roughness on adhesive properties of acrylate copolymers, *International Journal of Adhesion & Adhesives* 30, 245-254 (2010).

A.Diethert, Y.Peykova, N.Willenbacher, P.Müller-Buschbaum: Near -surface composition profiles and the adhesive properties of statistical copolymer films being model systems of pressure sensitive adhesive films; *ACS Applied Materials & Interfaces* Vol. 2, No. 7, 2060-2068 (2010).

Part of this work was present in the following conferences:

References

How probe roughness, surface energy and polymer chemical composition influence the adhesion of acrylate polymers. 11th International Conference on the Science and Technology of Adhesion and Adhesives, 7 Sep. 2011, University of York, UK.

Adhesion of acrylate polymers: the role of the chemical composition of polymer film and substrate. 34rd Annual Meeting of the Adhesion Society, Inc. Feb.2011, Savannah, Georgia, USA.

The influence of the roughness and chemical composition of the substrate on the adhesion of acrylate copolymers. 4th World Congress on Adhesion and Related Phenomena, September 26th-30th 2010, Arcachon, France.

The influence of the interaction Substrate-Polymer on the adhesion of acrylate copolymers. 33rd Annual Meeting of the Adhesion Society, Inc. 21 Feb.2010, Daytona Beach, Florida, USA.

Diploma thesis:

Yichi Zhang "Adhäsion von Haftklebstoffen: Einfluß von Oberflächenenergie und Rauigkeit" Januar 2009.

Wieke Maaßen "Adhäsion:Einfluss der chemisch funktionalisierten Substratoberfläche"
Juni 2010

Lebenslauf

Persönliche Daten

Yana Rüdener, geb. Peykova
geboren am 2. Juli 1979
in Sevlievo, Bulgarien

Arbeitserfahrung

2008-2012 Wissenschaftlicher Mitarbeiter: Angewandte Mechanik (KIT)
2007 Wissenschaftlicher Mitarbeiter am Institut für Wasser und
Gewässerwirtschaft (KIT)
2003-2007 Chemisch -technische Beraterin BONERO Ltd Sofia ,Bulgarien.

Bildung

2008-2012 Promotion: Einfluss von Grenzflächeneffekten auf die Adhäsion
weicher Polymere.
2002 Diplomarbeit am Institut für Abwasserwirtschaft, Technische
Universität Hamburg-Harburg.
1997-2002 Chemieingenieurwesen an der Universität für Chemische
Technologie und Metallurgie (UCTM) - Sofia,

Schulischer Bildungsweg

1993 – 1997 Gymnasium Vasil Levski, Sevlievo, Bulgarien
1986 – 1993 Grundschule Sevlievo, Bulgarien

Stipendien

2011 Abschlussstipendium

2007	Deutsche Bundesstiftung Umwelt (DBU)
2002	ERASMUS
2001	DAAD